# Connectivity-specified targeting and manipulation of the motor thalamus

Rahul S. Shah

Thesis submitted for the degree of Doctor of Philosophy (D.Phil.)




Magdalen College

MRC Brain Network Dynamics Unit

Department of Pharmacology

University of Oxford

Student No: 842686

**Connectivity-specified targeting and manipulation of the motor thalamus**

Rahul Shah

Magdalen College

DPhil in Biomedical and Clinical Sciences

Trinity Term 2019

Understanding the nature and consequences of information flow between the basal ganglia, cerebellum, thalamus and motor cortex on the acquisition and execution of motor skills may lead to better circuit therapies for brain disorders. Although basal ganglia and cerebellar output is thought to influence motor cortex activity via projections arising from distinct zones of ventral 'motor' thalamic nuclei (ventral medial [VM], ventral anterior [VA] and ventral lateral [VL] nuclei), the consequences of their activity on motor skills in rodents remains uncertain. Here, we first utilise an anterograde transsynaptic viral strategy to confirm that anatomically and functionally distinct basal ganglia-recipient and cerebellar-recipient neuron populations exist in the mouse motor thalamus. To address the behavioural significance of these two neuron populations for motor skill learning, Vglut2-Cre mice with either targeted chronic motor thalamus silencing (using overexpression of the inward-rectifier potassium channel Kir2.1) or acute optogenetic silencing of VM or VL (using the light-sensitive proton pump ArchT) thalamus were trained in a novel operant task monitoring the self-paced acquisition of a covert, temporally-constrained lever press sequence (fixed ratio of 3 lever presses within 2 seconds [FR3/2s]) over multiple sessions. Surprisingly, rather than causing gross motor impairment or impaired acquisition of the FR3/2s action pattern, mice receiving acute VM-ArchT silencing or chronic motor thalamus silencing showed faster early learning of the sequence compared to controls or VL-ArchT silencing. Simultaneous adaptation of peak within-press acceleration with learning was deficient in mice receiving VL-ArchT silencing. Our results suggest that manipulating the motor thalamus in mice can alter the pattern of within-day and between-day performance gains during task acquisition, potentially via downstream network effects which promote learning occurring via competing circuits.

**Acknowledgements**

I would like to thank my primary supervisor Dr Andrew Sharott for the support and enthusiasm he has showed during the entirety of my doctoral fellowship, and my co-supervisors Professor Peter Magill and Professor Peter Brown for their mentorship and strategic advice. I also would like to thank all of the current and former members of the Sharott lab for their varied culinary, intellectual and practical contributions: Dr Colin McNamara, Dr Abbey Holt, Dr Eric Tam, Ms Andreia Madalena, Ms Naomi Berry, Dr Magdalena Baaske, Dr Anders Meihdahl, Dr Eszter Kormann, Dr Farid Garas, Mr Max Rothwell, and Dr Oliver Härmson.

Special thanks goes to Dr Natalie Doig, Dr Paul Dodson, Dr Kouichi Nakamura, Dr Amy Wolff, Dr Julien Carponcy, Dr Jennifer Kaufling, Dr Guy Yona, Dr David Dupret, Dr Stéphanie Trouche, Dr Pavel Perestenko, Dr Linda Katona, Dr Mohamady El-Gaby, Dr Hayriye Cagnan, Dr Emilie Syed, Dr Gabriela Martins, Dr Rafal Bogacz, Dr Simon Butt, and Dr Abhilasha Joshi for their willingness to discuss specific aspects of my project. Undertaking this project would not have been possible without the support of Ms Lisa Conyers, Mrs Jane Westcott, Ms Grace Tennant, Dr Hua Zhang, Mr Ben Micklem, Ms Savita Anderson and Dr Vivienne Collins. I would also like to thank Dr Bernard Balleine and Dr Rui Costa for giving me the opportunity to train in their respective labs, and to Dr Tommas Ellender for undertaking critical *in vitro* experiments, as well as Dr Zengcai Guo, Mr Myles Billard, Mr Martin Preston, Mr Jon Beyor, and Mr Buddy Brow. This work could not have been undertaken without generous funding from the Wellcome Trust (WT_RS_109030/Z/15/Z) and the Medical Research Council.

Lastly, I would like to thank my sister, Rupal, and my parents, Jyotsna and Surendra, for their support in all of my endeavours.

**Declaration**

I, Rahul Shah, confirm that the work presented in this thesis is my own. Where information has been derived from other sources, I confirm that this has been indicated in the thesis.

**Table of Contents**


Acknowledgements ..... 3
Declaration ..... 4
Table of Contents ..... 5
List of Figures and Tables ..... 8
List of Abbreviations ..... 10
1. Introduction ..... 12
1.1 The motor thalamus: anatomy and connectivity ..... 14
1.1.1 Parcellation of motor thalamus by subcortical inputs ..... 14
1.1.2 Parcellation of motor thalamus by output targets ..... 18
1.2 Motor thalamus: physiology ..... 22
1.2.1 Intrinsic firing properties of motor thalamus neurons ..... 22
1.2.2 Task-related activity of motor thalamus neurons ..... 23
1.2.3 Basal ganglia (BG) modulation of motor thalamus neurons ..... 24
1.2.4 Cerebellar modulation of thalamocortical neurons ..... 25
1.2.5 Corticothalamic modulation of thalamocortical neurons ..... 26
1.2.6 Thalamic reticular nucleus (TRN) modulation of thalamocortical neurons ..... 26
1.2.7 Motor thalamus modulation of downstream targets ..... 27
1.3 Motor thalamus: skill execution and learning ..... 31
1.3.1 Neuroimaging evidence of motor skill learning-related activity ..... 32
1.3.2 Lesion studies in human motor thalamus ..... 33
1.3.3 Lesion and optogenetic studies in the non-human primate and rodent ..... 34
1.4 Summary ..... 37
1.5 Specific Aims ..... 38
2. Materials and Methods ..... 39
2.1 Animals ..... 39
2.2 Viral Constructs ..... 39
2.3 Stereotactic viral injections ..... 39
2.4 Implant surgeries ..... 40
2.5 *In vivo* anaesthetised electrophysiology and optogenetic stimulation ..... 41
2.6 Head-fixed awake or anaesthetised *in vivo* electrophysiological recordings to validate optogenetic silencing ..... 43
2.7 Immunofluorescence ..... 44
2.8 Behavioural training ..... 44
2.8.1 Housing and food restriction ..... 44
2.8.2 Operant lever press training. ..... 45
2.8.3 Light delivery during behaviour ..... 46
2.9 Slice electrophysiology ..... 48

2.10 Quantification and data analysis ..... 50
2.11 Statistical analysis ..... 54
2.12 Key resources table ..... 57
3. Connectivity-specified targeting of the motor thalamus ..... 60
3.1 Introduction ..... 60
3.2 Experimental aims ..... 63
3.3 Basal ganglia- and cerebellar-recipient motor thalamus can be parcellated by immunoreactivity to Calbindin-1, GAD67 and VGLUT2 in mice ..... 63
3.4 Anterograde transsynaptic trafficking of WGA-Cre from substantia nigra or deep cerebellar nuclei can target distinct populations of post-synaptic motor thalamus neurons ..... 68
3.5 Direct targeting of VM or VL thalamus in Vglut2-cre mice shows differences in the density of laminar targeting ..... 75
3.6 Discussion ..... 78
3.6.1 Technical considerations ..... 79
3.6.2 Summary ..... 80
4. Designing a novel task to monitor self-paced acquisition of a covert motor skill ..... 81
4.1 Introduction ..... 81
4.2 Experimental aims ..... 84
4.3 Adapting a commercial operant chamber for detailed behavioural monitoring ..... 84
4.4 Extinction-induced motor variability in operant lever pressing identifies a demanding covert target for motor skill learning in mice ..... 87
4.5 Mice covertly switched from a strict FR1 to a FR3/2s lever pressing schedule acquire it in the first test session but continue to improve efficiency over days ..... 90
4.6 Real-time accelerometer data can capture lever dynamics during acquisition of FR3/2s lever pressing ..... 97
4.7 Discussion ..... 101
4.7.1 Technical considerations ..... 104
4.7.2 Summary ..... 105
5. Acute and chronic silencing of motor thalamus during behaviour ..... 106
5.1 Introduction ..... 106
5.2 Experimental aims ..... 108
5.3 Kir2.1 expression in the motor thalamus of Vglut2-Cre mice causes chronic hyperpolarisation ..... 108
5.4 Light-induced ArchT silencing of VM or VL thalamus does not disrupt learned operant lever pressing ..... 110
5.5 MThal-Kir2.1 and VM-ArchT mice show faster self-paced FR3/2s sequence acquisition without significantly different performance endpoints ..... 116
5.6 Refinement of accelerometer profile during sequence learning only occurs in untethered control mice ..... 125
5.7 Manipulating motor thalamus alters the pattern of within-day and between-day performance gains during early FR3/2s sequence acquisition ..... 128

5.7.1 Effect of recording day, daily session and experimental group on the absolute percentage of ≥ 3 press bouts ..... 128
5.7.2 Significant differences for within-day and between-day performance gains exist within each experimental group during early sessions ..... 129
5.7.3 Significant differences in within-day and between-day performance gains exist between each experimental group during early sessions ..... 131
5.8 Discussion ..... 135
5.8.1 Technical considerations ..... 139
5.8.2 Summary ..... 142
6. Discussion ..... 144
6.1 Summary of Main Findings ..... 144
6.2 Anatomically distinct motor thalamus neuron populations are conserved in mice ..... 145
6.3 Discrete acquisition of a demanding non-dextrous motor sequence shows refinement in multiple behavioural domains in mice ..... 147
6.4 Silencing of motor thalamus may facilitate motor sequence learning in mice ..... 149
6.5 Future directions ..... 151
6.6 Conclusion ..... 152
References ..... 153

**List of Figures and Tables**

Figure 1.1 Schematic of salient connections in cortico-basal ganglia-thalamocortical and cortico-cerebellar-thalamocortical loops. ..... 13
Figure 1.2 Afferent inputs to motor thalamus neurons. ..... 15
Figure 1.3 Motor thalamus classification systems across species organised based on predominant input from either basal ganglia or cerebellar nuclei. ..... 17
Figure 1.4 Projection patterns of motor thalamic neurons. ..... 19
Figure 1.5 Parallel cortico-basal ganglia-thalamocortical loops. ..... 21
Table 2.1 Summary of mice trained for FR3/2s behavioural analysis. ..... 48
Table 2.2 Key Resources Summary. ..... 59
Figure 3.1 Immunohistochemical and projection-based identification of basal ganglia-receiving zone of motor thalamus in coronal mouse brain sections. ..... 65
Figure 3.2 Comparison of thalamic GAD67+ zones and projection fibres from deep cerebellar nuclei. ..... 67
Figure 3.3 Anterograde transsynaptic tagging from basal ganglia or cerebellar output nuclei targets distinct populations of motor thalamus neurons. ..... 70
Figure 3.4 Optogenetic mapping of transynaptically identified basal ganglia- or cerebellar-recipient motor thalamus neurons shows distinct patterns of cortical activation in mice. ..... 73
Figure 3.5 Targeting VM and VL thalamic nuclei in Vglut2-Cre mice results in a degree of differential targeting in frontal cortex. ..... 77
Figure 4.1 Recording setup for operant lever pressing. ..... 86
Figure 4.2 Identifying the patterns of self-paced operant lever pressing elicited by extinction. ..... 89
Figure 4.3 A novel self-paced motor refinement task encouraging mice to acquire a ballistic pattern of lever pressing. ..... 92
Figure 4.4 Individual self-paced learning trajectories during acquisition of FR3/2s lever pressing. ..... 94
Figure 4.5 Refinement of multiple task parameters during self-paced acquisition of a FR3/2s lever press sequence in control mice. ..... 96
Figure 4.6 Accelerometer recordings from the lever allow detailed analysis of lever-pressing movement kinematics. ..... 99
Figure 4.7 Lever accelerometer recordings during press-initiation from bouts with ≥ 3 presses in control mice. ..... 101
Table 5.1 Complex relationship between role of brain areas and observed behavioural effects of their manipulation ..... 107
Figure 5.1 Kir2.1-ZsGreen expression results in hyperpolarization of motor thalamus neurons. ..... 109

Figure 5.2 Custom setup for quiescent head-fixed electrophysiological recordings. ..... 112
Figure 5.3 Sustained light-induced *in vivo* silencing of motor thalamus neurons expressing ArchT in mice. ..... 114
Table 5.2 Within group comparison of mean rates of head entries, licks and lever presses in light-on versus light-off periods during well learnt fixed-ratio 1 lever pressing. ..... 116
Figure 5.4 Refinement of multiple task parameters during self-paced acquisition of a FR3/2s lever press sequence in untethered control and MThal-Kir2.1 mice. ..... 118
Figure 5.5 Optic fibre sites for all VM-ArchT and VL-ArchT mice used for opto-behaviour experiments. ..... 120
Figure 5.6 Refinement of multiple task parameters during self-paced acquisition of a FR3/2s lever press sequence in VM-ArchT, VL-ArchT and tethered control mice ..... 121
Figure 5.7 Refinement of lever press duration for bouts with 1, 2, or ≥ 3 presses during self-paced acquisition of a FR3/2s lever press sequence in MThal-Kir2.1, VM-ArchT, VL-ArchT, and respective control mice. ..... 124
Figure 5.8 Accelerometer recordings from bouts of ≥ 3 presses in untethered control and MThal-Kir2.1 mice. ..... 126
Figure 5.9 Accelerometer recordings from bouts of ≥ 3 presses in tethered control, VM-ArchT and VL-ArchT mice. ..... 127
Figure 5.10 Within group comparisons of early task performance improvement within days and between days for VM-ArchT, VL-ArchT and tethered control mice. ..... 130
Figure 5.11 Between group comparisons of early task performance improvement within days and between days for MThal-Kir2.1 and control groups ..... 132
Figure 5.12 Between group comparisons of early task performance improvement within days and between days for VM-ArchT, VL-ArchT and tethered control groups. ..... 134

**List of Abbreviations**

| | |
|---|---|
| AAV | Adeno-Associated Virus. Typically the capsid and ITR are from AAV-2, but surface proteins from a different AAV (e.g. AAV1, AAV2, AAV5, etc) or a mixture of several (e.g. AAV-DJ). |
| ANOVA | Analysis of variance |
| ArchT | Archaerhodopsin from *Halorubrum* strain TP009 |
| BZ / BG-MThal | Basal ganglia recipient zone of motor thalamus (e.g. VM, VA, VLa) |
| CAG | Hybrid "promoter" consisting of the cytomegalovirus (CMV) early enhancer fused to the chicken beta-actin promoter and rabbit beta-globin |
| Calb1 | Calbindin 1 (Calbindin D-28K) |
| CaMKII | Calcium/calmodulin dependent protein kinase II promoter |
| ChR2 | Channelrhodopsin-2, a rhodopsin from Chlamydomonas reinhardtii |
| CMV | Cytomegalovirus promoter |
| Cre | Cre recombinase enzyme which catalyzes the site-specific recombination of DNA between loxP sites in DIO or FLEX switches to allow transcription |
| CTIP2 | Chicken ovalbumin upstream promoter transcription factor-interacting protein 2 |
| CZ / CB-MThal | Cerebellar recipient zone of motor thalamus (e.g. Vim, VL, VLp) |
| D1-MSN | D1-receptor expressing medium spiny neuron |
| D2-MSN | D2-receptor expressing medium spiny neuron |
| DAPI | 4′,6-diamidino-2-phenylindole |
| DCN | Deep cerebellar nuclei. |
| DIO | Double-floxed inverse orientation |
| Ef1a | Elongation factor 1-alpha promoter |
| EP | Entopeduncular nucleus. Rodent analogue of primate globus pallidus pars interna. |
| eYFP | Enhanced yellow fluorescent protein |
| FLEX | Flip excision switch |
| FR1 | Fixed-ratio 1 schedule. Reinforcer earnt per single lever press. |
| FR3/2s | Fixed-ratio 3 / 2 seconds schedule. Reinforcer earnt when three lever presses are initiated within any 2 second window. |
| GABA | Gamma-aminobutyric acid. An inhibitory neurotransmitter. |
| GAD67 | Glutamic acid decarboxylase 67. Marker for inhibitory GABAergic neurons and their projections. |
| GFP | Green fluorescent protein |

| | |
|---|---|
| GPi | Globus pallidus pars interna. The major basal ganglia output nucleus in primates. |
| Kir2.1 | Inward-rectifier potassium channel 2.1 |
| M1 | Primary motor cortex |
| M2 | Secondary motor cortex (rodent) |
| mCherry | A type of red fluorescent protein |
| MThal | Motor thalamus |
| NA | Numerical aperture |
| PB3 | Percentage of pressing bouts with ≥ 3 presses |
| S1, S2, etc | Specific FR3/2s training session (Session 1 – Session 14) |
| SEM | Standard error of the mean |
| SNr | Substantia nigra pars reticulata. The major basal ganglia output nucleus in rodents. |
| STN | Subthalamic nucleus |
| TRN | Thalamic reticular nucleus. |
| VA | Ventral anterior thalamic nucleus |
| Vglut2 | Vesicular glutamate transporter 2. Marker for glutamatergic axons arising from subcortical nuclei. |
| VL | Ventral lateral nucleus of the thalamus |
| VM | Ventral medial nucleus of the thalamus |
| Wfs1 | Wolframin syndrome 1 transmembrane ER glycoprotein |

# 1. Introduction

Motor skills are task-specific learned motor sequences critical for goal-directed behaviour such as speech or playing a musical instrument. Motor skill learning refers to the process by which temporally ordered movement sequences are prepared and executed with increasing speed and accuracy (Willingham, 1998). Sudden or progressive impairment of motor skills and/or onset of unwanted movements are seen in a range of devastating neurological and psychiatric disorders (e.g. stroke, movement disorders, obsessive-compulsive disorder, Tourette syndrome) at great cost to individuals, their families and society. Systematically improving our understanding of how and when manipulating specific brain areas affects motor performance and the acquisition of skills may facilitate novel strategies for neuromodulation, neuroprosthetic control and neurorehabilitation (Cagnan et al., 2019; Patel and Lieber, 2019).

Neural activity patterns associated with both normal motor control and movement disorders are distributed across brain networks known to be interconnected via a deep brain structure called the thalamus (Hwang et al., 2017). In particular, the motor thalamus – which consists of several adjacent ventral thalamic nuclei – receives widespread input from motor-related subcortical areas (basal ganglia and cerebellum) and has reciprocal connections to cortical circuits important in disorders of movement and cognition (Figure 1.1) (Albin et al., 1989; Redgrave et al., 2010; Lanciego et al., 2012; Guo et al., 2018; Aoki et al., 2019). Despite the privileged connectivity of the motor thalamus, its clinical utility has remained restricted to being a target for treating tremor (or rarely focal dystonia) for decades and very little progress has been made on understanding how its computations relate to motor behaviour (Bosch-Bouju et al., 2013; Goldberg et al., 2013; Crossman and Obeso, 2016). Here, I will summarise what is currently known about the motor thalamus with respect to its anatomical connectivity, physiological activity and potential role in motor behaviour.

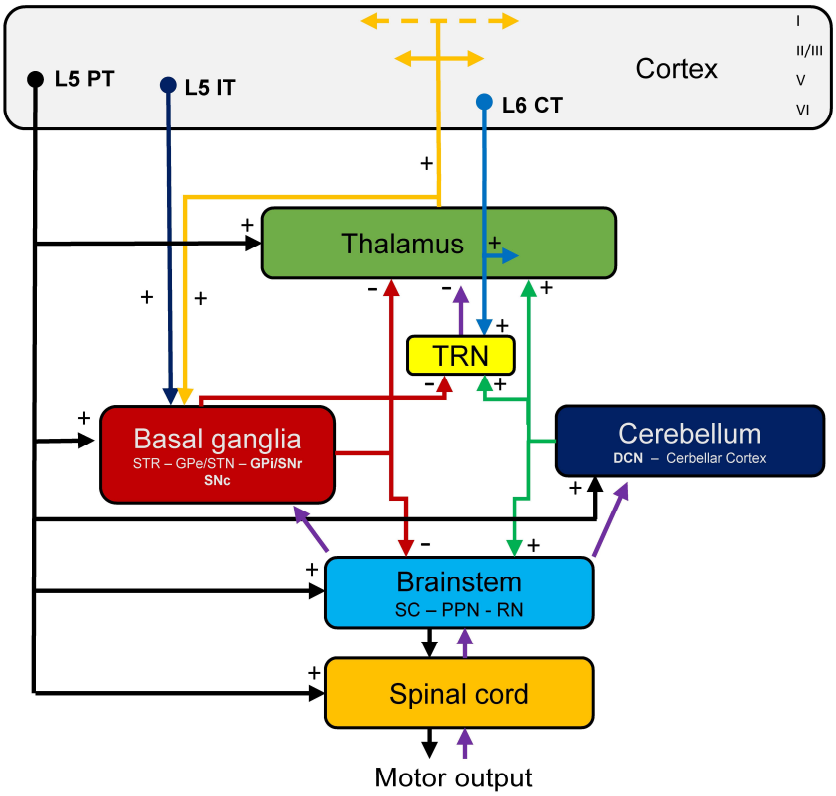



**Figure 1.1 Schematic of salient connections in cortico-basal ganglia-thalamocortical and cortico-cerebellar-thalamocortical loops.**

Branching of individual axons means a single neuron can influence multiple structures, though how this same information is differentially transformed at each target site and their relative importance to a specific aspect of ongoing behaviour is challenging to dissect. DCN, deep cerebellar nuclei; GPe, globus pallidus pars externa (globus pallidus in rodents); GPi, globus pallidus pars interna (entopeduncular nucleus in rodents); L5PT, Layer 5 pyramidal tract neurons; L5IT, layer 5 intratelencephalic neurons (projections to contralateral striatum/cortex not shown); L6 CT, layer 6 corticothalamic projection neurons; PPN, pedunculopontine nucleus; RN, red nucleus; SC, superior colliculus; STR, striatum (caudate-putamen in primates); SNc, substantia nigra pars compacta; SNr, substantia nigra pars reticulata; STN, subthalamic nucleus; TRN, thalamic reticular nucleus. (Based on Albin et al., 1989; Redgrave et al., 2010; Guo et al., 2018; Aoki et al., 2019).

## 1.1 The motor thalamus: anatomy and connectivity

The thalamus is a midline, symmetrical deep brain structure conserved across mammals, reptiles and birds (Butler, 2008). It has a common structure of dorsal and ventral nuclei (composed mostly of glutamatergic neurons) flanked by a lateral shell of GABAergic inhibitory neurons (the thalamic reticular nucleus; TRN). However, there are large number of nuclei with distinct anatomical connectivity and functional properties, and only a small number of nuclei support the canonical 'relay' function attributed to the thalamus (Sherman and Guillery, 1996). Today, thalamic nuclei are commonly classified as being first order or higher order nuclei depending on the nature of the afferents they receive. Those nuclei receiving 'driver' input (i.e. large axon glutamatergic input to proximal dendrites or perisomatic zones of thalamic neurons capable of reliably generating action potentials) from subcortical regions are considered first order thalamic 'relay' nuclei. Those nuclei receiving driver input from the cortex are termed higher-order nuclei and are thought to actively participate in cortical functioning by facilitating cortico-cortical information transfer (Sherman, 2016). Motor thalamus does not fit neatly into this classification given substantial input from cortex, cerebellum and basal ganglia (Bosch-Bouju et al., 2013). In primates, thalamic nuclei contain a mixture of calbindin-1 expressing 'matrix' neurons, which target superficial layers of cortex, and parvalbumin expressing 'core' neurons which target deeper cortical layers (Jones, 2001). The limitations of these existing classification systems, which do not demand understanding of complete input-output functional connectivity schemes of individual thalamic neurons ('thalamocortical motifs') is becoming clear in the modern search to understand what their effect on cortical computations might be (Halassa and Sherman, 2019).

### *1.1.1 Parcellation of motor thalamus by subcortical inputs*

A practical definition of the motor thalamus is the region in the ventral thalamus which is both i) the major receiver of basal ganglia and cerebellar afferents and ii) the major origin of projections to the motor cortex (Hintzen et al., 2018). It is conveniently parcellated in rodents and primates by

immunoreactivity for GAD67+ (marking GABAergic basal ganglia afferents) and VGLUT2+ (marking subcortical glutamatergic afferents from deep cerebellar nuclei) (Figure 1.2) (Kuramoto et al., 2011; Rovo et al., 2012). Unfortunately, these immunohistochemically defined zones do not adhere to the classic borders of thalamic nuclei defined over the last century by Nissl staining. In rodents, where the largest basal ganglia output nucleus is the substantia nigra pars reticulata (SNr), Nissl borders parcellate the motor thalamus into ventral medial (VM) and ventral antero-lateral (VAL) nuclei (Paxinos and Watson, 1996). In general, VM receives mostly SNr input while the more rostral part of VAL ("VA") receives SNr and entopeduncular nucleus (EP) input, and the more caudal part of VAL ("VL") receives cerebellar input. As such, some authors have favoured a functional parcellation of ventral motor nuclei into simply a basal ganglia-recipient zone (BZ) or cerebellar-recipient zone (CZ) (Nakamura et al., 2014).

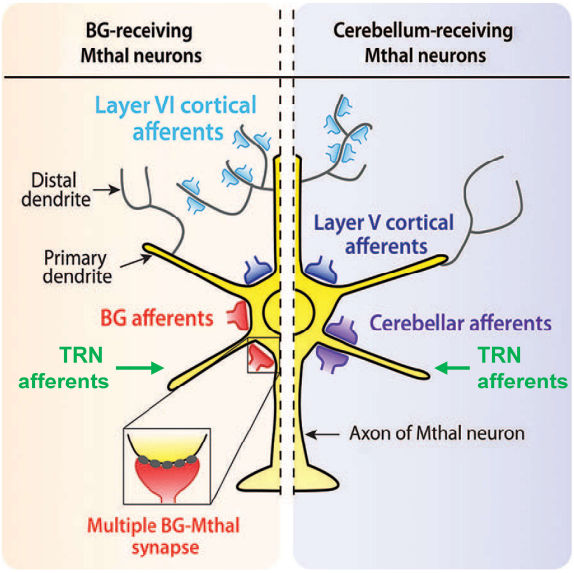



**Figure 1.2 Afferent inputs to motor thalamus neurons.** Basal ganglia inputs are axo-somatic, whereas others are axo-dendritic. Layer V (5) input innervates perisomatic areas and proximal dendrites, cerebellar input innervates proximal dendrites and Layer VI (6) input innervates distal dendrites. Input from layer 5 or layer 6 cortical projection neurons is typically used to differentiate between higher order and first order thalamic nuclei, but the situation is less clear in motor thalamus. Inhibitory input from

the thalamic reticular nucleus can also powerfully control spike rate (image adapted from Bosch-Bouju, 2013).

In human and non-human primates, where the major basal ganglia output nucleus is the globus pallidus pars interna (GPi), many more classification schemes exist based on Nissl staining and have been variably adopted (Krack et al., 2002) (Figure 1.3). In non-human primates, the medial magnocellular part of VA receives SNr input (VAmc), while the larger lateral parvocellular VApc and VLo receives GPi input, while cerebellar input goes to VPLo, VLc, and Area X (Vitek et al., 1994; Vitek et al., 1996). In human motor thalamus surgery, only the cerebellar-receiving thalamus is commonly targeted for movement disorders (usually tremor) and often referred to as Vim thalamus (equivalent to posterior VL). Single neuron tracing studies in rodents suggest that the same basal ganglia efferents targeting VA/VM also ascend to target the intralaminar (i.e. centromedian, parafasicular, paracentral and centrolateral nuclei) and mediodorsal nuclei which predominantly project to striatum and prefrontal cortex respectively (Kha et al., 2000; Cebrian et al., 2005). Equally, cerebellar nuclei efferents additionally target the lateral dorsal thalamus and intralaminar nuclei projecting to visual cortex and striatum respectively (Chen et al., 2014). Additionally, there may be species specific inputs to motor thalamus from subthalamic nucleus (Rico et al., 2010) and midbrain dopaminergic neurons (Sanchez-Gonzalez et al., 2005).

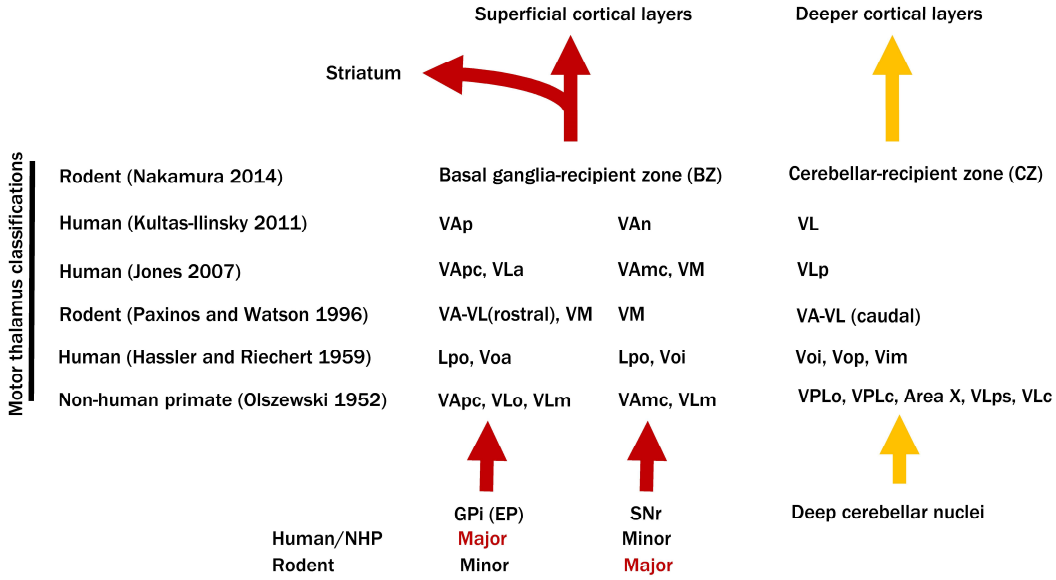



**Figure 1.3 Motor thalamus classification systems across species organised based on predominant input from either basal ganglia or cerebellar nuclei.** EP, entopeduncular nucleus; LP, lateral posterior thalamic nucleus; Lpo, lateropolaris; NHP, non-human primate; SNr, substantia nigra pars reticulata; VA, ventral anterior thalamic nucleus; VAp, ventral anterior thalamic nucleus, pallidal part; VApc, ventral anterior thalamic nucleus, parvocellular part; VAmc, ventral anterior thalamic nucleus, magnocellular part; VAn, ventral anterior thalamic nucleus, nigral part; Vim, ventral intermediate nucleus; VL, ventral lateral thalamic nucleus; VLa, ventral lateral anterior nucleus (Jones) = VLo (Olszewski); VLc, ventral lateral thalamic nucleus, pars caudalis (Olszewski) = VLp (dorsal part) (Jones); VLo, ventral lateral thalamic nucleus, pars oralis (Olszewski) = VLa (Jones); VLp, ventral lateral posterior nucleus (Jones); VLps, ventral lateral thalamic nucleus, pars postrema (Olszewski) = VLp (posterodorsal part) (Jones); VM, ventromedial thalamic nucleus; Voa, ventralis oralis anterior; Voi, ventralis oralis interus; Vop, ventralis oralis posterior; VPLa, ventral posterior lateral nucleus, anterior division (Jones) = VPLc (Olszewski); VPLc, ventral posterolateral thalamic nucleus, pars caudalis (Olszewski) = VPLa (Jones); VPLo, ventral posterolateral thalamic nucleus, pars oralis (Olszewski) = VLp (ventral part) (Jones). (Olszewski, 1952; Hassler and Riechert, 1959; Hirai and Jones, 1989; Paxinos and Watson, 1996; Jones, 2007; Kultas-Ilinsky et al., 2011; Nakamura et al., 2014)

### *1.1.2 Parcellation of motor thalamus by output targets*

At a gross anatomical level, BZ and CZ differ considerably in the density of their axonal projections to different cortical areas and the laminar distribution of their axonal terminals (Figure 1.4). Single neuron tracing studies show that axons of BZ thalamic neurons project densely to neocortical layer 1 over a wide area of prefrontal cortex and motor cortex, and arborise in dorsal striatum (Kuramoto et al., 2009; Garcia-Munoz and Arbuthnott, 2015; Kuramoto et al., 2015). In contrast, CZ neurons preferentially target cortical layers 3-5 in primary motor and somatosensory cortex (Kuramoto et al., 2009; Kuramoto et al., 2015). This general organisation in similar in non-human primates (McFarland and Haber, 2000; McFarland and Haber, 2002). Consistent with these findings, cholera toxin B-based retrograde tracing of primary and secondary motor cortex inputs lead to more retrogradely labelled neurons in VL and VM respectively (Hooks et al., 2013). The distinction on the basis of striatal projections, however, is not supported by a recent monosynaptic retrograde tracing study with modified rabies virus in the mouse dorsal striatum revealed input from VM, VA and VL thalamus to medium spiny neurons (D1 and D2) and ChAT interneurons (although the largest input was from intralaminar thalamus as expected) (Hoover and Strick, 1999; Hunnicutt et al., 2014; Guo et al., 2015b).

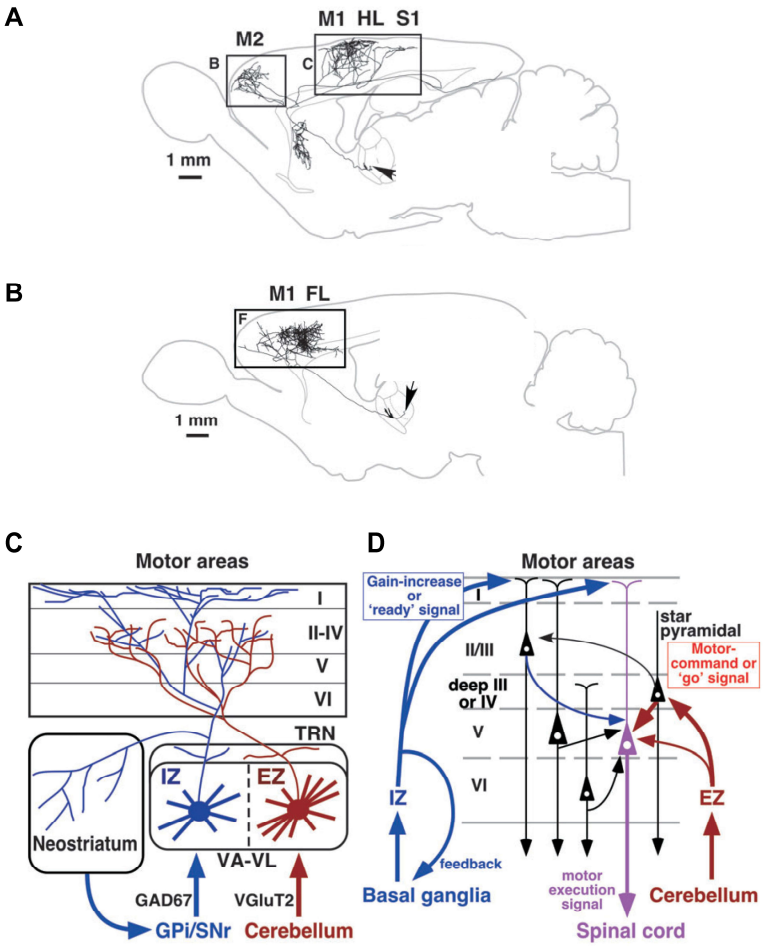



**Figure 1.4 Projection patterns of motor thalamic neurons. (A) and (B)** Example single sagittal plane neuron axonal reconstruction of thalamocortical neurons in basal ganglia- (inhibitory zone, IZ) and cerebellar-recipient (excitatory zone, EZ) parts of rat motor thalamus, respectively. Note the widespread, superficial targeting of cortex by the IZ neuron relative to more focal, deeper layer projection of EZ neuron. **(C)** Schematic summary of projection patterns of IZ and EZ neurons. **(D)** Schematic of cortical pyramidal neuron elements potentially targeted by IZ and CZ neurons (image adapted from Kuramoto et al. 2009).

Motor thalamus neurons may receive afferents from layer 5 and layer 6 corticothalamic neurons, GABAergic input from thalamic reticular nucleus, and either glutamatergic cerebellar or GABAergic basal ganglia afferents (Kakei et al., 2001; Kultas-Ilinsky et al., 2003). The location of

cerebellar, basal ganglia and layer 5 corticothalamic inputs on proximal dendrites of MThal neurons indicate they are all likely to have a powerful effect on spiking activity (Kakei et al., 2001). Basal ganglia and cerebellar input is generally assumed to target distinct motor thalamus neuron populations, but some neurons (particularly in border regions) do receive input from both systems raising questions about the utility of such an interaction prior to reaching cortex (Hintzen et al., 2018). Layer 5 input to motor thalamus is from pyramidal tract neurons which also target other subcortical motor nuclei (e.g. striatum, SNr, STN) on their way to spinal cord. There is some uncertainty as to whether layer 5 corticothalamic neurons only synapse onto BZ neurons in motor thalamus (as seen with other higher order thalamic nuclei) or also target CZ neurons, largely because anatomical studies to date have used either Nissl borders to parcellate thalamus and layer 5 specific tracing in transgenic mice only targets sub-populations of layer 5 neurons. Recent tracing studies agree with the only available *in vivo* recordings that suggest layer 5 output targets BZ and not CZ, whereas layer 6 output targets the distal dendrites of both BZ and CZ neurons (Sawyer et al., 1994; Jeong et al., 2016). The role of layer 6 inputs to the distal dendrites of MThal neurons is less clear, but interestingly their branches also target thalamic reticular nucleus (TRN) neurons, which in turn send GABAergic inhibitory projections to thalamic neurons. Although cortico-basal ganglia-thalamocortical loops are largely thought to exist as parallel circuits that process limbic, associative and sensorimotor information separately (Figure 1.5) (McFarland and Haber, 2002; Galvan et al., 2015; Guo et al., 2018) recent evidence suggests that motor thalamus is also involved in an open cortico-subcortical loop facilitating limbic control over motor loops (Aoki et al., 2019).

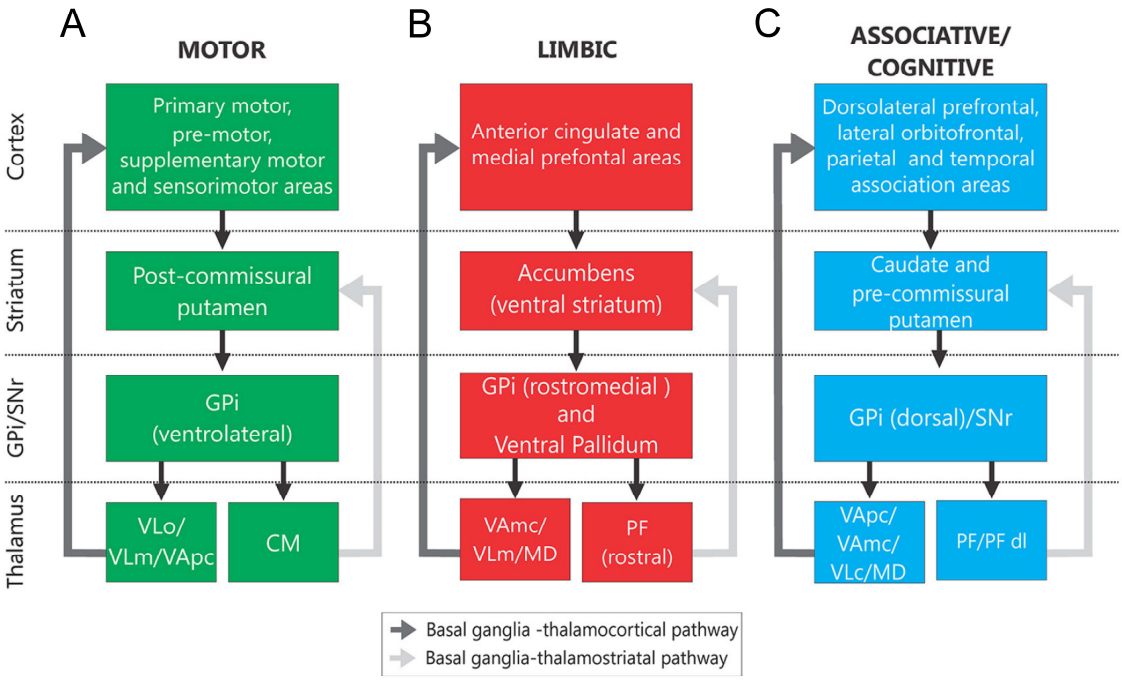



**Figure 1.5 Parallel cortico-basal ganglia-thalamocortical loops. (A)** The motor loop flows through frontal cortex, post-commissural putamen (dorsolateral striatum in rodents), ventrolateral GPi (entopeduncular nucleus and substantia nigra pars reticulata in rodents) and to motor thalamus (thalamo-cortical projecting) or centromedian (CM) nuclei (thalamo-striatal projecting). **(B)** The limbic loop flows through medial frontal cortex, ventral striatum, rostromedial GPi and ventral pallidum (entopeduncular nucleus, substantia nigra pars reticulata, and ventral pallidum in rodents) and to motor thalamus, mediodorsal thalamus or parafascicular thalamus. **(C)** The cognitive loop flows from lateral frontal areas to the caudate/pre-commissural putamen (dorsomedial striatum in rodents), GPi/SNr, motor thalamus (VA-VL)/mediodorsal thalamus (MD) or parafascicular thalamus (PF). GPi, globus pallidus pars interna; SNr, substantia nigra pars reticulata. Adapted from Galvan et al., 2015.

## 1.2 Motor thalamus: physiology

### *1.2.1 Intrinsic firing properties of motor thalamus neurons*

Thalamocortical neurons are excitatory and exhibit either tonic or burst firing of action potentials. The tonic firing mode encodes information via the timing of individual spikes such that frequency is proportional to signal strength (Bosch-Bouju et al., 2013; Halassa and Acsady, 2016). A burst of spikes significantly increases the probability of neurotransmitter release and thus increases the reliability of synaptic transmission (Lisman, 1997). In the burst firing mode, high frequency bursts of 3-5 spikes (termed low threshold calcium spike [LTS] bursts) occur following a prolonged period of hyperpolarisation below -70 mV (Bosch-Bouju et al., 2013). This period of hyperpolarisation is required to de-inactivate the CaV3.1 α-1 subunit T-type calcium channels expressed by thalamocortical neurons making them responsive to depolarising events, which then cause the T-type channel to briefly open and allow influx of calcium ions ($I_T$ calcium current) further depolarizing the membrane. This leads to activation of voltage-gated sodium channels and generation of action potentials. Because the membrane potential of thalamic neurons remains depolarized by the T-type calcium channels for a relatively long duration (∼50 ms) a burst of action potentials occurs, characteristic of LTS bursts. The T-type channel then inactivates and the gate closes, permitting repolarization of the membrane potential.

One function of LTS bursts during awake states may be to trigger state changes such as between inattentive rest and active movement, though there is growing evidence that bursts also allow complex coding of information (Mease et al., 2017). Although bursts have been seen in the thalamus in awake animals, only tonic firing has been shown in the motor thalamus of awake monkeys while LTS-like events occur during skilled reaching in rats (Bosch-Bouju et al., 2014). In the songbird homolog of basal ganglia-recipient motor thalamus, the dorsolateral division of the medial thalamus (DLM), LTS bursts can be induced by GABAergic synaptic events coming from the basal ganglia output Area X *in vitro* (Luo and Perkel, 1999).

*1.2.2 Task-related activity of motor thalamus neurons*

Despite the complex ways in which motor thalamus neurons may be modulated by cortical and either inhibitory or excitatory subcortical inputs, some consistent findings regarding the contextual and topographic nature of their firing do exist. While initial primate studies were unclear (Anderson and Turner, 1991), later work showed that somatotopic territories in response to either passive or active movement are present in some (VLo, VPLo, VLc) but not other (VA, Area X) motor thalamus areas and this pattern also determined likelihood of eliciting movements due to microstimulation. Neurons in VLo, VA and Area X were much more likely to respond with active movement compared to areas with more proprioceptive driving (VPLo and VLc) (Vitek et al., 1994; Vitek et al., 1996). Microstimulation of VA and VL thalamus in primates under ketamine anaesthesia showed that only the latter reliably evoked movements, which were often multi-joint (Miall et al., 1998). Activity in a small proportion of both pallidal and cerebellar-receiving human thalamus neurons was directly related to phantom upper extremity movements in an amputee, and to imagined movements (Anderson et al., 2011). MThal firing rate in control rats is modulated in a temporally precise pattern during reach-to-grasp movements, with a peak at the time of the reach-end and troughs just before and after it. LTS-like events were rare, but also modulated, decreasing in incidence just after reach-end (Bosch-Bouju et al., 2014). In a nose poke decision making task, motor thalamus neurons in rats were shown to respond to action onset, delay period and reward consumption (Gaidica et al., 2018). Recently, two-photon calcium imaging of thalamocortical axonal activity in the motor cortex of mice learning a self-initiated lever-pull task has found that layer 1 axons exhibit activity at lever-pull initiation and termination, while layer 3 axons did so at lever-pull initiation (Tanaka et al., 2018). Optogenetic stimulation of the substantia nigra pars reticulata activated more L1 than L3 axons, whereas deep cerebellar nuclei stimulation did the opposite (Tanaka et al., 2018). Lastly, activity of VM calbindin1-positive cells is high in wake and rapid eye movement (REM) sleep and low in non-rapid eye movement (NREM) sleep, and increases before cortical activity at the sleep-to-wake transition (Honjoh et al., 2018). Furthermore, optogenetic stimulation of VM cells rapidly awoke all mice from NREM sleep and consistently caused electrocorticograph (EEG) activation during slow

wave anaesthesia but could not waken mice from REM sleep. As such, motor thalamus activity seems to correlate with a range of behavioural phenomena, but whether the computations it performs are essential to them remains unclear.

### *1.2.3 Basal ganglia (BG) modulation of motor thalamus neurons*

Although early models of basal ganglia function posit that the motor thalamus (and inhibitory control of its activity by basal ganglia output) is critical for voluntary movement, the lack of motor deficits in humans following thalamotomy or pallidotomy suggest otherwise. Nonetheless, how the BG thalamic pathway communicates task-related information remains unclear (Goldberg et al., 2013). The BG-thalamic projection is composed of GPi/SNr GABAergic neurons that fire at high tonic rates at rest and terminate on soma of thalamocortical relay neurons and, in some species, distal dendrites of thalamic GABAergic interneurons in some species (Ilinsky et al., 1997). One theory suggests the high tonic firing rate of BG output neurons normally prevents thalamic neurons from responding to excitatory inputs (e.g., from cortex), but a task-related pause in BG output would act as a disinhibitory opening of the gate allowing a temporally-coordinated task-related activation of thalamus (Albin et al., 1989). Although strong inhibitory effects of individual BG efferents onto thalamic neurons allowing entrainment of thalamic spiking to the inter-spike intervals of BG efferents have been observed in the birdsong circuit, this has a unique anatomy and unlikely to be the case in rodents and primates (Goldberg et al., 2012).

A competing theory hypothesizes that transient task-related increases in BG output may hyperpolarise thalamic neurons causing activation in the form of rebound firing of low threshold spikes (Person and Perkel, 2005). This idea is supported by evidence that i) inactivation of BG output does not abolish task-related activity in the BG-recipient thalamus (Inase et al., 1996), ii) task-related increases in firing are far more common in both BG-output neurons (Mitchell et al., 1987) and BG-recipient thalamus (Anderson and Turner, 1991); and iii) that the task-related activity in BG output

neurons does not clearly lead that in the BG-recipient thalamus (Turner and Anderson, 1997). Recently, it has been shown that synchronized optogenetic stimulation of entopeduncular nucleus GABAergic terminals in motor thalamus can produce rebound firing (although unclear if single spikes or bursts) which are also dependent on T-type calcium channels and have a strong impact on downstream motor circuits producing parkinsonian-like rigidity and akinesia (Kim et al., 2017). While this suggests inhibitory BG input can generate excitatory motor thalamus-motor cortex responses in mammals, it is unclear if this the type of synchronised BG firing occurs in normal physiological circumstances to produce voluntary movements. Nonetheless, although studies support the idea that striatal direct and indirect pathway activation cause a net increase or decrease thalamic activity respectively (Lee et al., 2016), recent evidence suggests these pathways are likely to be co-active during voluntary behaviour (Tecuapetla et al., 2014) presumably producing a more complex activity pattern in motor thalamus. These findings have led some to suggest that BG output only modulates thalamic activity and corticothalamic input may actually serve as the primary driver of spiking. How this might be altered during skill learning compared to execution of well learnt behaviour is also currently unknown.

### *1.2.4 Cerebellar modulation of thalamocortical neurons*

In contrast to the inhibitory input from the basal ganglia, cerebellar input to the thalamus is excitatory and modulated by glutamate. *In vitro* work suggests that cerebellar dentate input to the thalamus targets VM, VL and CL nuclei in a slightly different dendritic location (Gornati et al., 2018) and VL neurons show more robust responses to optogenetic stimulation of cerebellar terminals than neurons in VM or CL. *In vivo*, the net effect of silencing cerebellum is a drop off in cortical firing rate (presumably through reduced drive of first order thalamocortical neurons) and the opposite effect is seen when excited (Gao et al., 2018; Chabrol et al., 2019). Furthermore, it is also known that cerebellar input to thalamostriatal neurons in intralaminar thalamus can directly modulate activity in the striatum (Chen et al., 2014; Xiao et al., 2018).

### *1.2.5 Corticothalamic modulation of thalamocortical neurons*

*In vivo* intracellular recordings in motor thalamus of urethane-anaesthetised rats show that stimulation of cerebellar afferents produces strong fast excitatory events in motor thalamus neurons with a shorter rise time than after ipsilateral motor cortex stimulation suggesting that cortico-thalamic terminals are more distally located (Sawyer et al., 1994) and thus likely to be layer 6 in origin. In primates, optogenetic stimulation of layer 5 and 6 corticothalamic projections in awake monkeys resulted in long-latency increases or decreases in firing of BG-MThal and CB-MThal neurons suggesting the simultaneous recruitment of intrathalamic GABAergic circuits from reticular thalamus and GABAergic interneurons, rather than predominantly driving thalamocortical spiking (Galvan et al., 2016). As such, while layer 5 input may be the main driver this will be difficult to test experimentally in primates while obscured by the TRN-mediated effects of layer 6 co-activation. Recently, photoinhibition of anterolateral motor cortex in mice was found to significantly decrease the activity of VM/VAL neurons supporting the idea that cortico-thalamic driver input does exist (Guo et al., 2017).

### *1.2.6 Thalamic reticular nucleus (TRN) modulation of thalamocortical neurons*

Until recently, TRN function was rarely discussed in the context of basal ganglia or cerebellar modulation of cortex but it may be a powerful, indirect route by which they can modulate motor thalamus activity. TRN inhibition is a scalable system that controls thalamic spike rates across behavioural states and cognitive needs, whereas extrathalamic inhibition (e.g. basal ganglia, zona incerta) likely impacts spike timing in well-defined thalamic regions and limited behavioural contexts (Halassa and Acsady, 2016). Through this mechanism dependent on cortical layer 6 output to thalamus, TRN could gate or recruit thalamocortical input with changing cognitive demands. One study (Lam and Sherman, 2015) demonstrates that TRN inputs to VA/VL are topographic and overlap with those to CL, but that some, presumably higher order neurons, received input from a

greater spread of TRN neurons while others received unitary input. Furthermore, they demonstrated that stimulation of VA/VL produced disynaptic inhibition in neighbouring thalamic nuclei via TRN although the purpose of this is unclear. Interestingly, deep cerebellar nuclei neurons, basal ganglia indirect pathway GPe neurons, and output SNr neurons all target the TRN, although it is unclear if the TRN neurons they contact modulate VA/VL or completely different thalamic nuclei (Cavdar et al., 2002; Gulcebi et al., 2012). Again, this may provide another mechanism for recruiting more cortical neurons or increasing the susceptibility of thalamocortical spike-timing to other dimensions of basal ganglia activity. While indirect pathway activation would presumably increase TRN bursting and hence thalamic inhibition, TRN neurons are known to laterally inhibit their neighbours, hence could provide a route for basal ganglia to modulate thalamic firing rate while the direct inputs from GPi/SNr to BZ modulate spike timing. This may also potentially account for dramatic behavioural effects of optogenetic GPe stimulation reported by some (Mastro et al., 2017). What is less clear is whether a combination of TRN and extrathalamic inhibitory output is aimed at altering spike timing, mean firing rate or inducing LTS bursting. Indeed, the first evidence of basal ganglia-TRN effects *in vivo* suggests the system can be used to bias attention to auditory or visual cues by adjusting the relative activity in auditory or visual thalamic nuclei (Horisawa et al., 2019).

### *1.2.7 Motor thalamus modulation of downstream targets*

Basal ganglia modulation of cortex has been assumed by classic models to drive cortical activity and hence movement, but evidence of feed-forward effects in motor cortex has only recently been published (Oldenburg and Sabatini, 2015). As expected, optogenetic stimulation (light-on continuously for 2 seconds) of striatal D1-receptor expressing ('direct pathway') medium spiny neurons (MSN) results in an excitatory response in motor cortex for the entire duration of stimulation (~80% increase). However, while D2-receptor expressing ('indirect pathway') MSN stimulation resulted in a ~50% decrease in firing rate in motor cortex, there was also a transient excitatory response at light onset and offset seen in a subpopulation (~30%) of motor cortex units, and they

were more superficially located than those without this response (550-610 μm vs. 830-910 μm). Even though the synchronous input as generated by optogenetic stimulation is unlikely to be physiological, taken together with other D1- and D2-MSN stimulation (20 s at 20 Hz) experiments showing opposite modulation of motor thalamus units that fail to produce opposing cortical responses (Lee et al., 2016), it suggests a more complex picture of basal ganglia influence on motor cortex than predicted by existing models.

The apical dendrites of pyramidal neurons in neocortical layer 2/3 and layer 5 are a major constituent of layer 1. The terminals of BZ neurons can form synapses with the spines of these apical dendrites in the outer half of layer 1, which can be clearly visualized by enriched labelling for the thalamic terminal marker VGlut2 (Rubio-Garrido et al., 2009). These thalamocortical synapses provide a mechanism through which BZ can potentially drive excitation in any population of cortical projection neuron. Indeed, monosynaptic retrograde tracing studies targeting CaMKIIa-Cre expressing excitatory neurons in primary and secondary motor cortex have shown the two biggest long-range inputs to be from somatosensory cortex (~57%) and motor thalamus (~8%) (Zhang et al., 2016). While inputs to inhibitory GABAergic neurons in motor cortex are not known, thalamocortical input constitutes a much higher proportion of total input to inhibitory neurons in other areas of cortex (Wall et al., 2016). In addition, the layer 1 dendritic spines of pyramidal neurons are highly plastic and are reorganized during motor learning (Xu et al., 2009), providing a substrate though which BZ neurons can contribute to cortical motor memory. While there is evidence for BZ terminals on layer 2/3 pyramidal neurons (Cruikshank et al., 2012), and generally onto CaMKII-Cre expressing excitatory neurons in motor cortex (Zhang et al., 2016), it has only recently been shown that they make monosynaptic connections with layer 5 projection neurons (Collins et al., 2018). The active intrinsic properties of L5 pyramidal neurons allow them to couple inputs arriving at the tuft and basal dendrites simultaneously. This mechanism could potentially facilitate the integration of superficial BZ and deeper CZ input in the motor cortex.

Interspersed with the pyramidal neuron apical dendrites in layer 1 are at least two populations of GABAergic interneuron, which have been investigated predominantly in sensory cortex. Extended neurogliaform cells (ENGCs) have multipolar dendrites and axonal arbors that are mostly contained within the outer half of layer 1 (Jiang et al., 2013; Lee et al., 2015). In contrast, single bouquet cells (SBCs) are more commonly located in the inner half of layer 1 and their axons project down into layer 2/3. Both types of layer 1 interneuron mediate complex effects on cortical microcircuits through both direct inhibition and disinhibition of layer 2/3 and layer 5 pyramidal neurons (Larkum, 2013). In line with this view, optogenetic terminal stimulation of matrix thalamocortical projections neurons in layer 1 of prefrontal cortex leads to fast excitatory post-synaptic potentials (EPSPs) in putative ENGCs, which mediate feedforward inhibition in layer 2/3 pyramidal neurons (Cruikshank et al., 2012).

CZ is considered to be a first order thalamic area and its neurons share several features of sensory thalamic relay nuclei. Although sensory thalamic nuclei send their densest thalamic input to layer 4 of sensory cortex, this granular layer is absent in frontal cortical areas. Recent work, however, has demonstrated the motor cortices do possess a functional layer 4 that receives monosynaptic input from CZ (Yamawaki et al., 2014) and that these neurons form unidirectional projections to neurons in layer 2/3. In addition, Yamawaki et al demonstrated that stimulation of CZ afferents produces a distinct activation peak in the lower part of layer 5, consistent with the large number of terminals from VL neurons (Kuramoto et al., 2009; Kuramoto et al., 2015). Indeed it has been shown that thalamocortical synapses in layer 5 show task-related post-synaptic plasticity in their connections with corticospinal neurons targeting the C8 level (forelimb muscles supply), but not those targeting the C4 level (neck muscle supply), after training in a forelimb reaching task (Biane et al., 2016). Monosynaptic retrograde tracing with modified rabies virus has also shown inputs from VL thalamus neurons to parvalbumin-, somatostatin- and vasoactive intestinal peptide-expressing GABAergic interneurons in barrel cortex (Wall et al., 2016).

In sensory transmission, there is a clear one-way drive of cortical activity by first order thalamic nuclei to accurately transfer transient sensory events to the cortex. Given the preserved somatotopy in human and primate CZ, one may again expect similar principles of functioning to sensory thalamus. In a recent study, Guo et al. showed that persistent activity (the neural correlate of motor preparation, working memory, decision making or other mental representation) in the anterior lateral motor cortex (ALM) normally occurring during the delay prior to a directional lick could be almost completely abolished (resulting in lick errors) by optogenetic stimulation of TRN-only or all GABAergic terminals (i.e. basal ganglia afferents to BZ and thalamic reticular afferents to both BZ and CZ) in the region of the motor thalamus in Vgat-ChR2-eYFP mice (Guo et al., 2017). Furthermore, in the same mice, optogenetic stimulation of cortical GABAergic neurons in the ALM abolished activity in motor thalamus, presumably due to a reduction in layer 5 driver input to motor thalamus. Critically, it was shown that intrinsic frontal cortex and corticocortical connections alone are not sufficient to produce persistent delay activity. In the frontal cortex at least, there is a continuous reverberation of activity between the cortex and thalamus that persistently maintains information in the cortex.

Given that recent *in vitro* work shows that MD but not VM neurons can elicit spikes in prefrontal cortex (Collins et al., 2018), much of the layer 5 ALM firing rate reduction following motor thalamus silencing may be primarily related to silencing first order CZ rather than higher order BZ activity. As such, it is it remains unclear if inhibiting BZ in isolation could disrupt persistent activity without abolishing cortical firing. Evidence supporting this possibility comes from two other recent studies of 'higher order' thalamic nucleus, both with only modest reductions in prefrontal cortical activity due to optogenetic silencing of mediodorsal thalamus but nonetheless significant task impairment. Schmitt et al found that cortical pyramidal cells displayed robust, rule-specific firing (attend to light or attend to sound) that was absent from the thalamic neurons they converge on during delay period-specific activity, suggesting that the output of thalamocortical neuron is not just a 'relayed' representation of its input but actually a novel signal generated in the thalamus (Schmitt et al., 2017). Bolkan et al also concluded that the role of the thalamus is not to make cortical cells fire but to

promote synaptic interactions among cortical cell ensembles, allowing the unfolding of synfire chains necessary to represent the actual rule (that is, attend to light or sound) explaining why augmenting MD thalamus activity led to better categorical representation in the cortex and augmented behavioural performance (Bolkan et al., 2017).

While it is likely that both BZ and CZ synapse onto both excitatory and inhibitory neurons in the cortex – it is unclear if the guiding principles of these connections favour improving centre signal and reducing surround noise. While this makes sense for CZ, who's internal topography is presumably maintained (albeit spatially expanded) in line with the cortical sensorimotor map, the situation is less clear for BZ which lacks somatotopy and is modulated by converging GABAergic inputs which represent already dimensionally reduced information passed through successively smaller basal ganglia nuclei. The function of a signal requiring a network to reach and synchronise such vast areas of cortex (conserved between species) is likely to be to global rather than specific (e.g. attention, value, urgency) (Garcia-Munoz and Arbuthnott, 2015; Thura and Cisek, 2017; Sieveritz et al., 2019).

### 1.3 Motor thalamus: skill execution and learning

A motor skill is defined by the ability to i) quickly identify an appropriate movement goal in a particular task context, ii) select the correct action and iii) execute that action with accuracy and precision. Motor learning refers to the diverse range of processes which underlie i) experience-dependent acquisition of a skill (and further improvements to asymptotic performance) and ii) skill maintenance under changing conditions. Although the main fascination in studying skill execution and motor learning surrounds expert skills like those possessed by professional athletes and musicians, most research focuses on more elementary forms of learning. Although simple, these tasks may provide fundamental insights into components of learning which may be important for

more impressive skills or the recovery of basic motor skills after brain injury. Different motor learning tasks stress improvement at one or more stages of goal selection, action selection or action execution. In general, they are categorized into tasks assessing motor adaptation (e.g. prism glasses, force field adaptation, visuomotor rotation adaptation), sequence learning (e.g. simple sequences, serial reaction time task, discrete sequence), *de novo* learning (e.g. arbitrary visuomotor association, mirror reversal learning, brain machine interface) and motor acuity (e.g. reaching and grasping).

Although motor learning may ultimately result in an implicit, procedural memory this does not mean only implicit processes were used in its construction – declarative (explicit) processes may have been important in the early stages. In general, the brain areas consistently implicated in various types of motor learning include the prefrontal cortex, premotor and motor cortex, basal ganglia, hippocampus and cerebellum (Doyon and Benali, 2005) . Despite being an important connecting site between many of these areas, the thalamus is generally omitted from most reviews on the topic of motor skill learning.

### *1.3.1 Neuroimaging evidence of motor skill learning-related activity*

Thalamic activity has been probed non-invasively using functional magnetic resonance imaging (fMRI) during motor tasks and particular motor learning paradigms. Though the fMRI blood-oxygen-level-dependent (BOLD) contrast signal has a temporal resolution of seconds and an uncertain relationship to neural activity, it has undeniably increased the ability to investigate physiological activity in humans during behavioural tasks. Several neuroimaging studies in the last 10-15 years have assessed thalamic BOLD activity during learning. One study undertook fMRI during extended one month practice of a known sequence of finger movements (Lehericy et al., 2005). The associative premotor territories of the basal ganglia, including the dorsal parts of the putamen and more rostral striatal areas, the anterodorsal globus pallidus, the corresponding output nuclei of the thalamus, as well as the STN, were active only during the early learning stage. In another finger tapping task, BOLD signal in premotor areas, the anterior putamen and the ventral

posterolateral thalamus increased regularly with increasing movement frequency and complexity. In rostral frontal areas, the caudate nucleus, the subthalamic nucleus and the ventral anterior/ ventrolateral thalamus, signal increased mainly during the complex task and the high frequency task (3 Hz) (Lehericy et al., 2006).

In another study, combined fMRI and repetitive transcranial magnetic simulation (rTMS) were used to investigate the intermanual skill transfer of a serial reaction time task using finger movements (Perez et al., 2007). The fMRI results showed that individuals who demonstrated better transfer to the left hand showed more activity in the supplementary motor area (SMA) and ventrolateral anterior (VLa) thalamic nucleus after. By contrast, activity in the ventrolateral posterior (VLp) thalamic nucleus, correlated with future successful transfer consistent with the view that the cerebellum has a role in procedure learning, particularly for the initial phases of acquisition when the time contingencies of the motor sequence need to be learned. The cerebellar input (via VLp) may condition trial-to-trial learning in a manner suitable to future transfer while the basal ganglia input (via VLa) may contribute to online adjustments required once the intermanual transfer process has already occurred (Birbaumer, 2007). In a similar vein, other groups have shown parallel contributions of basal ganglia and hippocampal processing to motor sequence learning (Albouy et al., 2008; Pinsard et al., 2019).

### *1.3.2 Lesion studies in human motor thalamus*

As transcranial magnetic stimulation can only transiently perturb function in more superficial brain areas, most human lesion studies attempt to draw conclusions from patients who have experienced a localised thalamic stroke, undergone thalamic deep brain stimulation or a unilateral thalamotomy. Although attempts to draw conclusions from small series of localised strokes have been made, in general the vascular territories are too broad to draw reliable conclusions about the role of specific thalamic nuclei while the lack of specific motor tasks also limits their utility (Carrera and Bogousslavsky, 2006). In one study that attempted to control for this as much as possible, patients

with chronic focal thalamic lesions showed reduced behavioural error detection and post-error adjustments in a task requiring fast, accurate pointing to an on screen target with the appropriate hand. When the lesions specifically affected the thalamic VA/VLa nuclei, these effects were pronounced and associated with complete absence of an error-related negativity signal on EEG. These results reveal that the thalamus, particularly its VA/VLa region, is a necessary constituent of the performance-monitoring network, anatomically well connected and functionally closely interacting with the anterior midcingulate cortex (Seifert et al., 2011). Despite this, a unilateral Vo complex thalamotomy is performed with good effect for patients with focal dystonia – often in patients who are professional musicians and go back to performing (Horisawa et al., 2019). In line with this, bilateral DBS of VA thalamus does not seem to cause major motor side effects (Maarouf et al., 2016). Cerebellar-receiving motor thalamus, by contrast, is much more frequently targeted clinically and again does not have any gross motor effects although fluency of speech may be affected. In a study of force field adaptation, patients with DBS-ON/thalamotomy of CZ showed impaired motor adaptation (Chen et al., 2006). It should be noted that bilateral thalamotomy is rarely performed, or if it is each side is lesioned several months apart due to the significantly higher risk of dysarthria and ataxia.

### *1.3.3 Lesion and optogenetic studies in the non-human primate and rodent*

The classical view of the role of basal ganglia input to thalamus is that an increase in direct pathway activity inhibits SNr and results in disinhibition of thalamocortical circuitry facilitating movement, whereas indirect pathway activation prevents movement by increasing SNr inhibition of thalamocortical projections to motor cortex (Oldenburg and Sabatini, 2015; Lee et al., 2016). However, this prediction has never been convincingly shown in rodents or primates during movement. Instead, the most consistent finding in GPi and motor thalamus recordings has been the co-activation of spiking activity either coincident or slightly after the onset of electromyograph (EMG) activity (Mitchell et al., 1987; Anderson and Turner, 1991). Furthermore, lesioning the GPi

(pallidotomy) in humans can restore normal movements to patients with both hyper- and hypokinetic movement disorders without producing the other (Piron et al., 2016). In addition to these long-standing basal ganglia paradoxes, it is now also clear that both direct and indirect pathways are concurrently active during movement, and subtle changes in the relative activity of one pathway over the other has the ability to exert profound effects on motor output (Tecuapetla et al., 2014). These findings suggest that while basal ganglia-thalamic signal may be important in regulating aspects of motor control, it is unlikely to be selecting routine motor programs and transmitting them to motor cortex for execution in primates. However, infusion of GABA-A receptor agonists into GPi of primates during reaching tasks have consistently shown that movement vigour (e.g. speed, amplitude, and frequency) is disrupted, rather than the constituent parts of the movement itself (Desmurget and Turner, 2010; Turner and Desmurget, 2010; Dudman and Krakauer, 2016). Two recent primate studies also suggest the basal ganglia send an urgency signal to cortex for actions which have already been planned there and facilitate the learning of new reward contingencies (Crossman and Obeso, 2016; Piron et al., 2016; Thura and Cisek, 2017).

Although the motor thalamus is an important node for propagating abnormal activity underlying movement disorder symptoms and thus also a clinically important target, clear evidence for its role in healthy motor performance and skill learning is lacking (Hikosaka et al., 2000; Turner and Desmurget, 2010; Goldberg et al., 2013; Kawai et al., 2015). Mammals exhibit akinesia / bradykinesia and their posture is acutely impaired following electrolytic lesions of VA, VLa, VLp and VM (but these tend to recover after several weeks) or thalamic injection of GABA receptor agonists or glutamate receptor antagonists (Di Chiara et al., 1979; Starr and Summerhayes, 1983a; Starr and Summerhayes, 1983b; Klockgether et al., 1986a; Klockgether et al., 1986b; Wullner et al., 1987; Canavan et al., 1989; Jeljeli et al., 2003). Large lesions of the VA, VLa and VLp nuclei produce acute ataxia and dysmetria in the contralateral arm of primates but again these recover (Bornschlegl and Asanuma, 1987). The VLa appears to be particularly important in learning motor tasks because large lesions that included the VLa severely impaired relearning in primates, whereas lesions confined to VA did not (Canavan et al., 1989). Results from lignocaine infusions into specific

motor thalamus nuclei imply that VPLo and VLo play a role in the production of movements in general regardless of whether they are internally generated or visually triggered, but that VPLo contributes more specifically to the execution of visually triggered and guided movements while area X contributes specifically to their initiation. By contrast, VApc appears to play a role in the execution of movements based on internal cues (van Donkelaar et al., 2000). Interestingly, activation of corticothalamic excitatory projections in motor thalamus does not have any acute behavioural effect in primates (Galvan et al., 2016).

VM lesions also impair forms of striatum-dependent learning such as retention of two-way conditioned active avoidance (Zis et al., 1984). In a recent study which found impairments in rotarod and single seed reaching (but not locomotion, water maze, or a two-lever choice task) after immunotoxin-mediated deletion of CL projecting DCN neurons, ibotenic acid lesion of bilateral rostral VA/VL thalamus (which received a larger DCN input than CL thalamus) did not impair rotarod or single-seed reaching success rate relative to sham control (Sakayori et al., 2019). In a head-fixed lever pull task, where mice had been trained over several sessions to pull a lever for > 600 ms to receive a water reinforcer, optogenetic silencing (3 min light-on, 3 min light-off for 30 min) of the contralateral motor thalamus in expert mice slightly impaired task performance, and excitatory lesions of either the thalamus or motor cortex before training caused a general failure to reach expert level performance (Tanaka et al., 2018) although the effect on recorded lever trajectory was not discussed. In a Parkinson's rat model, patterned (i.e. stimulation mimicking previously recorded neural activity during reaching) and theta burst stimulation but not any tonic optogenetic stimulation in motor thalamus improved reaching (Seeger-Armbruster et al., 2015). In a different head-fixed task, reducing the mean firing rate in unilateral motor thalamus, by driving the local activity in GABAergic terminals, during a directional licking task in mice caused a bias towards ipsilateral licking (Guo et al., 2017). In a different task in mice, optogenetic stimulation of VM thalamus triggered by a lever press resulted in acquisition of self-stimulation behaviour and muscimol blockade of VM reduced acquisition of D1-MSN optogenetic self-stimulation (Lalive et al., 2018) consistent with older studies showing electrical stimulation of rat VM or VL thalamus

supports intracranial self-stimulation (Clavier and Gerfen, 1982). Interestingly, more robust motor effects have been reported for parafascicular (Pf) thalamus where optogenetic silencing of Pf terminals in striatum causes a delay in initiation of lever press sequences (Diaz-Hernandez et al., 2018) and silencing of Pf thalamus in a mouse model of parkinsonism restores movement (Parker et al., 2016).

### 1.4 Summary

Voluntary performance of skilled movements is critical to goal-directed human behaviour and their recovery (or halting their loss) is a key goal in the treatment of neurological disorders. Skilled movements are generated by the joining together of movement sequences, in a process that has been thought to depend on activity in the basal ganglia, cerebellum and cortex to varying degrees depending on task demands such as dexterity, sequence complexity and timing. The motor thalamus has, by virtue of receiving major input from the basal ganglia and cerebellum, and reciprocal connections to motor cortical areas, long been assumed to play a key role in supporting cortically-dependent motor behaviour. Manipulation of motor thalamus activity has been shown to acutely impair dexterous skills such as reach and grasp which rely on corticospinal communication in primates and rodents. Due to the difficulty of separating cortical processes required for dexterity from those required for motor learning, non-dextrous motor skill learning has been more comprehensively studied in rodents, but the effect of motor thalamus lesions on patterns of basal ganglia-dependent (Jin and Costa, 2010; Santos et al., 2015) motor sequence acquisition has not been specifically studied. Here we aim to investigating the role of the motor thalamus in self-paced acquisition of non-dextrous complex motor sequences utilising acute and chronic circuit manipulations in mice.

It should be noted that for both basal ganglia and cerebellar output, the projections to the thalamus are one branch of an axon that also projects directly to lower order motor centres in the brainstem (e.g. pedunculopontine nucleus / mesencephalic locomotor region, red nucleus). Thus, it is unclear

which of the various normal functions attributed to the basal ganglia (or cerebellum) critically rely on thalamo-cortical more than direct brainstem information transfer. Indeed, optogenetic stimulation of the SNr and EP output fibres in brainstem have recently been reported to drive locomotion and rotatory behaviour respectively in rodents (Roseberry et al., 2016; Kim et al., 2017). Other skilled movements have also been shown to become retrievable directly from specific brainstem nuclei after learning in rodents (Esposito et al., 2014), and their related feedback circuitry identified (Azim et al., 2014). Indeed, this capacity may explain why decortication studies in lower mammals have repeatedly shown a seemingly normal basic movement repertoire provided that the basal ganglia remain intact (Kawai et al., 2015). We hypothesise that the signal received by motor thalamus (and on to cortex) is likely an efference copy of ongoing basal ganglia and cerebellar output to brainstem motor centres (Goldberg et al., 2013), presumably necessary for activities requiring conscious supervision of brainstem and spinal motor neuron output in response to the real-time discrepancy between predicted and actual motor outcomes (e.g. skilled movements of individual digits, rapid motor adaptation to unexpected situations and motor learning).

### 1.5 Specific Aims

1.5.1 *To confirm anatomically and functionally distinct basal ganglia and cerebellar receiving populations of motor thalamus neurons exist in mice.*

*1.5.2 To design a behavioural setup and task to monitor self-paced non-dextrous motor skill learning in mice.*

*1.5.3 To assess the impact of basal ganglia- and cerebellar-biased motor thalamus manipulations on self-paced non-dextrous motor skill learning in mice.*

# 2. Materials and Methods

## 2.1 Animals

Experimental subjects were adult (2- to 9-month-old) male C57BL/6J (Charles River Laboratories), Vglut2-IRES-Cre (C57BL/6J background; Jax Strain ID 028863) or PV-IRES-Cre (C57BL/6J background; Jax Strain ID 008069) mice. All mice were group housed in a 12 h light/dark cycle and all experiments were performed during the light cycle. Food and water was available ad libitum, except during behavioural training when food intake only was restricted. All animal procedures were performed in accordance with institutional guidelines and Animal (Scientific Procedures) Act 1986 (UK).

## 2.2 Viral Constructs

The following AAVs were used: AAV2-hSyn-ChR2(E123A)-eYFP (UNC vector core; $3.4x10^{12}$; Dr Karl Deisseroth), rAAV5-EF1a-DIO-hChR2(E123T/T159C)–eYFP (UNC Vector Core; 4.9 - 6.2 x $10^{12}$ vg/ml; Dr Karl Deisseroth), AAV5-Ef1a-mCherry-IRES-WGA-Cre (UNC vector core; 1.6 x $10^{12}$ vg/ml; Dr Karl Deisseroth), AAV5-CAG-FLEX-ArchT-GFP (UNC vector core; 8.2 x $10^{12}$ vg/ml; Dr Edward Boyden), AAV5-CAG-FLEX-GFP (UNC vector core; 4.5 x $10^{12}$ vg/ml; Dr Edward Boyden), and AAVDJ-CMV-DIO-Kir2.1-ZsGreen (Stanford vector core; 1 x $10^{13}$ vg/ml).

## 2.3 Stereotactic viral injections

Isoflurane (IsoFlo ®, induction 4%, maintenance 2%; Abbott Laboratories) in oxygen-enriched air (Novo Lite, Mark 5) was used to anaesthetize mice fixed in a stereotactic frame (Kopf Instruments 1430 series). A feedback-controlled heating pad (Harvard Apparatus) ensured

maintenance of core body temperature and eyes were covered with a thin layer of Lacri-lube (Allergan, UK). The scalp was cleaned with 0.5% chlorhexidine gluconate and 70% ethanol (Hydrex Clear, Ecolab). Marcaine (20 µl of 0.25% solution) was injected under the scalp for topical anaesthesia. Skin was incised and burr hole(s) drilled and pulled glass pipettes (15-20 µm tip microcapillary tube) were lowered to the target coordinates and virus manually pressure-injected at a rate of < 1 µl/min and the glass pipette was removed slowly no sooner than 8 minutes post-injection. Virus volume of 75 nl was used for all motor thalamus injections, whereas 150 nl was used in SNr and DCN. Coordinates for virus injections were: SNr (AP −3.3 mm, ML ± 1.6 mm, DV −4.5 mm), DCN (AP -5.9 mm, ML ± 2.4 mm, DV 2.2 mm), VM (AP -1.3 mm, ML ± 0.9 mm, DV 4.0 mm) and VL (AP -1.2 mm, ML ± 1.1 mm, DV 3.3 mm).

**2.4 Implant surgeries**

All surgeries used standard aseptic procedures. Mice (2–6 months old, males) were deeply anesthetized with isoflurane (by volume in O2; SurgiVet; Smiths Medical) and mounted in a stereotaxic apparatus (Kopf Instruments, California, USA). Mice were kept on a thermal blanket (Harvard Apparatus) and their eyes were covered with a thin layer of Lacri-lube (Allergan, UK). The scalp was cleaned with 0.5% chlorhexidine gluconate and 70% ethanol (Hydrex Clear, Ecolab). Marcaine (20 µl of 0.25% solution) was injected under the scalp for topical anaesthesia. A flap of skin, approximately 1 $cm^2$, was removed from the dorsal skull. The remaining gelatinous periosteum was removed. The skull was cleaned and dried with sterile cotton swabs and hydrogen peroxide solution. The bone was scored in a crosshatched pattern with a scalpel for better bonding with the glue. Skin edges were glued down using VetBond (3M, Minnesota, USA) and different protocols used for either fibre optic implants or head plate surgery at this point.

*Head plate implantation*

A burr hole for the cerebellar reference screw was drilled prior to covering the exposed skull with a thin layer of Precision cyanoacrylic glue (Bostick, UK) onto which the head bar was

positioned directly. Once stable, the cerebellar screw was passed though the appropriate rear hole in the headplate and screwed into bone. Once the glue was dry, silicone was applied within the centre well of the head plate to cover the midline and bregma as well as future craniotomy sites. Once this had set, Jet Denture Repair acrylic (Lang Dental, Illinois, USA) was added to cover any exposed areas of skull, the cerebellar screw, and the horizontal bar of the head plate. Once this was dry the mouse was removed from ear bars and allowed to recover. Close post-op monitoring was done for approximately 7 days.

*Optic fibre implantation*

Existing burr holes from previous virus injection surgery were re-drilled at the correct sites for VL-ArchT (AP -1.1 mm, ML 0.9 mm) or VM-ArchT (AP -1.3 mm, ML 0.9 mm) mice, as well as frontal and cerebellar burr holes for anchoring screws. With the anchoring screws in place, the optic fibre implant was then lowered to the appropriate depth (DV -3.3 mm for VM and -2.8 mm for VL). Jet Denture Repair acrylic was added to cover any exposed areas of skull, anchoring screws and the base of the fibre optic connector screw in several stages. When the cement had hardened, the implant tool was unscrewed from the implant and replaced with a plastic dust cap before removing the ear bars and allowing the mouse to recover. Close post-op monitoring was done for approximately 7 days.

### 2.5 *In vivo* anaesthetised electrophysiology and optogenetic stimulation

A C57/BL6 mouse injected with AAV-Ef1a-mCherry-IRES-WGA-Cre in SNr or DCN, and AAV-Ef1a-DIO-ChR2(E123T/T159C)-eYFP in motor thalamus, > 6-8 weeks previously was anesthetized with isoflurane. ECoG screws (1.0 x 3 mm) were implanted bilaterally over the frontal lobe (AP +2.0 mm, ML +2.0 mm) and references screws over the cerebellum. Bilateral craniotomies were performed over motor cortex (centred over the M1/2 border [AP +1.0 mm, ML 1.0 mm]). A burr hole was drilled over the opsin-expressing thalamus (AP - 1.3 mm, ML

0.9 mm). A unilateral optic fibre was inserted 3.7 mm below the brain surface above VM thalamus. Light intensity was adjusted pre-implantation with an integrating-sphere optical power meter (Thorlabs PM100USB and S140C) to reach 5, 10 or 20 mW at the end of the implanted optic fibre (200 μm, 0.22NA). The use of high light powers in optogenetic experiments has recently gained attention give the potential for non-specific thermal effects on neural activity and specifically the propensity to cause neuronal silencing (particularly if long durations of light delivery), possibly via an effect on inward-rectifier potassium channels expressed by neurons and glia (Wiegert et al., 2017; Owen et al., 2019). As such, ideal control experiments would involve GFP injected mice undergoing similar recordings (not done here). To partially address this, recordings at the highest light intensity were performed in the contralateral hemisphere (thalamus and cortex) of the same mouse for future comparison of their contribution to stimulus evoked responses.

For optical stimulation of ChR2, laser light of 473 nm (Cobolt, Sweden) was applied driven by TTL pulses from a CED Power 1401 mkII console controlled by Spike 2 software (v8.13, Cambridge Electronic Devices). Unilateral local field potential recordings were made with a linear silicon probe (A1x32-15mm-50-703-A32; Neuronexus, Ann Arbour, MI) positioned in M1 (ipsilateral or contralateral to the optic fibre) with the top recording site at the brain surface (depth = 0 μm). The extracellular signals picked up by each electrode were buffered directly above the head of the animal through an A32-Omnetics32 adapter (Neuronexus, Ann Arbour, MI) connected to an analogue to digital headstage (RHD2164, Intan Technologies) and sent to an interface board (RHD2000; Intan Technologies) where they were synchronized with signals from laser stimulation and filtered data was saved to a computer with a 20 kHz sampling rate (DSP cut-off = 1 Hz, low-pass filter = 0.1 Hz, high-pass filter = 7500 Hz). All recordings took place inside a Faraday cage.

## 2.6 Head-fixed awake or anaesthetised *in vivo* electrophysiological recordings to validate optogenetic silencing

A wild type mouse injected with AAV-Ef1a-mCherry-IRES-WGA-Cre in SNr and AAV-CAG-Flex-ArchT-GFP in motor thalamus (or a Vglut2-IRES-Cre mouse injected with AAV-CAG-Flex-ArchT-GFP in motor thalamus) > 6 weeks previously and had recovered from headplate surgery was habituated to the head fixation apparatus for at least 3 days for increasing periods of time (Day 1: 15 min training, 30 min break, 15 min training; Day 2: 30 min training, 30 min break, 30-45 min training; etc) until they were comfortable for at least one hour with intermittent sucrose rewards. Twenty-four hours prior to recording, unilateral craniotomy was performed under anaesthesia over thalamus (large window centred over AP - 1.3 mm, ML 0.9 mm) large enough for the passage of multi-shank probe or optrode. This was sealed with silicone prior to recovery and the mouse was single housed until perfused (3-5 days). After 24 hours, silicone was removed while the animal was head fixed and a unilateral optrode was inserted 3.7 mm below the brain surface above VM thalamus (AP -1.3 to -1.5 mm, ML 1.2-1.4 mm, with 10-degree medial angulation). Once daily recordings (< 3 h head fixation per session) were performed over 3-5 days per mouse. Electrophysiological signals in the thalamus were recorded using Neuronexus silicone optrodes (A4x8-100-200-177-OA32; 105 µm 0.22NA fibre on inner shank 200 µm above top contact site), digitised via an Intan recording system and captured in Spike 2 (v8.14) using the Intan Talker module (v1.4) at ~ 20 kHz with simultaneous video and piezo movement sensor attached to a 1401 DAQ. For optical stimulation of ArchT, laser light of 561 nm (Cobolt, Sweden) was applied driven by TTL pulses from a CED Power 1401 mkII console controlled by Spike 2 software v8.14 (Cambridge Electronic Devices, Cambridge, UK). Light intensity was adjusted pre-implantation with an integrating-sphere optical power meter (Thorlabs PM100USB and S140C) to reach 5, 10 or 20 mW at the end of the implanted optrode. All recordings took place inside a Faraday cage. Anaesthetised ArchT recordings took place without the steps for head plate implantation and habituation (as in section 2.5).

## 2.7 Immunofluorescence

After completion of experiments, mice were transcardially perfused with 4% paraformaldehyde in phosphate-buffered saline (PBS). Fixed brains were cut in cold PBS on a vibratome in 50 µm coronal slices. Antibody incubations were performed on single-well floating tissue sections. Sections were incubated overnight in primary antibodies at 4 °C followed by one overnight incubation with secondary antibodies at 4 °C. Primary antibodies used in this study were as follows: rabbit anti-calbindin 29k 1:500 (Swant), mouse anti- GAD67 1:200 (Millipore), chicken anti-GFP 1:1,000 (Alves), rat anti-RFP 1:500 (Chromtek), rabbit anti-vGlut2 1:200 (Synaptic systems), guinea pig anti-NeuN 1:200 (Synaptic systems), mouse anti-tyrosine hydroxylase 1:1000 (Sigma). Fluorophore-tagged secondary antibodies used were Alexa Fluor 488 donkey anti-chicken IgG 1:1,000 (703-545-155, Jackson), Cy3 donkey anti-rat IgG 1:1,000 (711-165-152, Jackson), Alexa Fluor 647 donkey anti-mouse IgG 1:500 (706-605-148, Jackson). Stained brain sections were mounted on glass slides and coverslipped with mounting medium (Vector Labs). Slides were imaged using an epifluorescence microscope (Zeiss Axioscan). Placement of the optical fibres and probes was assessed on the basis of DiI staining (painted on to fibre tip and back of probe).

## 2.8 Behavioural training

### *2.8.1 Housing and food restriction*

All mice were group housed, generally in pairs to minimise any weight differences during food restriction. Food pellets were restricted so that mice maintained 85-90% of their free feeding weight, but mice retained free access to water. Mice were trained daily at approximately the same time of day including over weekends.

*2.8.2 Operant lever press training.*

Behavioural training took place in operant chambers (21.6 cm × 17.8 cm × 12.7 cm; Med Associates, VT, USA) housed within a sound attenuating box (Campden Instruments, UK) and equipped with one retractable lever on the left side of the liquid magazine and a house light (3 W, 24 V) (see Figure 4.1). Sucrose solution (20%) was covertly delivered into a metal cup in the magazine through a syringe pump located on a shelf below the sound attenuating chamber. Magazine head entries were recorded using an infrared beam and licks using a contact lickometer. Behavioural timestamps (lever press, lick, reward delivery, head entry, vertical infrared beam break, and laser pulses delivered) were relayed from the Med Associates interface to a TDT RZ5P processor and captured using Synapse software (Tucker-Davis Technologies) using a custom made 8-channel 28V to TTL converter. All time stamps of lever presses, duration of press, magazine entries and licks for each mouse were recorded with a resolution of 10 ms. The lever was retrofitted with a light weight (0.3g) accelerometer moving in the Z-axis (Analog Devices ADXL326) and able to output a continuous analogue signal to the TDT processor. Mice were trained in the same chamber for the duration of experiments. Due to the physical limitation of tethered and implanted mice undertaking tasks in operant chambers, a custom 3D printed liquid delivery port was utilised in all 3 chambers to ensure rhythmic/stereotyped lever pressing behaviour was not disturbed by implants or tethers catching on commercially supplied fluid receptacles.

Training started with two 20-min magazine training sessions per day in which a 4 µl reinforcer was delivered on a random time schedule, on average every 30 s, until mice showed > 750 licks. Mice were first trained to acquire a regular lever pressing under a strict fixed-ratio 1 schedule where either licking or head entry must have occurred before another press can trigger the delivery of the next reinforcer**.** To support lever acquisition, mice were initially allowed to gain up to 30 reinforcers of 15 µl sucrose (20%) per day, then transitioned to up to 60 reinforcers of 10 µl once per day, and finally had 60 reinforcers of 5 µl twice per day. Mice had 1-2 h breaks between

sessions when being trained twice daily. The behaviour was self-paced and throughout training there was no explicit signal for the animal to initiate or terminate a sequence of lever press. Mice continued to be trained twice daily until they could gain all 60 reinforcers in less than 90 lever presses (i.e. mean press rate of < 1.5 per reinforcer delivered). Once this criterion was achieved and maintained for at least 6 sessions (3 days) mice could be moved on to specific training schedules which differed for untethered mice (UT-Control and MThal-Kir2.1) compared to that for tethered mice (T-Control, VM-ArchT, and VL-ArchT). Untethered mice could either undergo a single 45min extinction session or be covertly switched a fixed-ratio 3 schedule where three presses must be initiated within any 2 second window (FR3/2s) to deliver a three-fold larger reinforcer (12 µl; maximum 15 reinforcers per session). By contrast, tethered mice (for optogenetic silencing) were habituated to the tether (minimum 2 days or 4 sessions) and then tether plus light delivery (minimum 2 days or 4 sessions) prior to being covertly switched to the FR3/2s reinforcement schedule. During FR3/2s training, mice were trained twice daily without interruption and the training started at approximately the same time each day. Mice who could gain at least 10 (out of 15) reinforcers in their first FR3/2s session (S1, maximum 90 minutes) continued on this training schedule twice daily. Mice who failed to achieve this minimum transition to FR3/2s pressing were reinstated on FR1 pressing for 3 days then given a second attempt at FR3/2s, although these mice are not analysed in this thesis.

*2.8.3 Light delivery during behaviour*

Yellow 100 mW DPSS lasers (561 nm; Cobolt, Sweden) were connected via a 200 µm 0.22NA optic fibre to an intensity-splitting rotary joint (Doric, Quebec, CA) which was, in turn connected via a custom patch cord to a dual ferrule fibre optic cannula implanted in the animal. The same fibre optic implant was used in all mice, and had two 200 µm 0.37NA optic fibres 10 mm long with a centre distance spaced 1.7 mm apart, allowing implantation with a mediolateral coordinate of 0.7-0.9 mm. Laser power was checked at the start of the day using a integrating sphere power meter accommodating the patch cord connector attached to a phantom dual optic fibre ferrule (Thorlabs, UK). In all optogenetic lever press sessions, light was delivered as 30 s

long continuous pulses with a pseudorandom interval of 5-20 s controlled by a custom RPvdsEx circuit script for TDT processors (written by Myles Billard, Tucker Davis Technologies).

### *2.8.4 Composition of control and experimental groups*

Vglut2-IRES-Cre knock in mice (on a C57/BL6 background; Vglut2-Cre) were imported from Jackson Laboratories. Despite initially successful breeding, delays in having sufficient heterozygous males during a key experimental period and the inherent problem of individual mice failing FR3/2s transition at first attempt (despite identical performance in FR1 to mice who successfully transitioned) meant that we had to use wild type or mixed control groups (Table 2.1). In the comparison with Vglut2-Cre MThal-Kir2.1 group we used a purely wild type (non-injected) untethered control group (Chapter 5), instead of the ideal control group of Vglut2-Cre mice bilaterally injected with MThal-GFP. Equally, for comparisons with optogenetic silencing VM-ArchT and VL-ArchT groups, the tethered control group (n = 6) was composed of 3 mice which were truly matched (i.e. Vglut2-Cre males with bilateral VM-GFP expression and bilateral optic fibre implantation and light delivery during FR3/2s training sessions), but the other three mice had bilateral injections of AAV5-Ef1a-mCherry-IRES-WGA-Cre in SNr, either AAV5-CAG-Flex-ArchT-GFP (n = 2) or AAV5-CAG-Flex-GFP (n = 1) in the motor thalamus, and bilateral fibre implantation, but did not receive light delivery during FR3/2s sessions. Early wild type untethered controls that did not have simultaneous accelerometer recordings (n = 5) were included in early part of Chapter 4 (Figures 4.2, 4.3 and 4.4; n = 12 mice).

| Group | Tethered or untethered (Group) | FR3/2s Successful on 1st attempt (accelero-meter data available) | FR3/2s Successful on 2nd attempt | Unable to acquire FR3/2s | Total mice |
|---|---|---|---|---|---|
| WT Control | Untethered (control) | 12 (7) | 1 | 4 | 17 |
| Vglut2-Cre MThal-Kir2.1 | Untethered (MThal-Kir2.1) | 4 (4) | 0 | 3 | 7 |
| Vglut2-Cre VM-GFP | Tethered (control) | 3 (3) | 0 | 1 | 4 |
| SNr WGA/ MThal-ArchT | Tethered (control) | 2 (2) | 0 | 0 | 2 |
| SNr WGA/ MThal-GFP | Tethered (control) | 1(1) | 0 | 0 | 1 |
| Vglut2-Cre VM-ArchT | Tethered (VM-ArchT) | 7 (7) | 2 | 2 | 11 |
| Vglut2-Cre VL-ArchT | Tethered (VL-ArchT) | 5 (5) | 1 | 3 | 9 |
| Summary | - | 34 (29) | 4 | 13 | 51 |
| Summary (%) | - | 66.7% | 7.8%% | 25.5% | 100% |

**Table 2.1 Summary of mice trained for FR3/2s behavioural analysis.**

Only mice that were successful at first attempt on acquiring FR3/2s and could subsequently maintain the behaviour over 14 sessions were analysed in Chapter 4 and Chapter 5 of this thesis.

## 2.9 Slice electrophysiology

Adult male Vglut2-Cre mice ~10 weeks after bilateral motor thalamus injection of AAVDJ-CMV-DIO-Kir2.1-ZsGreen virus and completion of lever press training were given to Dr Tommas Ellender for *in vitro* electrophysiological recordings and analysis as outlined here. Acute brain slices containing the thalamus were made from mice anaesthetised with isoflurane and then decapitated. Brain was removed and coronal 350-400μm slices were cut using a vibrating microtome (Microm HM650V). Slices were prepared in artificial cerebrospinal fluid (aCSF) containing (in mM): 65 Sucrose, 85 NaCl, 2.5 KCl, 1.25 NaH2PO4, 7 MgCl2, 0.5 CaCl2, 25 NaHCO3 and 10 glucose pH 7.2-7.4, bubbled with carbogen gas (95% O2, 5% CO2).

Slices were immediately transferred to a storage chamber containing aCSF (in mM): 130 NaCl, 3.5 KCl, 1.2 NaH2PO4, 2 MgCl2, 2 CaCl2, 24 NaHCO3 and 10 glucose pH 7.2–7.4, at 32°C and bubbled with carbogen gas until used for recording. Slices were transferred to a recording chamber and continuously superfused with aCSF bubbled with carbogen gas with the same composition as the storage solution (32°C and perfusion speed of 2 ml/min). Whole-cell current-clamp and voltage-clamp recordings were performed using glass pipettes, pulled from standard wall borosilicate glass capillaries and containing for current-clamp experiments (in mM): 110 potassium gluconate, 40 HEPES, 2 ATP-Mg, 0.3 Na-GTP, 4 NaCl and 4 mg/ml biocytin (pH 7.2–7.3; osmolarity, 290–300 mosmol/l) and for voltage-clamp recordings (in mM): 120 cesium gluconate, 40 HEPES, 4 NaCl, 2 ATP-Mg, 0.3 Na-GTP, 0.2 QX-314 and 4 mg/ml biocytin (pH 7.2–7.3; osmolarity, 290 –300 mosmol/L). Recordings were made using Multiclamp 700B amplifiers and acquired using WinWCP software (University of Strathclyde, UK).

*Slice stimulation and recording protocols*

Native fluorescence of zsGreen in Kir2.1 overexpressing neurons was used to identify neurons for patching. Adjacent, non-fluorescent neurons were patched and used as controls. Recording of resting membrane potential was performed in whole-cell current-clamp mode. Hyperpolarising and depolarising current steps were used to assess the intrinsic properties of the recorded thalamocortical neurons including input resistance and action potential frequency. Data were analyzed offline using custom written programs in Igor Pro (Wavemetrics, RRID:SCR_000325).

*Histological analyses on slices*

Following whole-cell patch-clamp recording, slices were fixed in 4% paraformaldehyde in 0.1 M phosphate buffer (PB; pH 7.4). Biocytin-filled cells were visualized using streptavidin fluorescent-conjugated antibodies (ThermoFisher Scientific, S32351) performed using standard procedures. All sections were pre-incubated in 10–20% normal goat serum (NGS; Vector

Laboratories; Cat# S-1000, RRID:AB_2336615) in PBS containing 0.3% Triton-X (PBS-Tx) for more than 1h at RT. Slices were co-stained with anti-calbindin1 (Swant, 1:500) and anti-GAD67 (Millipore, 1:500) antibodies in PBS-Tx to facilitate the delineation of brain structures. All sections were mounted in Vectashield (Vector Laboratories, H-1000) and images were captured with a LSM 710 (Carl Zeiss Ltd, Cambridge, UK) confocal microscope using ZEN software (Carl Zeiss Ltd, Cambridge, UK).

### 2.10 Quantification and data analysis

*Counting of transynaptically tagged VM neurons*

Stereological counting was performed in three C57/BL6 mice injected 7 weeks previously with AAV5-Ef1a-mCherry-IRES-WGA-Cre in SNr and AAV5-Ef1a-DIO-ChR2(E123T/T159C)-eYFP in VM thalamus. 50 µm sections were incubated in anti-GAD67 and anti-GFP antibodies as above. Starting sections were chosen at random, and every 1 in 4 serial sections (50 µm sections) spanning the whole of VM thalamus were selected for incubation, with 11-13 sections of each combination per animal. An epifluorescent microscope with a 20x objective and ApoTome (Zeiss, Cambridge, UK) was used to image the motor cortex of each section using Stereo Investigator software (MBF Bioscience, VT, USA). The optional fractionator method was used to carry out systematic random sampling. The probe depth was 8 µm, with a 2 µm guard zone and 1 µm interval. The grid size and counting frame were 350 x 250 µm. Contours were drawn around basal ganglia-recipient zone of motor thalamus using GAD67 as a guide, and a mouse brain atlas (Paxinos and Franklin, 2012) for a guide to the ventrolateral borders of the thalamus. Neurons were counted if the point at which the nucleolus (marked by DAPI) first appeared was within the probe, or the top of the neuron (marked by GFP). Cells touching the green inclusion line on the counting frame were included, and those touching the red exclusion line excluded. Numbers of each marker combination were counted, and the proportion as a percentage of total GFP neurons within each protocol for each animal were calculated.

*Image processing*

Images were acquired using Stereo Investigator software (MBF Bioscience, VT, USA). Whole brain images were stitched together in Zen Black (Zeiss, Cambridge, UK) and further processed in the Fiji distribution of ImageJ2. Region of interest analysis (laminar fluorescence histograms) were performed in Fiji.

*Cortical laminar electrophysiology*

Electrophysiological recordings were analysed using custom scripts (written by Dr Andrew Sharott) in MATLAB (Mathworks, version: R2014b). Stimulus-evoked local field potential (LFP) recordings were calculated by averaging each trace around the first pulse of each "burst" of optogenetic stimuli at a given frequency. These evoked potentials were then normalised using a standard z-score and plotted in order of contact depth (superficial to deep).

*Thalamic multi-unit activity plots*

Electrophysiological data recorded in Spike2 software (with the IntanTalker module) via an Intan headstage and RHD2000 evaluation board were processed in Neuroexplorer (v5.201). A python script customised to channel identities in our rig was used to remove global movement-related artefacts (by subtracting the mean local field potential from each channel) and subsequently high pass filter recordings from 300-6000 Hz. Subsequently, each channel was processed using the 'detect spikes' function in Neuroexplorer (median sigma = -6, segment before threshold = 0.2 ms; segment after threshold = 1 ms; minimum time between spikes = 1 ms). Data was then visualised as perievent rasters of spike-times and perievent rasters of continuous data. Data from 3 adjacent contacts on the same shank of the silicone probe (100 μm spacing) is shown and presented from highest to lowest, to show effects are not purely due to proximity to optic fibre.

*Accelerometer-lever press validation*

To characterise how the temporal profile of the z-axis accelerometer trace corresponded to lever press timestamps recorded by the Med-PC software, we compared both signals with 'ground truth' high speed video recording (150 frames per second [fps]) in a subset of mice that had already acquired FR3/2s press sequences. Briefly, a 150 Hz TTL pulse from the Tucker Davis RZ5P processor being used to record behavioural data (from both Med-PC system and accelerometer) was used to drive monochrome frame capture of a mvBlueFOX3 camera (Matrix Vision, Germany) via Streampix 7 software (Norpix, Quebec, CA). This high-speed camera was positioned to have a side view of a lever marked with a white dot (its diameter was approximately one third of the vertical thickness of the lever) during FR3/2s training sessions. High speed video recordings were then analysed offline to track arc-like lever movements during presses. The video files were analysed by idTracker software (Perez-Escudero et al., 2014) to produce a trajectories dataset which could be mapped to the camera-trigger TTLs which accompanied behavioural data in the Synapse recording file for that session in MATLAB. The two-dimensional tracking of the lever dot position was then reduced to a single vertical dimension (by using the difference between coincident x and y coordinates) so it could plotted against session time along with accelerometer trace and lever timestamps.

*Behavioural analysis*

Tables describing folder structure of behavioural data recorded via TDT Synapse software were created for each animal. Timestamps of magazine head entries, lever on/off, lever duration, licks and reinforcer delivery were imported from TDT files to MATLAB using the TDT script "TDT2mat." All further analysis was performed using custom MATLAB scripts (written by Dr Andrew Sharott). Lickometer timestamps were edited so that only licks occurring within head entry periods were analysed. The temporal properties of lever press sequences were analysed using inter press interval (IPI) histograms constructed from the derivative of the lever press time

series. Histograms were constructed using IPI bins of exponentially increasing size to aid visualisation and comparison of very short (< 1 s) and very long (< 20 s) IPIs. IPI return plots were constructed by plotting each IPI (x-axis) against the following IPI (y-axis). Each point on the IPI return plot thus represents a sequence of 3 lever presses. In order to be able to mean these data across animals, they were normalised using the same bins as the IPI histograms using a 2-dimensional histogram. These 2D histograms could then be used to show the mean number of times a given consecutive IPI occurs across animals at each stage of training.

In line with previous work (Jin and Costa, 2010), lever press sequences were divided into bouts of uninterrupted pressing, as defined using existing criteria (Jin et al., 2014), i.e. a bout of pressing was one or more presses separated by detected magazine head entry, lick, or 2 seconds of inactivity. These criteria could be applied to lever press sequences in any of the training regimes (FR1, FR3/2s, extinction). Having divided the overall sequence lever presses during a session into bouts with different numbers of presses (1, 2, or ≥ 3 presses) and defining their indices, certain analyses (e.g. mean accelerometer traces) were carried out using lever presses that formed part of specific bout sizes. In the FR3/2s trials, the percentage of bouts with ≥ 3 presses (PB3) was used as the main metric of performance, as it best reflected the ability of the animal to achieve the covert target (i.e. if this measured 100%, all lever presses would have contributed to reinforcer delivery assuming they occurred within 2s). In animals where optogenetic inhibition was applied, in the last 4 FR1 sessions the number of lever presses, head entries and licks was counted in for each individual epoch where the laser was on or off. These parameters where then converted to rate (e.g. number of lever presses/minute) to normalise for the unequal amount of time that the laser was on (~60%) or off (~40%).

To allow synchronisation between these data and the accelerometer, each series of time stamps was converted to a binary event channel at the sampling rate of the accelerometer (6 kHz). Accelerometer data was analysed by triggering off the Med Associates lever onset timestamp. The peak within-press acceleration was analysed by detecting the most negative (trough) value

in the 100 ms prior to the lever press onset timestamp in Med-PC. For analysis of accelerometer traces between experimental groups in FR3/2s sessions, any lever press that occurred within a bout with ≥ 3 presses was included.

### 2.11 Statistical analysis

As eluded to in section 2.8.1 and Table 2.1, only mice which i) acquired and maintained FR3/2s for 14 sessions at the first attempt and ii) had lever accelerometer data for all 14 sessions were included in analysed datasets in Chapter 4 and Chapter 5. Given that mice were trained twice daily for 7 days on FR3/2s task, we use the following notation to describe data timepoints: Day 1 (first session = S1, second session = S2), Day 2 (S3, S4), Day 3 (S5, S6), Day 4 (S7, S8), Day 5 (S9, S10), Day 6 (S11, S12), and Day 7 (S13, S14). Analysis of data across the FR3/2s trials was performed using several analytical methods. Firstly, one-way ANOVA was were calculated for several output variables (total lever number, % of ≥ 3 press bouts, head entry rate, reinforcer delivery rate, total time) at specific time points across the first 14 sessions (S1, S5, S9 and S13) of control mice undergoing FR3/2s to establish whether there was a consistent increase or decrease in these metrics with learning. Next, to test whether light delivery had a gross effect on behavioural output, multi-way ANOVA was performed to assess the effect of experimental group and light condition on rate of lever pressing, head entry or licks during the last 4 FR1 sessions (prior to starting FR3/2s).

One-way Kruskal-Wallis ANOVAs were calculated for each of the previously described metrics to compare the differences in parameter values on FR3/2s session 1, 7 and 13 between groups (untethered control vs MThal-Kir2.1; tethered control vs VM-ArchT; tethered control vs VL-ArchT, VM-ArchT vs VL-ArchT).

Multi-way ANOVA (MATLAB function: ANOVAN) was next used to test the influence of experimental group and between-session differences (S1 vs S5, S1 vs S9, S1 vs S13, S5 vs S9, S9 vs S13) on task parameters during FR3/2s training. As several key task parameters showed early

(i.e. S1 vs S5) significant differences on post-hoc testing, this analysis was repeated for differences between early sessions (S1 vs S2, S1 vs S3, S1 vs S4, S2 vs S3, S2 vs S4, S3 vs S4). As training consisted of two sessions per day, multi-way ANOVA was then used to test the relationship of multiple variables (recording day, recording session, experimental manipulation) on the percentage of ≥ 3 press bouts in the first two days of FR3/2s training. The choice of the first two recordings days was based on the analysis of the first 14 FR3/2s sessions showing that this period represented the biggest difference between experimental groups. Models were calculated both for the absolute percentage of ≥ 3 press bouts and the difference in percentage of ≥ 3 press bouts across two *consecutive* training sessions, either within the first (S1-S2) or second (S3-S4) training day, or between the first and second (S2-S3) or second and third (S4-S5) training days. A positive difference (increase) in the percentage of ≥ 3 press bouts between two consecutive training sessions suggested learning or performance gain. The Shapiro-Wilk test was used to verify normal distribution of data points for each experimental group within a session. Where appropriate/necessary, Mauchly's test was applied to verify that the assumption of sphericity for a given data set had not been violated.

Median-adjusted accelerometer data was analysed using Spearman's rank correlation coefficients (R-values and $R^2$-values) to assess whether there was a consistent increase or decrease in mean trough values (i.e. mean peak within-press acceleration) over recording sessions 1-14.

### 2.12 Key resources table

| Reagent or Resource | Source | Identifier |
|---|---|---|
| *Antibodies* | | |
| Anti-Calbindin1 | Swant | Rabbit CB38 |
| Anti-GFP | Alves | Chicken GFP-1020 |
| Anti-GAD67 | Millipore | Mouse MAB 5406 |
| Anti-TH | Sigma Aldrich | Mouse T2928 (TH-16) |
| Anti-RFP | Chromtek | Rat 5F8 |
| Anti-Ctip2 | Abcam | Rat AB18465 |
| Anti-Wfs1 | Proteintech | 11558-1-AP |
| 4′,6-Diamidino-2-phenylindole dihydrochloride (DAPI) | Sigma Aldrich | D8417 |
| Anti-Vglut2 | Synaptic Systems | Rabbit 135 403 |
| *Viruses* | | |
| AAV2-hSyn-ChR2(E123A)-eYFP | University of North Carolina Vector Core | Dr Karl Deisseroth (MTA #34) |
| AAV5-Ef1a-mCherry-IRES-WGA-Cre | University of North Carolina Vector Core | Dr Karl Deisseroth (MTA #36) |
| AAV5-Ef1a-DIO-hChR2(E123T/T159C)-eYFP | University of North Carolina Vector Core | Dr Karl Deisseroth (MTA #27) |
| AAV5-CAG-Flex-ArchT-GFP | University of North Carolina Vector Core | Dr Ed Boyden |
| AAV5-CAG-Flex-GFP | University of North Carolina Vector Core | Dr Ed Boyden |
| AAVDJ-CMV-DIO-Kir2.1-ZsGreen | Stanford Vector Core | GVVC-AAV-61 |
| *Experimental models: organisms/strains* | | |
| C57BL/6J mice | Charles River, UK | Strain code 632 |
| Vglut2-IRES-Cre mice | https://www.jax.org | Stock #028863; RRID: IMSR_JAX:028863 |
| PV-IRES-Cre mice | https://www.jax.org | Stock #008069; RRID: IMSR_JAX:008069 |
| *Software and Algorithms* | | |
| Intan RHD2000 Evaluation system software | Intan technologies, California, USA | Version 1.5.3 |
| Fiji | National Institutes of Health, USA | ImageJ1.52p |
| Stereo Investigator | MBF Bioscience, Vermont, USA | Version 9.0 |
| Synapse | Tucker Davis Technologies, Florida, USA | v90 |
| Med-PC V | Med Associates, Vermont, USA | SOF-736 |
| idTracker | de Polavieja lab, Cajal Institute, Madrid, Spain | Version 2.1 |
| Neuroexplorer | Neuroexplorer, Colorado, USA | V5.201 |

| *Other* | | |
|---|---|---|
| Dual optic fiber ferrule 10 mm | Doric Lenses, Québec, Canada | DFC_200/245-0.37_10mm_GS1.7_FLT |
| optic rotary joint | Doric Lenses, Québec, Canada | FRJ_1x2i_FC-2FC |
| Dual Fibre optic patch cable | Doric Lenses, Québec, Canada | DFP_200/220/900-.37_0.75m_GS1.7-2FC |
| Jet Denture Repair Power | Lang Dental, Illinois, USA | 1230CLR |
| Methyl methacrylate monomer | Mr Dental, Surrey, UK | Meadway Rapid Repair Liquid |
| 32 Channel Silicone probe (single shank) | Neuronexus technologies, Michigan, USA | A1x32-15mm-50-703-A32 |
| 32 Channel Silicone optrode (4 shank; 200 µm 0.22NA fiber on inner right shank 200 µm above top contact) | Neuronexus technologies, Michigan, USA | A4x8-5mm-100-200-177-OA32LP |
| Probe adaptor and holder compatible with Intan headstage | Neuronexus technologies, Michigan, USA | Adpt.A32-Omnetics32 |
| 473 nm diode laser | Cobolt, Solna, Sweden | 06-MLD-473-100 mW |
| 561 nm diode pumped laser | Cobolt, Solna, Sweden | 06-DPL-561-100 mW |
| 561 nm diode pumped solid state laser | Cobolt, Solna, Sweden | Jive 561-100 mW |
| Z-axis Analogue Accelerometer | Analog Devices | ADXL-326 |
| Accelerometer circuit board and analog output | Electronics workshop, Department of Pharmacology, Oxford | Custom design |
| 8 Channel x 28V to TTL converter box | Electronics workshop, Department of Pharmacology, Oxford | Custom design |
| Fiber photometry system | Tucker Davis Technologies, Florida, USA | RZ5P |
| Head-stage amplifier | Intan technologies, California, USA | RHD2164 and/or RHD2132 |
| Electrophysiology acquisition board | Intan technologies, California, USA | RHD2000 Evaluation board |
| TTL Generator for electrophysiology | Cambridge Electronic Design, Cambridge, UK | CED Power 1401 mkII |
| Vibrating Microtome | Leica Microsystems, Wetzlar, Germany | VT1000S |
| Thorlabs integrated sphere power meter | Thorlabs, Germany | PM100USB/S140C |
| Operant chamber | Med Associates, Vermont, USA | ENV-307W-CT |
| Head-implant and tether compatible magazine | MRC Brain Network Dynamics Unit, Oxford | 3D-printed custom design |
| Liquid delivery cup | Med Associates, Vermont, USA | ENV-303RMA-3 |
| Head entry detector | Med Associates, Vermont, USA | ENV-303HDW |
| Contact Lickometer | Med Associates, Vermont, USA | ENV-250 |

| | | |
|---|---|---|
| Ultrasensitive retractable lever for mice | Med Associates, Vermont, USA | ENV-312-2W |
| Syringe pump | Med Associates, Vermont, USA | PHM-100A |
| Shielded Sound attenuated chamber | Campden Instruments, UK | 80604-SAC-H1 |
| BenchTop Faraday Cage | TMC, Massachusetts, USA | 81-334-03 |
| 100 μm optic fiber patch cable (FC to 1.25 mm ferrule) | Thorlabs, USA | |
| Animal tunnel holder for head-fixed recordings | Thorlabs, USA | |
| Head-fixation apparatus | Custom design/Howard Hughes Medical Institute | |

**Table 2.2 Key Resources Summary.**

# 3. Connectivity-specified targeting of the motor thalamus

## 3.1 Introduction

The term 'motor' thalamus refers to the ventral thalamic nuclei which receive input from basal ganglia or cerebellum and in turn predominantly project to motor associated cortical areas. The majority of literature on the anatomy of motor thalamic neurons has been derived from experiments in rats, non-human primates, cats and dogs (Hintzen et al., 2018). In rats, motor thalamus can be functionally divided into the basal ganglia-receiving zone (BZ) consisting of the ventromedial (VM; substantia nigra pars reticulata (SNr)-receiving) and ventral anterior (VA; entopeduncular (EP) nucleus-receiving) thalamic nuclei, and the cerebellar-receiving zone (CZ) consisting of the ventrolateral thalamus (VL) (Nakamura et al., 2014). In practice, BZ and CZ are identified as motor thalamus zones with either glutamic acid decarboxylase (GAD67; GABAergic projections from SNr or EP) or vesicular glutamate transporter 2 (VGLUT2; glutamatergic projections from deep cerebellar nuclei) immunoreactivity respectively (Kuramoto et al., 2011). Axons of BZ thalamic neurons are known to densely target layer 1 over a wide area of frontal cortex and arborise in dorsal striatum whereas CZ neurons do not have any branches in striatum and preferentially target cortical layers 3-5 (Kuramoto et al., 2009; Kuramoto et al., 2015; Guo et al., 2018). Furthermore, electrical stimulation studies have shown differential cortical responses from activation of BZ (i.e. VM/VA) and CZ (i.e. VL), termed 'recruiting' and 'augmenting' responses respectively (Castro-Alamancos and Connors, 1997). Given that VL thalamocortical synapse strength in cortical layer 5 becomes biased toward task relevant corticospinal neurons during skilled reach training (Biane et al., 2016) and that VM neurons projecting to frontal cortex also make monosynaptic connections onto layer 5 pyramidal tract neurons but do not elicit action potential firing (Collins et al., 2018), it has become a priority to understand their differential effect on motor skill learning. Since VM neurons target the L1 apical dendrites of the same corticospinal neurons as VL neurons they may facilitate spine

formation in apical dendrites of L5 pyramidal neurons important for motor memory formation (Xu et al., 2009; Yang et al., 2009; Peters et al., 2014).

Nissl borders of thalamic nuclei have long been used to imply a functional distinction and been the primary target of lesions. Exactly what the computations of the basal ganglia- and cerebellar-thalamocortical pathways contribute to the gamut of normal motor behaviour in mammals remains unclear due to the need to overcome the technical challenges of targeting one thalamic nucleus while sparing the other. In purely spatial terms, selectively targeting BZ or VM distinctly from CZ or VL is more difficult than, for example, functionally distinct subregions or motor cortex of striatum. The juxtaposed nature of basal ganglia and cerebellar territories within the motor thalamus means that lesions, drug infusions and non-restricted expression of viral actuators will mostly manipulate both pathways. Additionally, single axon tracing from basal ganglia output nuclei to the thalamus suggests that multiple thalamic nuclei are targeted by a single ascending axon in the order of motor thalamus, intralaminar thalamus and mediodorsal thalamus (Cebrian et al., 2005; Wallace et al., 2017). As such, a radiofrequency lesion in the motor thalamus may affect the distal axon and thus the activity of other downstream thalamic nuclei known to have significant cognitive or motor roles. Equally, it may damage thalamocortical axonal projections from an adjacent/more posterior nucleus. Lastly, there is also evidence that cerebellar and basal ganglia input targets the same motor thalamus neurons although the degree of this may vary between species (Hintzen et al., 2018).

Neuronal cell types in a specific brain region can usually be segregated by protein expression, firing pattern, morphology, and afferent/efferent connections (‘connectome’ at the single cell level) (Molyneaux et al., 2007). In recent decades, mice have become a popular experimental model due to advantageous breeding and cell type specific targeting using transgenic lines (Wolff and Olveczky, 2018). The use of promoter targeted site-specific recombinase (e.g. Cre or Flp) knock-in mice can restrict expression of virally delivered Cre- or Flp-dependent transgenes to only those cells with gene promoter activity of interest. Previous attempts at parcellating thalamus using this approach had some success in selectively targeting motor thalamic nuclei only, but no pattern

suggestive of BZ or CZ neuron selectivity (Gerfen et al., 2013). In practical terms, this problem of selective targeting favours more generic motor thalamic targeting strategies recently used with optogenetic tools (Guo et al., 2017; Lalive et al., 2018; Tanaka et al., 2018). The expression of Calbindin-1, a marker for matrix thalamocortical neurons in primates, does seem to adhere to the borders of VM and VA thalamic nuclei and has been used for specifically targeting VM thalamus (Guo et al., 2018; Honjoh et al., 2018). A recently published molecular analysis of thalamic architecture in the mouse brain does appear to support Calbindin 1 in VM/VA and Tnnt1 in VL, though these are also expressed in intralaminar/mediodorsal and sensory thalamic nuclei respectively (Phillips et al., 2019).

Given the time and resources required to engineer and test new transgenic mouse lines, others have focused on connectivity-based approaches which may parcellate brain regions in more functionally relevant ways. Recent attempts to selectively target motor thalamus neurons have used modified AAVs with a propensity to be taken up at projection site terminals (Tervo et al., 2016) and has meant that motor thalamus parcellation has occurred based on cortical projection sites (Collins et al., 2018). Because motor thalamic nuclei do not send reciprocal axonal projections to the cerebellar- or basal ganglia output nuclei they receive afferents from, unfortunately this approach cannot be used to segregate motor thalamus in a cerebellar or basal ganglia specific manner. Despite the widespread adoption of retrograde monosynaptic tracing using modified rabies virus (Kim et al., 2016), using other viruses which jump across synapses in an anterograde fashion (e.g. vesicular stomatitis virus, herpes simplex virus) remains problematic in terms of toxicity and degree of simultaneous retrograde transmission (Beier et al., 2011; Zingg et al., 2017; Saleeba et al., 2019). Another transsynaptic approach which has been used predominantly for retrograde transsynaptic targeting involves viral expression of a wheat germ agglutinin-Cre recombinase (WGA-Cre) fusion protein, which appears to be transynaptically trafficked at low efficiency retrogradely (Gradinaru et al., 2010; Xu and Sudhof, 2013; Gunaydin et al., 2014; Gompf et al., 2015; O'Shea et al., 2018) or anterogradely (Libbrecht et al., 2017).

Cerebellar and basal ganglia territories have only recently been subjected to anterograde viral tracing in the mouse thalamus and show considerable axon overlap in ventral motor nuclei which are already challenging to target selectively due to their small size (Kim et al., 2017; Wallace et al., 2017; Gao et al., 2018; Tanaka et al., 2018; Phillips et al., 2019). However, i) the extent to which cerebellar and basal ganglia projections overlap in their postsynaptic targeting of motor thalamus neurons and ii) whether populations of motor thalamus neurons identified as receiving either basal ganglia or cerebellar inputs still show differential targeting of deep and superficial cortical layers in mice remains unknown. Given this uncertainty, here we attempt to clarify which of the features of BZ and CZ neurons previously described in other species may be conserved in mice and thus justify attempts to target these two neuronal populations separately in the same motor skill learning task.

### 3.2 Experimental aims

1) To clarify the degree of conserved segregation of basal ganglia-thalamic and cerebellar-thalamic inputs and post-synaptic targets in the mouse motor thalamus

2) To select and validate an appropriate approach for targeting basal ganglia or cerebellar-receiving motor thalamus neurons to be used in behavioural manipulations.

### 3.3 Basal ganglia- and cerebellar-recipient motor thalamus can be parcellated by immunoreactivity to Calbindin-1, GAD67 and VGLUT2 in mice

Calbindin-1 (Calb1) has been used to identify 'matrix' thalamocortical neurons (Kuramoto et al., 2009; Kuramoto et al., 2011; Kuramoto et al., 2015) and appears to mark the borders of Nissl-defined VM thalamus in mice (Fig 3.1C), but only a subregion of this Calb1+ zone is GAD67 immunoreactive (Fig 3.1D) and thus receives GABAergic projections from basal ganglia. VGLUT2 immunoreactivity (Fig 3.1E) pattern is at low levels in VM but overlaps with GAD67 in border regions as well as in the paracentral nucleus (consistent with dual innervation of intralaminar thalamus) and in zona incerta. Due to the discrepancy between GAD67 and

Calbindin1 in their definition borders of BZ/VM, we injected a Cre-dependent AAV-Ef1a-DIO-ChR2-eYFP into the substantia nigra pars reticulata (SNr) of PV-Cre mice (Fig 3.1F-G; n = 3) to confirm the location of basal ganglia input. We found that projections of PV+ SNr neurons projecting to motor thalamus was highly congruous with GAD67 immunoreactivity (Fig 3.1H-J) but that axosomatic synapses were formed onto Calb1+ thalamic neurons in this zone (Fig 3.1K, white arrow). As such, we confirmed that GAD67 is a faithful marker of basal ganglia input into motor thalamus, but that the lateral portion of VM thalamus consists of Calb1+ neurons but lacks GAD67 immunoreactivity.

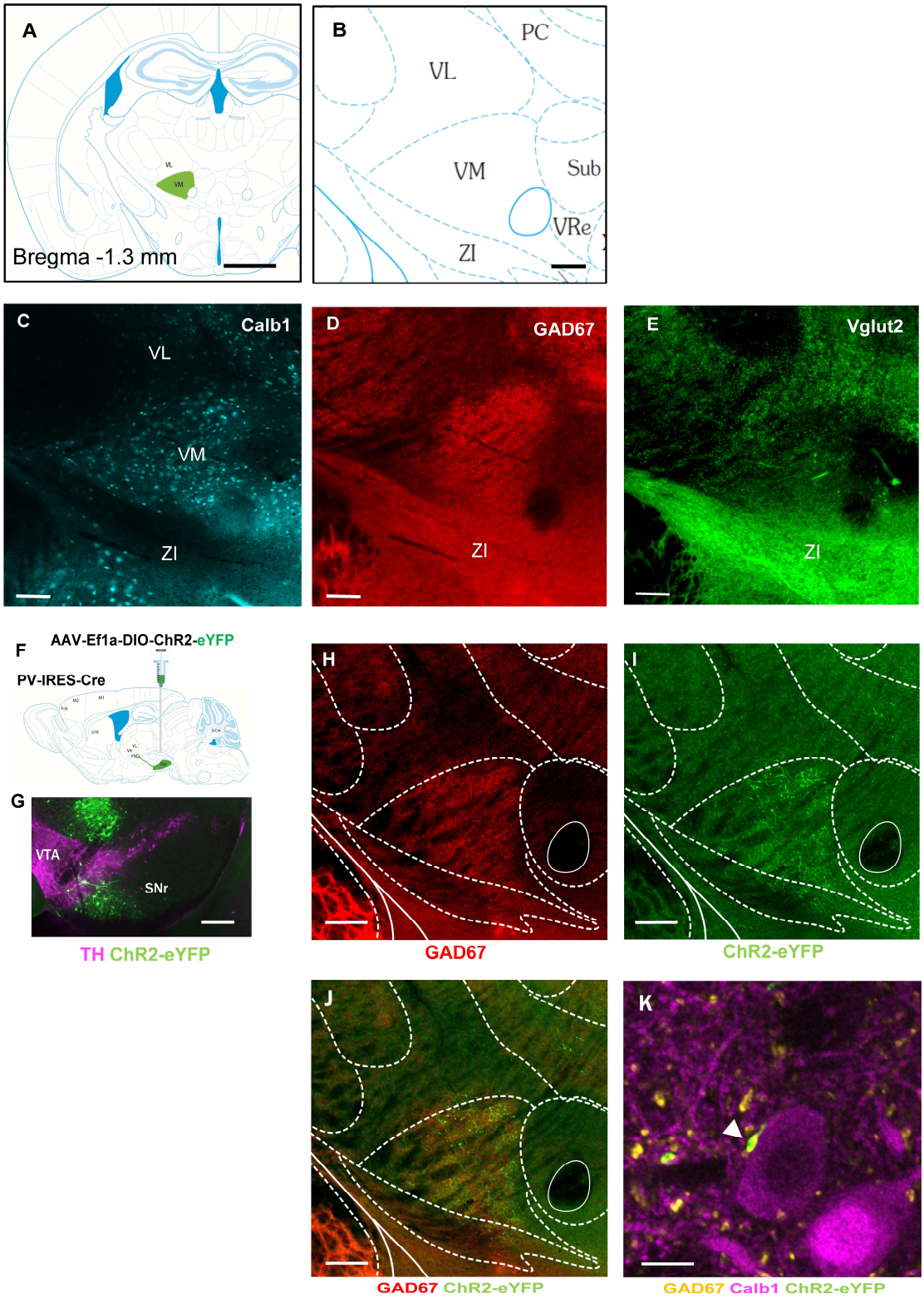



**Figure 3.1 Immunohistochemical and projection-based identification of basal ganglia-receiving zone of motor thalamus in coronal mouse brain sections. (A)** Coronal section and **(B)** magnified view from Paxinos mouse brain atlas showing relative position of basal ganglia receiving VM and cerebellar

receiving VL thalamic nuclei. **(C)**, **(D)** and **(E)** Adjacent sections through the motor thalamus (-1.3 mm relative to Bregma) stained for Calbindin 1, GAD67 and VGlut2. Note the partial overlap of GAD67+ zone and Calbindin1-expressing cell bodies in VM thalamus. **(F)** Schematic of small (~75 nl) viral injection in medial substantia nigra pars reticularis (SNr) in PV-IRES-Cre mice allowing anterograde viral tracing of SNr projections to thalamus. **(G)** Injection site image showing transduced PV GABAergic projection neurons in medial SNr, SNc and red nucleus. There is no transduction of putative dopaminergic neurons (tryosine hydroxylase, TH-positive). **(H-J)** Colocalisation of GAD67+ (red) and ChR2-YFP (green) expressing terminals of SNr PV+ cells projecting to motor thalamus, confirming the reliability of GAD67 immunopositivity to define the borders of the basal ganglia recipient zone in mice. **(K)** Confocal microscopy images of ChR2-YFP expressing terminals of SNr PV+ cells forming putative axo-somatic synapses onto Calbindin-1 positive cell bodies within VM thalamus (white arrow). Abbreviations: MTT, mamillothalamic tract (lies medial to VM); VTA, ventral tegmental area; PC, paracentral thalamic nucleus; SNc, substantia nigra pars compacta; SNr, substantia nigra pars reticulata; Sub, submedius nucleus; VL, ventral lateral nucleus; VM, ventral medial nucleus; VRe, ventral reuniens; ZI, zona incerta. Scale bars: **(A)** 1 mm, **(B-E, G, H-J)** 200 μm, and **(K)** 10 μm.

Given that GAD67 appeared to faithfully mark the basal ganglia input zone (BZ), we compared its relationship to cerebello-thalamic projection fibres mapped using anterograde viral tracing from the contralateral deep cerebellar nuclei (DCN) at multiple levels through the thalamus in the coronal plane (Figure 3.2). Cerebellar projection fibres were densest laterally, superolaterally and superior to BZ but also traversed it (Fig 3.2Bii-iii, Cii-iii, Dii-iii, Eii-iii). Some fibres were also visible in the thalamus ipsilateral to the injection site (Fig 3.2Bii), and dense cerebellar targeting of other thalamic nuclei was present such as intralaminar nuclei (centromedian, paracentral, centrolateral, and parafascicular) and lateral posterior nucleus. In general, this pattern supports some degree of segregation of post-synaptic targets in motor thalamus of cerebellar and basal ganglia input in mice.

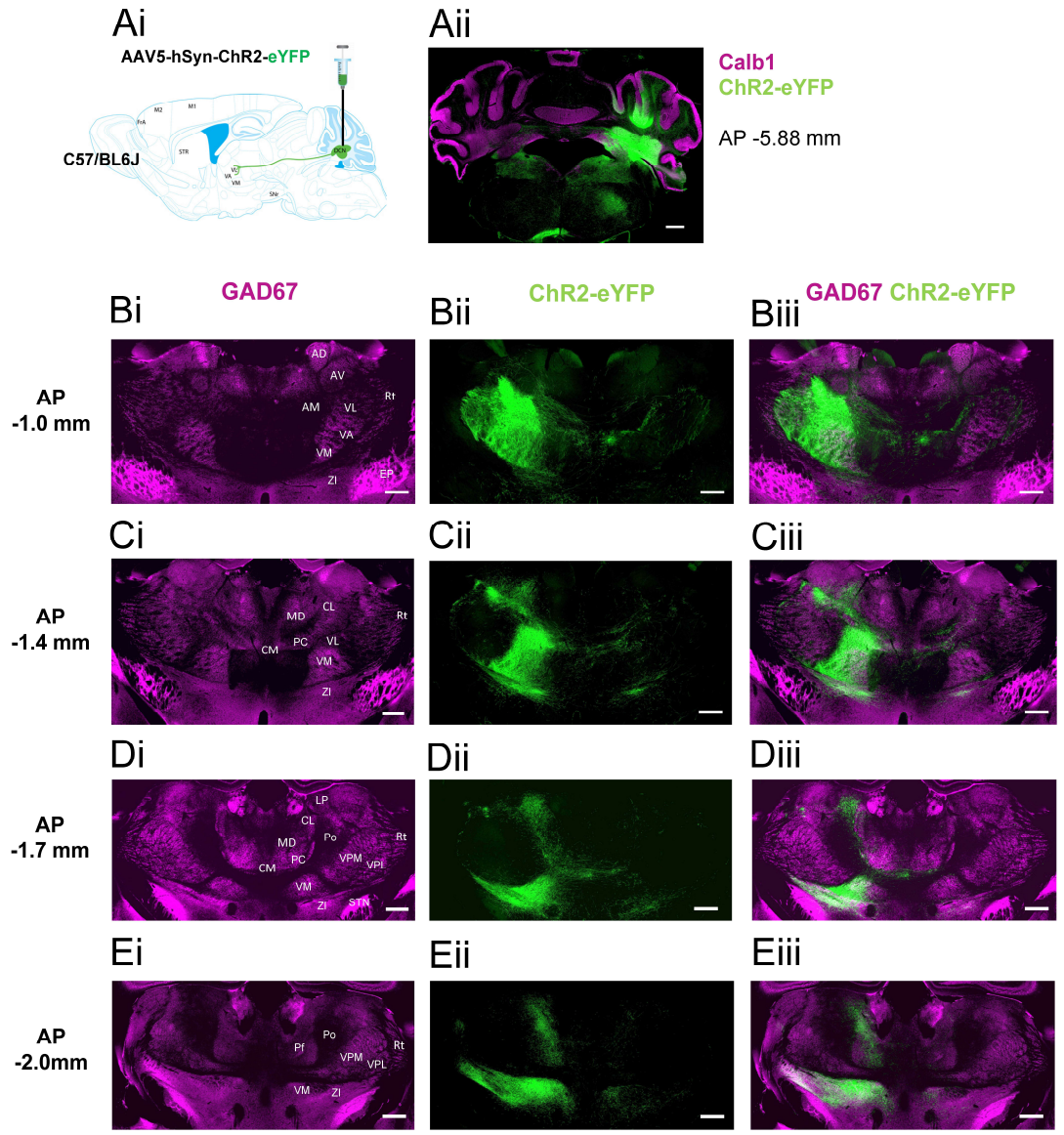



**Figure 3.2 Comparison of thalamic GAD67+ zones and projection fibres from deep cerebellar nuclei. (Ai)** Schematic of unilateral viral injection in deep cerebellar nuclei utilized to anterogradely trace projections to contralateral thalamus. **(Aii)** Injection site in cerebellum of brain utilized for panels in this figure. Calbindin 1 (Calb1) is expressed in cerebellar Purkinje cells. Coronal sections through the thalamus at AP -1.0 mm (Bi-Biii), - 1.4 mm **(Ci-Ciii)**, -1.7 mm **(Di-Diii)** and -2.0 mm **(Ei-Eiii)** relative to bregma demonstrating the passage of cerebellar projection fibres through the basal ganglia recipient motor thalamus (GAD67+ zone of VM-VA thalamus). Most eYFP positive fibres are visualized in the contralateral ZI, AM, VM, VA, VL, CM, PC, CL, LP, although sparse fibres are also seen in ipsilateral thalamus. Abbreviations: AD, anterior dorsal nucleus; AM, anterior medial nucleus; AV, anterior ventral nucleus; CL, centrolateral nucleus; CM, centromedian; EP,

entopeduncular nucleus; LP, lateral posterior nucleus; MD, mediodorsal nucleus; MTT, mamillothalamic tract (lies medial to VM); PC, paracentral nucleus; Pf, parafascicular nucleus; Po, posterior nucleus; Rt, reticular thalamus; SNc, substantia nigra pars compacta; SNr, substantia nigra pars reticulata; STN, subthalamic nucleus; VPM, ventral posteromedial nucleus; VPL, ventral posterolateral nucleus; VTA, ventral tegmental area; ZI, zona incerta. Scale bar in **(Aii)** 500 μm; **all other panels** 200 μm.

### 3.4 Anterograde transsynaptic trafficking of WGA-Cre from substantia nigra or deep cerebellar nuclei can target distinct populations of post-synaptic motor thalamus neurons

To test whether populations of basal ganglia- or cerebellar-recipient motor thalamus neurons are segregated in mice, we leveraged specific properties of the circuit (non-reciprocal connections) and recently developed viral tools. In the rodent, the bulk of SNr projections target the ventromedial nucleus of the thalamus. To target only the neurons in VM which received SNr input, we wanted to assess the viability of an anterograde transsynaptic approach to deliver Cre recombinase. The nigrothalamic projection was ideal for this for the following reasons: i) there is sufficient spatial separation between SNr and VM to avoid direct viral spread (unlike EP and VM), ii) there are no reciprocal projections between thalamus and SNr (ensuring viral or viral product transfer is to postsynaptic thalamic neurons).

C57BL/J6 mice were unilaterally injected in a single session with Cre-dependent channelrhodopsin-2 (AAV5-Ef1a-DIO-ChR2(E123T/T159C)-eYFP) in the VM and AAV5-Ef1a-mCherry-IRES-WGA-Cre in the SNr (Fig 3.3A and C; n = 6). The latter virus expresses mCherry and a fusion protein of Cre recombinase and the polysynaptic tracer wheat germ agglutinin (WGA), which can be transsynaptically trafficked retrogradely into presynaptic neurons or anterogradely into postsynaptic neurons in sufficient quantities to allow low level expression of Cre-dependent constructs (Libbrecht et al., 2017).

In the thalamus, ChR2-eYFP positive cell bodies were highly localised to the GAD67 immunoreactive zone defining VM (Fig 3.3E, left), and a small number in zona incerta. The major cortical target of YFP positive axons was the outer half of cortical layer 1 in motor cortex (Fig 3.3E, right) and frontal association/lateral orbital cortex (not shown). These features are consistent with the expected projection targets of single BZ neurons described previously (Kuramoto et al., 2009; Kuramoto et al., 2015). We hypothesised that targeting thalamic neurons which receive cerebellar input should produce a different distribution of fibres which do not target layer 1 neocortex. As such, C57BL/J6 mice were unilaterally injected with a virus expressing Cre-dependent channelrhodopsin-2 (AAV5-Ef1a-DIO-ChR2 (E123T/T159C)-eYFP) in VL thalamus and AAV5-Ef1a-mCherry-IRES-WGA-Cre in the contralateral deep cerebellar nuclei (Fig 3.3B and D; n = 5). This time, ChR2-eYFP positive cell bodies were localised to the GAD67 immuno-negative zone between VM, intralaminar thalamus and VPL/VPM which form the borders of VL (Fig 3.3F, left). The major cortical target of YFP positive axons was VGLUT2+ cortical layer 5b in motor cortex (Fig 3.3F, right) with minimal to no fibres in (densely VGLUT2 immunoreactive) layer 1 and Layer 3. These features are consistent with the expected targets of CZ neurons (Kuramoto et al., 2009). Distribution of YFP fluorescence intensity was performed in BZ and CZ mice and compared with markers for cortical layer 2 (Wfs1) and layer 5 (Ctip2) which confirmed this (Fig 3.3I-J).

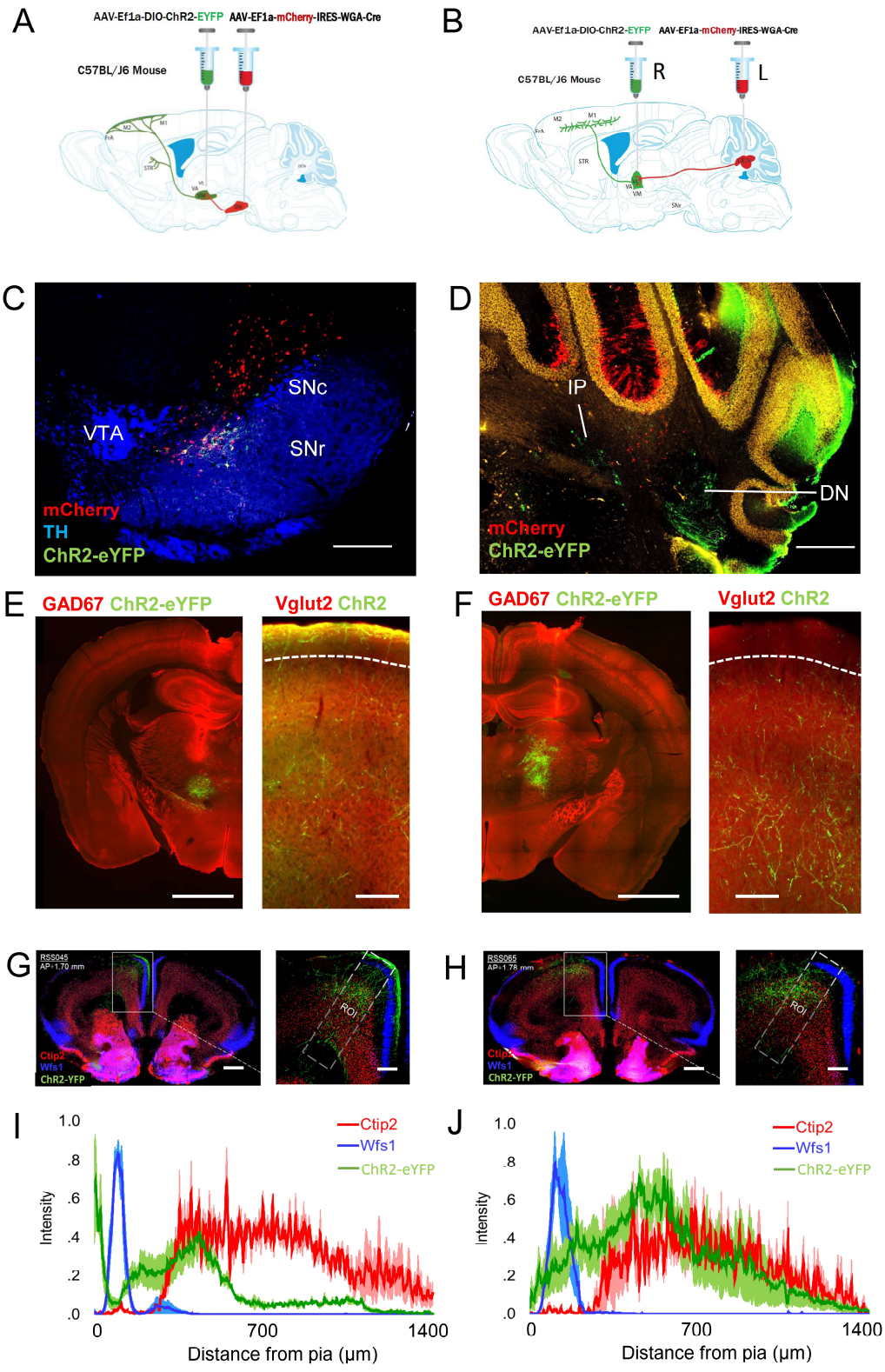



**Figure 3.3 Anterograde transsynaptic tagging from basal ganglia or cerebellar output nuclei targets distinct populations of motor thalamus neurons. (A)** and **(B)** Schematic showing dual virus targeting strategy where Cre-dependent channelrhodopsin expression in post-synaptic motor thalamus neurons is determined by transsynaptic delivery of WGA-Cre via pre-synaptic terminals arising from

substantia nigra pars reticulata (SNr) or deep cerebellar nuclei (DCN). Briefly, SNr or DCN neurons were infected with a virus (AAV-Ef1a-mCherry-IRES-WGA-Cre) driving expression of WGA-Cre (Cre recombinase enzyme fused to the transsynaptic tracer wheat-germ agglutinin) which is then anterogradely trafficked into post-synaptic thalamic neurons over weeks. Simultaneously, neurons in the motor thalamus were infected with a Cre-dependent viral transgene (coding for a light sensitive ion channel channelrhodopsin-2 [ChR2] and yellow fluorescent protein; AAV-Ef1a-DIO-ChR2(E132T/T159C)-eYFP). As such, transgene expression in the motor thalamus only occurs in those neurons having transsynaptically received WGA-Cre via a given pre-synaptic input from SNr or DCN. This approach allows selective study of motor thalamus neurons with identified input connectivity. **(C)** Injection site in SNr showing non-Cre-dependent mCherry expression in SNc and SNr, and YFP+ cell bodies retrogradely infected with AAV-Ef1a-DIO-ChR2(E132T/T159C)-eYFP delivered to motor thalamus. **(D)** Injection site in deep cerebellar nuclei, again showing mCherry expression and retrogradely infected YFP+ neurons in dentate nucleus (DN) and interpositus nucleus (IP). **(E)** *Left*, thalamic cross section showing localized GFP cell bodies in VM thalamus. *Right*, Motor cortex section in the same mouse showing projection fibres targeting Layer 1a of neocortex as expected. **(F)** *Left*, thalamic coronal section showing GFP positive cell bodies immediately above the GAD67+ border zone with VM/VA. *Right*, motor cortex section in the same mouse showing fibres target mostly deeper cortical layers. **(G)** *Left*, Coronal brain section from SNr-receiving motor thalamus tagged mouse used for laminar fluorescence analysis assisted by staining for Wfs1 (upper layer 2/3) and Ctip2 (layer 5). *Right*, Expanded view of inset RIO on the left image. **(H)** *Left*, Coronal brain section from cerebellar-receiving motor thalamus tagged mouse used for laminar fluorescence analysis assisted by staining for Wfs1 (upper layer 2/3) and Ctip2 (layer 5). *Right*, Expanded view of inset region of interest (RIO) on the left image. **(I)** and **(J)** Mean fluorescence intensity profiles (± SEM) at various distances from the pia (0-1400 μm) in the areas shown in **(G)** and **(H)** respectively. Signals from Wfs1 and Ctip2 immunostaining, which mark upper layer 2/3 and layer 5 neurons, respectively, shows that basal-ganglia receiving neurons show high intensity in layer 1 and lower intensity in layer 3 and 5, while cerebellar receiving neurons show low intensity in layer1, higher intensity in layer 3 and peak intensity in layer 5. Scale bars: **(C)** 200 μm, **(D)** 250 μm, **(E)** and **(F)** Left image 1 mm, right image 100 μm; **(G)** and **(H)** Left image 500 μm, right image 300 μm.

To confirm whether these anatomical differences may have obvious functional consequences for cortical information processing we undertook electrophysiological recordings (Fig 3.4Ai) in mice with ChR2 expression in either basal ganglia- or cerebellar-recipient motor thalamic neurons. Unilaterally injected mice were anaesthetised 8 weeks after viral injection and placed in a stereotactic frame, implanted with bilateral skull ECoG screws (M2; AP +2.5 mm, ML +2 mm) and craniotomy performed over motor cortex. A 32-channel linear probe was lowered to span the full depth of cortex (Fig 3.4i) at the M1/2 border of the ChR2-positive hemisphere (AP +1.0 mm, ML1.0 mm). A 200 μm optic fibre connected to a 473 nm laser was implanted in the thalamus in slightly different locations and depths for BZ or CZ stimulation. Isoflurane anaesthesia was then kept at 0.8-1.2% during light stimulation protocols (at various frequencies and light powers; only data for 5 ms pulse trains at 25 Hz in single animals shown). Single animal normalised (z-scored) LFP recordings during BZ (Fig 3.4C) or CZ (Fig 3.4E) stimulation show differing profiles of cortical activation, with CZ neurons provoking strong responses in deep layers and BZ having a more diffuse effect.

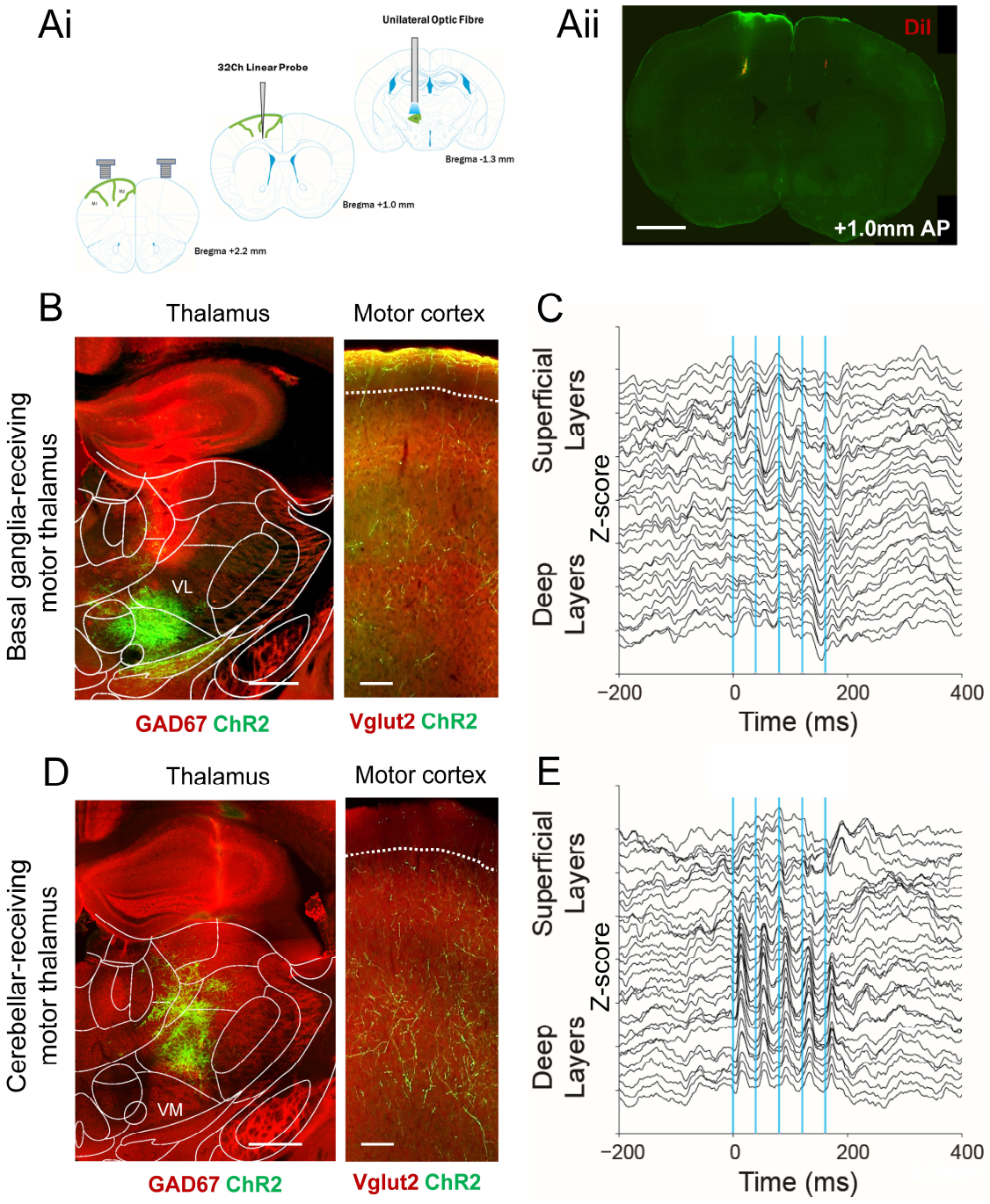



**Figure 3.4 Optogenetic mapping of transynaptically identified basal ganglia- or cerebellar-recipient motor thalamus neurons shows distinct patterns of cortical activation in mice. (Ai)** Schematic of recording arrangement for silicone probe recordings. **(Aii)** DiI labelling of cortical recording sites (bilateral) on border M1/M2 cortex (scale bar = 1 mm). **(B)** *Left*, Selective expression blue light-activated channelrhodopsin-2 (green) isolated to BG-MThal neurons in VM. *Right*, The axons of these thalamic neurons primarily innervate superficial cortical layers of the motor cortex. Basal ganglia terminals in MThal are GAD67+ while thalamocortical terminals in cortex are Vglut2+. **(C)** Single mouse recording

of electrical activity (local field potentials) across all layers of motor cortex using a linear 32-channel electrode during 25 Hz optogenetic stimulation of BG-MThal (blue lines indicate timing of light pulse). The average activity from 50 sets of 5 x 5 ms light pulses for each cortical electrode contact is shown as a z-score relative to the mean signal for that contact. In line with the projections, current flow is strongest in the superficial layers. (**D)** Isolated expression of ChR2 (green) in CB-MThal neurons in VL (*left*). The projections of these thalamic neurons primarily innervate deep layers of motor cortex (*right*)**. (E)** In line with this**,** light pulse stimulation of the neurons in CZ results in current flow in the deeper cortical layers. Scale bars = 500 μm (thalamus) and 100 μm (motor cortex). Together these stimulation protocols demonstrate that BG-MThal and CB-MThal neurons are functionally distinct populations in mice and modulate cortex in different ways.

Overall, although these findings suggested that we were able to selectively target the distinct motor thalamus neuron populations of interest to us, we also appeared to suffer from the low efficiency of viral transgene expression as reported by others (Libbrecht et al., 2017; O'Shea et al., 2018). As such, we thus undertook cell counting in VM to quantify how many transsynaptically targeted cell bodies were present in mice unilaterally injected with AAV5-Ef1a-DIO-ChR2(E123T/T159C)-eYFP in VM and AAV5-Ef1a-mCherry-IRES-WGA-Cre in the SNr. Coronal brain sections (approximating bregma AP -0.8 mm,-1.0 mm, -1.2 mm, -1.4 mm, -1.6 mm) from three mice were co-stained for GFP and GAD67 and the number of neurons in VM (defined by GAD67 intensity) or not in VM but still in thalamus or zona incerta were counted. Mean number of GFP+ neurons in VM were 6.88 ±1.51 (range 0-18; n = 3 mice) and in non-VM 23.88±3.80 (range 1 - 45; n = 3 mice), with the majority of non-VM neurons being in the zona incerta and the rest either in intralaminar or mediodorsal thalamus which are known to receive branches of the same SNr axon (Heise and Mitrofanis, 2004; Cebrian et al., 2005). Recent studies of thalamic neuron density and total neurons in visual thalamic nuclei (Evangelio et al., 2018; Keller et al., 2018) and expansion microscopy of the whole brain suggest that the VA-VL complex contain ~110, 000 neurons while the VM nucleus has ~60,000 neurons (Murakami et al., 2018). Given that VM thalamus is extends ~1 mm in the AP plane

and that we sampled using 50 µm thick sections, one can extrapolate that we may have tagged 120 VM neurons in total (~0.2% of total VM population) with an optogenetic construct.

### 3.5 Direct targeting of VM or VL thalamus in Vglut2-cre mice shows differences in the density of laminar targeting

Although not routinely reported, studies reporting behavioural effects from using optogenetic tools, and specifically ArchT, usually silence a significant proportion of cell type-specific neurons in the brain area of interest (Tecuapetla et al., 2016; Trouche et al., 2016). As we aimed to understand the behavioural contribution of neurons in BZ/VM vs CZ/VL our highly selective transsynaptic approach would not be targeting a meaningful number of neurons in either nucleus. Given our primary goal was to manipulate neurons during behaviour, we felt this would be better done using conventional targeting strategy in a Cre-dependent mouse line. As such, we utilised the Vglut2-Cre mouse line which targets glutamatergic thalamocortical neurons and has been used to target thalamic nuclei previously (Parker et al., 2016; Diaz-Hernandez et al., 2018). Small volume (~75 nl) injections of AAV5-CAG-Flex-ArchT-GFP were performed in either VM (n = 4 mice) or VL (n = 3 mice). Although there was much more thalamic viral transgene expression than using the WGA-Cre approach, a degree of expected laminar selectivity pattern is retained (i.e. VM injections targeting layer 1 vs VL injections targeting layer 3-5), but restricted to M2/frontal association areas but not more posteriorly in M1 (Fig 3.5Ci-ii, Di-ii). Furthermore, transgene expression is likely to be greater and less specific than the volume of ArchT-expressing neurons modulated by the cone of light. Given that ArchT needs minimum irradiance of > 7 mW/mm$^2$ to induce peak photocurrent levels (Han et al., 2011), using an online brain-tissue light penetration calculator (https://web.stanford.edu/group/dlab/cgi-bin/graph/chart.php) suggests that for a 200 µm fibre outputting 20 mW power at the tip this would only extend for ~800 µm in depth. Of note, when immunostaining for ArchT-GFP localisation was performed in mice who received chronic optogenetic stimulation we found consistent evidence of reductions in GFP expression in

close proximity to optic fibre tip position (Fig 3.5A, B, and Ei) resulting in a 'halo' effect. Mice who had also been injected with ArchT but undergone a single optrode recording did not demonstrate this pattern (Fig 3.5Ei) and although DAPI staining in the area did not show absence of nuclei (Fig 3.5Eii), this may indicate a chronic thermal tissue effect (e.g. altered protein expression, induction of apoptosis) in addition to purely within session silencing of thalamic neurons.

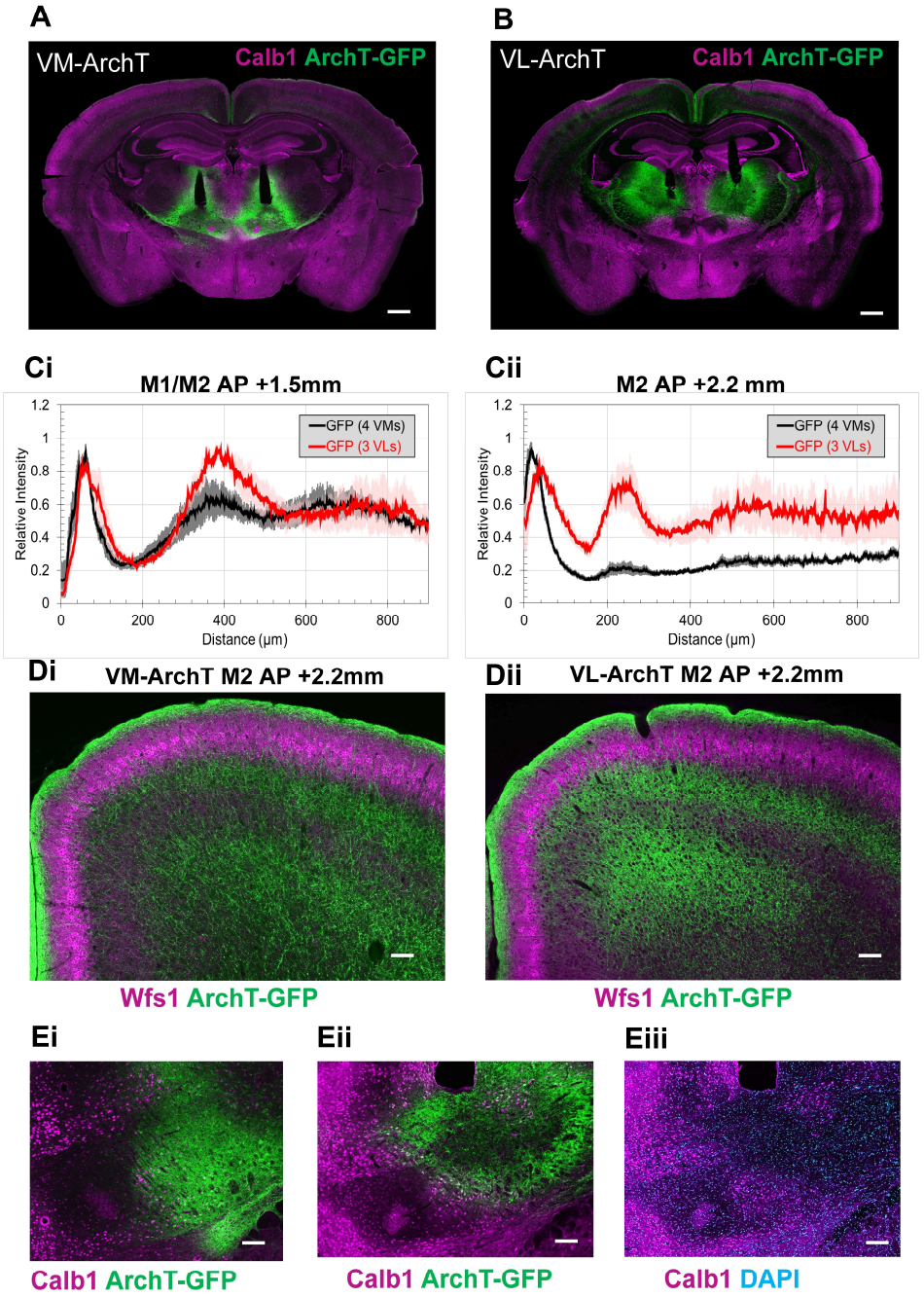



**Figure 3.5 Targeting VM and VL thalamic nuclei in Vglut2-Cre mice results in a degree of differential targeting in frontal cortex. (A)** and **(B)** Example injection and optic fibre implantation sites for VM-ArchT and VL-ArchT mice respectively. Calbindin 1 (Calb1) staining highlights the location of VM thalamus. **(Ci)** and **(Cii)** ArchT-GFP mean fluorescence intensity profile (± SEM) across cortical laminae in motor cortex at +1.5 mm AP or +2.2 mm AP respectively analysed in single hemispheres from VM-ArchT mice (black line; n = 4 mice) or VL-ArchT mice (red line; n = 3 mice). There is minimal difference at +1.5 mm AP, but more anteriorly VL-ArchT mice have greater projection

intensity in lower cortical layers. **(Di)** and **(Dii)** Example of cortical projection fibres at AP +2.2 mm in VM-ArchT or VL-ArchT mice, respectively. Wfs1 immunostaining is used to identify neocortical layer 2. Note the slightly denser patter of GFP positive fibres in deeper cortical layers in Dii. **(Ei)** VM thalamus expressing ArchT-GFP imaged after a single optogenetic probe recording. **(Eii)** Halo appearance of VM/VAL thalamus expressing ArchT-GFP after chronic optogenetic stimulation. **(Eiii)** DAPI counterstaining in the same section does not show any focal loss of nuclei. Scale bars: **(A) and (B)** 500 μm; **(Di) and (Dii)** 100 μm; **(Ei), (Eii), and (Eiii)** 150 μm.

### 3.6 Discussion

With the ultimate aim of studying the distinct contributions of basal ganglia-thalamic and cerebellar-thalamic pathways to motor skill learning we attempted to use a dual virus targeting strategy in wild type mice to selectively target basal ganglia- or cerebellar-recipient motor thalamus. As there is no reciprocal output from the thalamus to its subcortical input structures, we were able to anterogradely tag post-synaptic thalamic neurons with a WGA-Cre fusion protein delivered from either SNr or DCN. This allowed expression of Cre-dependent viral transgenes in the motor thalamus in a pattern representative of either SNr or DCN projection targets (Figures 3.2 and 3.3). This approach has confirmed that segregated populations of thalamic neurons receiving either basal ganglia or cerebellar input exist in mice, as in other species. Furthermore, the high selectivity of this approach allowed us to distinguish cortical projection patterns previously described by single neuron tracing in rats. In terms of morphology, SNr-recipient thalamic neurons densely targeted cortical layer 1 over a widespread area (including M1, M2, cingulate and PFC) and showed axonal arbors also in the dorsal striatum as expected. These differences were preserved when optogenetic stimulation was used to identify their laminar responses in motor cortex in example subjects (Figure 3.4). Despite this, only a very small fraction of neurons could be targeted/manipulated using this strategy and so it is unlikely to impair basal ganglia- or cerebellar-thalamocortical information transfer sufficiently to delineate their contribution to behaviour. As such, we performed injections in VM or VL thalamus

of Vglut2-Cre mice and demonstrated that differences in cortical targeting are reproduced to some degree and represent a worthwhile approach to delineating basal ganglia-biased or cerebellar-biased computations during the same motor skill learning task.

Although the data described in this chapter is largely descriptive, it supports the idea that populations of thalamocortical neurons differentially targeted by basal ganglia or cerebellar projections in the mouse thalamus are anatomically and functionally distinct, and show features consistent with findings in other species. Furthermore, it justifies further work aiming to target these populations with greater efficiency, either via advancements in anterograde transsynaptic tracing or use of newly identified cell markers (Phillips et al., 2019) to capture them in novel transgenic mouse lines.

### *3.6.1 Technical considerations*

Although this approach is highly selective and confers the knowledge that neurons being manipulated receive input from either basal ganglia or cerebellar output nuclei it also has several limitations. Firstly, since the AAV-Ef1a-mCherry-IRES-WGA-Cre construct delivered to either SNr or DCN is non-Cre-dependent, local spread of virus to adjacent nuclei also targeting the motor thalamus cannot be excluded. Using viruses at commercially available titres only resulted in a small number of post-synaptic thalamic neurons being tagged as predicted by other work (Libbrecht et al., 2017) and seen in studies using a similar construct for retrograde tagging. Efficiency may be improved by using higher viral titres or only driving WGA-Cre expression without mCherry. These issues limit the use of this highly specific approach in behavioural studies, where activity perturbations in larger numbers of neurons are often desired for a behavioural effect (or to ensure that the absence of an observed behavioural effect isn't due to local compensation).

Although the transsynaptic approach we used may not allow manipulation of a significant proportion of neurons in VM thalamus, it could still facilitate the study of connectivity defined single neurons *in vitro* – either in the thalamus or connected neurons in the cortex in a way that complements recent studies manipulating GABAergic or glutamatergic inputs to motor thalamus (Guo et al., 2017; Gornati et al., 2018) to study the effect on thalamic or downstream cortical activity. These latter protocols, though potentially identifying thalamic neurons receiving cerebellar or basal ganglia input, do not allow direct stimulation or silencing of thalamic neurons themselves and may be subject to known caveats of terminal fibre stimulation (e.g. antidromic activation). Ultimately, other approaches such as population activity monitoring (e.g. GCamp6) while differentially activating cerebellar or basal ganglia projections in the same mouse may shed light on how segregated BZ and CZ neurons really are.

### *3.6.2 Summary*

Our ability to selectively target and manipulate the thalamic neurons in the basal ganglia- or cerebellar-thalamo-cortical pathway lags behind our understanding of the functional diversity of neuronal subtypes based on connectivity, activity patterns, gene expression and location. To our knowledge, attempts to differentially tag postsynaptic thalamic neurons based on their input from basal ganglia or cerebellum have not been attempted before in mice. Although the targeting efficiency of our approach was low and not suitable for behavioural manipulations, this highly specific method provides first confirmation in mice that post-synaptic thalamic neurons receiving cerebellar- or basal ganglia input are likely to be anatomically and functionally distinct and may have differential effects on motor skill learning.

# 4. Designing a novel task to monitor self-paced acquisition of a covert motor skill

## 4.1 Introduction

Motor skills underlie most of our actions such as walking, speech or playing a musical instrument. Learning a motor skill involves organizing actions, or muscle synergies, into novel sequences that can be executed smoothly, accurately and reproducibly to solve a given task (Willingham, 1998; Hikosaka et al., 2002). Studies have demonstrated that the incremental acquisition of motor skills follows two distinct stages: an early, fast learning stage in which considerable improvement in performance can be seen within a single training session and a later, slow learning stage in which further gains can be observed across several sessions (and even weeks) of practice (Ungerleider et al., 2002). Conversely, skill learning can be considered to have cognitive, associative and autonomous stages (Fitts and Posner, 1967). In the initial cognitive stage, you learn which movements are needed to perform a skill and this requires high attentional demand, sufficient feedback, and frequent errors occur. In the associative stage, practice of the skill allows refinement of accuracy and consistency, reduction in the number of errors, greater fluency, and increasing use of intrinsic/kinaesthetic feedback rather than external evidence to know if it was performed correctly. Lastly, in the autonomous stage the sequencing and timing of subroutines becomes automatic, requires little conscious attention, and demonstrates high levels of smoothness, efficiency, and accuracy without stress. Notably, recovery of motor skills after brain injury involves a mixture of relearning and spontaneous reinstatement of lost functions, as well as adaptation and compensation via spared, residual function. Thus, mechanisms that support learning in the intact brain should mediate motor relearning and adaptation in the injured brain (Nudo, 2013).

Paradigms to study motor skill learning come in two main categories: i) measuring the incremental acquisition of movements into a well-executed behaviour (motor sequence learning), and ii) measuring the ability to compensate for environmental changes (motor adaptation) (Olveczky,

2011). In humans, motor adaptation tasks include force field adaptation of reaching and visuomotor adaptation (Held and Freedman, 1963; Chen et al., 2006), while motor sequence learning tasks involve learning sequential finger movement or multi-button press sequences, which can be varied in complexity/number and frequency (Lehericy et al., 2005; Bonstrup et al., 2019). In rodents, examples of motor adaptation tasks include the accelerating rotarod (Dunham and Miya, 1957; Cao et al., 2015), while another type of task relies on reaching and forepaw dexterity to manipulate uncooked pasta (Ballermann et al., 2001; Whishaw et al., 2017), food pellets (Guo et al., 2015a; Wang et al., 2017) or water droplets positioned in difficult to reach places (Galinanes et al., 2018). In rodents, motor sequence learning involves ordering simple actions (e.g. lever presses or nose pokes) into sequences of varying complexity or difficulty, either through trial and error (operant) or using sensory cues. Sequence complexity is commonly imposed through either the number of sequence elements, minimum speed/frequency of execution, or timing accuracy (e.g. minimum duration of lever hold, or specific timing between two sequence elements) (Kawai et al., 2015). However, compared to the study of brain regions in the performance of already well learnt skills, the study of acquisition of those same skills is complicated by the fact that impaired motor learning of dextrous tasks may be due to a primary impairment in dextrous control, or sequence learning, or both, suggesting that studies of sequence learning should utilise non-dextrous tasks.

Self-initiated or self-timed movements are thought to critically depend on the basal ganglia, such that they are impaired in Parkinson's disease but can be rescued by external cueing (Klaus et al., 2019). Acquisition of self-paced operant lever pressing by rodents relies on the modification of the probability of an initially spontaneous lever press by providing reinforcing consequences to its occurrence (Thorndike, 1898; Skinner, 1938; Ferster and Skinner, 1957). The striatum is important for reinforcement learning and chunking - the process by which sequences of motor actions are concatenated with training (Graybiel, 1998). Self-paced operant lever press tasks which covertly demand mice to perform increasingly concatenated action sequences to continue receiving a fixed reinforcer are associated with activity modulation in motor cortex, striatum, GPe and SNr (Jin et al., 2014; Santos et al., 2015). The output of SNr is

both to brainstem and thalamus, but it is unclear if the basal ganglia-thalamo-cortical pathway itself is required for either the acquisition of temporally-constrained motor sequences requiring a particular mean frequency of pressing (Jin et al., 2014; Santos et al., 2015) and/or those requiring accurate inter-press intervals (Kawai et al., 2015). The cerebellum is thought to function in error correction and control of ongoing movement, but similar lever press sequencing tasks have only recently demonstrated that conditional knock-out of FoxP2 cerebellar Purkinje cells or striatal medium spiny neurons impaired progression through successively higher speed press sequences (French et al., 2019).

Self-paced operant lever press studies in mice have used frequent, small increments in lever press sequence difficulty to reliably improve skill level until a certain level of performance has been reached before studying the effect of circuit perturbations on lever pressing performance (Jin et al., 2014; Santos et al., 2015; Matamales et al., 2017). Such training paradigms are designed to maximise the performance level of the largest number of mice rather than to characterise discrete learning curves. As such, they are not well suited to detect the effects of circuit manipulations on the acquisition of a single challenging target sequence over extended periods of training. Only in rats so far has attention been paid to what proportion of motor output is in the correct sequence, as opposed to incorrect/non-reinforced (Ostlund et al., 2009; Martiros et al., 2018) and how this changes with training. Despite its key position connecting basal ganglia and cerebellum to motor cortex, all three of which have been implicated in motor sequence learning in humans, no studies have monitored motor thalamus activity during motor sequence learning. We hypothesised that acquisition of a skill requiring both sequence and timing constraints may require basal ganglia-thalamo-cortical and cerebellar-thalamo-cortical information transfer. In this chapter, an operant task with a clear learning curve and subsequent stable performance period is first designed to ultimately allow testing of this hypothesis.

### 4.2 Experimental aims

1) To build an optogenetics-capable operant behaviour setup and augment it to maximise behavioural monitoring of lever press dynamics

3) Identify the maximal range of early variability of mouse lever pressing through a single unexpected non-reward session and used this to identify a suitable covert target pattern for mice to acquire over sessions.

4) Demonstrate a learning curve in key parameters of a novel sequence acquisition task, and characterise this behaviour based on lever pressing structure, overall action structure (pressing, head entry, licks) or other custom signals.

### 4.3 Adapting a commercial operant chamber for detailed behavioural monitoring

There is an increasing expectation that *in vivo* rodent studies should attempt to inform or map onto human behaviours commonly compromised by neurological disease. Although some types of rodent behaviour may be innate and require little additional apparatus to study (e.g. exploration in an open field), many behaviours of interest in motor and cognitive neuroscience require purpose built electro-mechanical devices and the knowledge of how to program them. Furthermore, commercially available systems are generally expensive, often provide only binary readouts of behavioural events (at most with durations but without amplitude/magnitude) and are less customisable as research demands change. As such, there is a growing movement of open source and home-brew low-cost alternatives for behavioural apparatus, often controlled through Arduino microprocessor boards, and it has understandably become the favoured option where commercial options are not yet available. For those lacking the prerequisite skills and experience, this route may require a significant time investment and risks increasing reproducibility gap by introducing variability in the kinematics of response devices (e.g. levers, joysticks) between labs and, potentially, the nature of motor responses the experimenter may see compared to that reported in the literature.

Given that cued behaviour has slightly different circuit dependency to purely self-initiated movement (Klaus et al., 2017), we were interested in studying self-paced mouse operant lever press behaviour in the extensively used Med Associates operant chambers (Yin, 2009; Jin and Costa, 2010; Jin et al., 2014; Tecuapetla et al., 2014; Santos et al., 2015; Tecuapetla et al., 2016; Matamales et al., 2017). The architecture of these operant chambers records events as either single timestamps (onset or offset; 'toggle' mode) or their duration ('level' mode). As such, we adopted this setup but optimised each chamber to output durations of behavioural events (e.g. head entries, lever presses) as variable length TTL pulses in real-time to an external acquisition system (RZ5P, Tucker Davis Technologies) capable of integrating this data with video monitoring or other custom behavioural signals, as well as generating TTL signals capable of triggering lasers or other equipment (Fig 4.1A and B). A single-axis lightweight accelerometer (AD326XL, Analog Devices) capable of continuous analogue output was retrofitted into a standard Med Associates ultra-light retractable lever (Fig 4.1C) allowing us to capture finer grain details of forces applied to the lever and identify lever related events (e.g. press onset time, subthreshold presses, or presses occurring when the lever was already breaking the infrared beam) which are normally not detected by the Med-PC software due to the reliance of the lever on a infra-red beam break registration system. Normally, Med Associates levers only register a press if the lever is moved through > 50% of its arc (there is a 4 mm maximum vertical range in lever position, hence > 2 mm motion has already occurred before a press is registered), and must return below this before another lever press can be registered (Fig 4.1D). Presses that either do not move the lever enough or occur when the lever is already > 50% of its arc go unregistered despite being initiated by mice. Although not a true readout of lever position such as that achieved in studies utilising a joystick potentiometer (rather than a lever), accelerometer data can be used in conjunction with existing Med-PC lever timestamps to provide a higher resolution picture of lever press vigour without the need for expensive high-speed cameras in each chamber and the associated data storage demands. Furthermore, the first deflection in the accelerometer trace is when the mouse actually initiates the lever press and is not detected by Med Associates equipment. In summary, behavioural timestamps (lever press, magazine entry, licks)

were collected with a 10 ms resolution, lever accelerometer data was collected with 6 kHz resolution, and video at 10 fps.

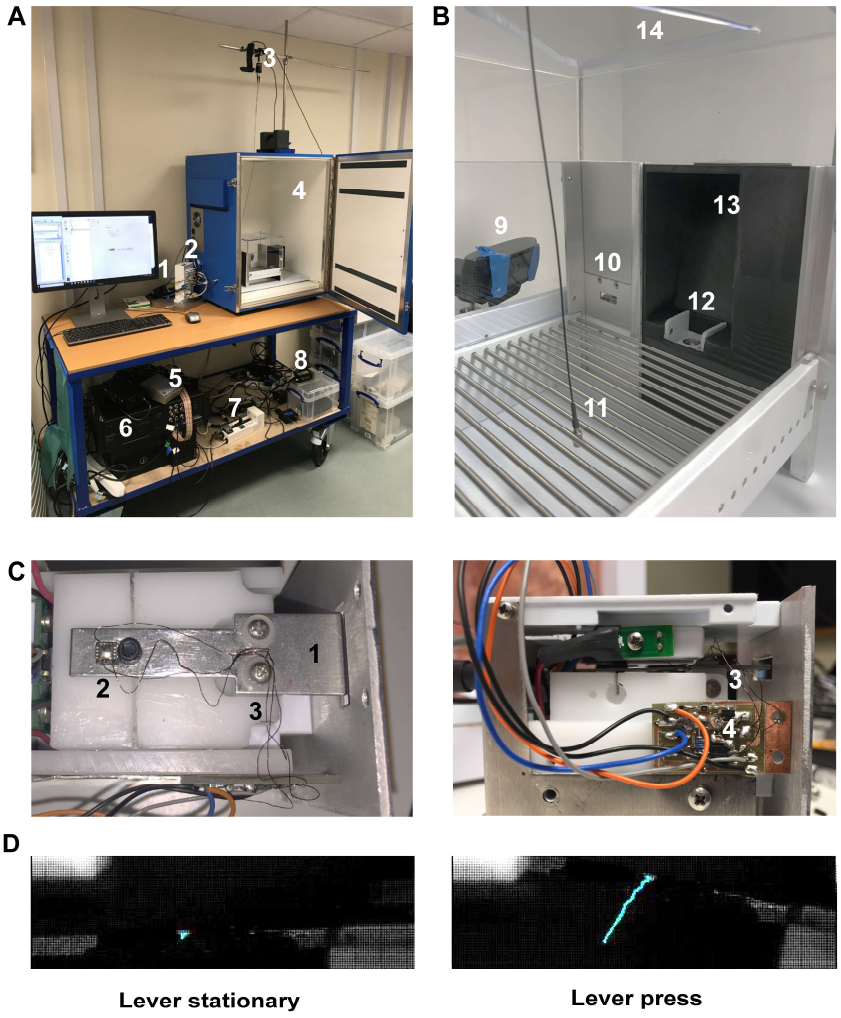



**Figure 4.1 Recording setup for operant lever pressing. (A)** Single behavioural rig. 1, Custom 28V to TTL converter; 2, Med-PC Interface box; 3, Fibre optic rotary joint; 4, Sound attenuating chamber housing operant box; 5, accelerometer control unit; 6, TDT Acquisition box; 7, syringe pump; 8, laser. **(B)** Inside view of customized operant chamber. 9, Webcam; 10, Retractable lever; 11, Dual fibre optic patch cable; 12, Liquid delivery cup with infra-red head entry detector; 13, custom printed wall opening compatible with implants and tethers; 14, custom roof opening for patch cord. **(C)** Lever accelerometer (top view, *left*, and side view, *right*). 1, Lever paddle; 2, Accelerometer position; 3, low tension copper enamel wires powering accelerometer and collecting analogue output; 4, circuit board for accelerometer. **(D)** Offline tracking of lever movement from resting (*left*) to fully pressed (*right*) position during mouse lever press using idTracker software (Perez-Escudero et al., 2014) with 150 fps video recording.

## 4.4 Extinction-induced motor variability in operant lever pressing identifies a demanding covert target for motor skill learning in mice

Frustration has a well-documented function of increasing motor variability in lever pressing in mice and is seen early during extinction training when mice no longer receive the reinforcer they were expecting on performing a previously learnt lever press (or sequence) (Burokas et al., 2012). The increased exploration of parameter space (timing, frequency and number of lever presses) which occurs during frustration response could represent an opportunity for incidental learning of a novel reinforced lever press sequence (Dhawale et al., 2017). A clear motor learning curve could be brought about by asking mice to directly switch from a baseline lever pressing behaviour to one at the limit of their spontaneous dynamic range in a single step, rather than via small increments in press number or minimum frequency. However, previous work has suggested that different mice have different limits of performance (Jin et al., 2014), hence a single large increment in task difficulty is likely to be associated with a much greater risk of mice abandoning the task if their learning ability or motivation is insufficient to meet task demands. Conversely, if the increment is too small it may not produce any clear learning response or may be limited to only the first session. Given that mice may have had significant experimental investment (e.g. viral injections and optic fibre implants) we attempted to identify a complex lever press pattern that most mice already performing fixed-ratio 1 (FR1) operant lever pressing might be able to acquire when introduced covertly but take multiple sessions to consolidate allowing sufficient opportunity to simultaneously monitor and manipulate neural activity.

To pick temporal constraints for a challenging covert target for motor learning in a non-arbitrary fashion, we first characterised the profile of early lever pressing patterns in FR1-trained mice who experienced a single 45 minute session of extinction in their normal operant chamber (Figure 4.2). Briefly, mice were food restricted to 85% of free feeding weight and underwent magazine training until they made > 1000 licks in a 20min session training before being trained on a self-paced fixed-ratio 1 lever pressing schedule. Initially, in the first session they could earn up to 30 x 15 µl

reinforcers once daily, then 60 x 10 µl reinforcers once daily, and then 60 x 5 µl twice daily until they could earn 60 reinforcers of 5 µl sucrose solution (20% w/v) twice daily. This was chosen to maximise lever pressing and based on our experience that food-restricted male mice reliably work for 600 µl of sucrose per day. Reinforcer delivery was unsignalled (e.g. no light or auditory cue), not directly visible to mice while engaging with the lever, and the syringe pump was located outside of the sound attenuating chamber on a different shelf (to minimise any auditory or vibration cue). We used sucrose reinforcer as this could be delivered more covertly in our equipment (in contrast to a food pellet), often in the middle of a press sequence and encouraged mice to make a cost-benefit decision about extra presses. Unlike previous studies which use a FR1 (or continuous reinforcement) schedule without any other constraints to ensure lever pressing is acquired quickly, we used a 'strict' FR1 schedule where licks must have occurred between sequential reinforcer deliveries (Fig 4.2A). This was to discourage mice from performing multiple presses to collect a larger single reinforcer volume per magazine check, and allowed us to have a readout of their efficiency in recognising the underlying rule. Once mice were gaining all 60 reinforcers for 6 sessions (over 3 days) in under 90 presses, they were exposed to the same chamber and lever the following day but without any available reinforcer for 45 minutes (Fig 4.2C-D). We found that mice naturally responded by increasing motor variability (range of inter-press interval) when single presses no longer earned the expected reinforcer (Fig 4.2B vs. D). We found that at the upper limit most mice could naturally press in genuine bursts (i.e. without seeking to check the magazine) was three presses. The occurrence of 3 press 'bursts' was associated with an increase in the number of inter-press intervals < 1s (Fig 4.2Eii and Fii) suggesting that the 1$^{st}$ and 3$^{rd}$ press was generally initiated within 2 seconds of each other (i.e. at least 1.5 Hz pressing). As they could do this early on into the training session, it was more likely to lead to discovery of the new skill requirement rather than outcome devaluation/demotivation. As such, we hypothesised that this may represent a reasonable target sequence for most mice to learn in order to continue receiving a reinforcer.

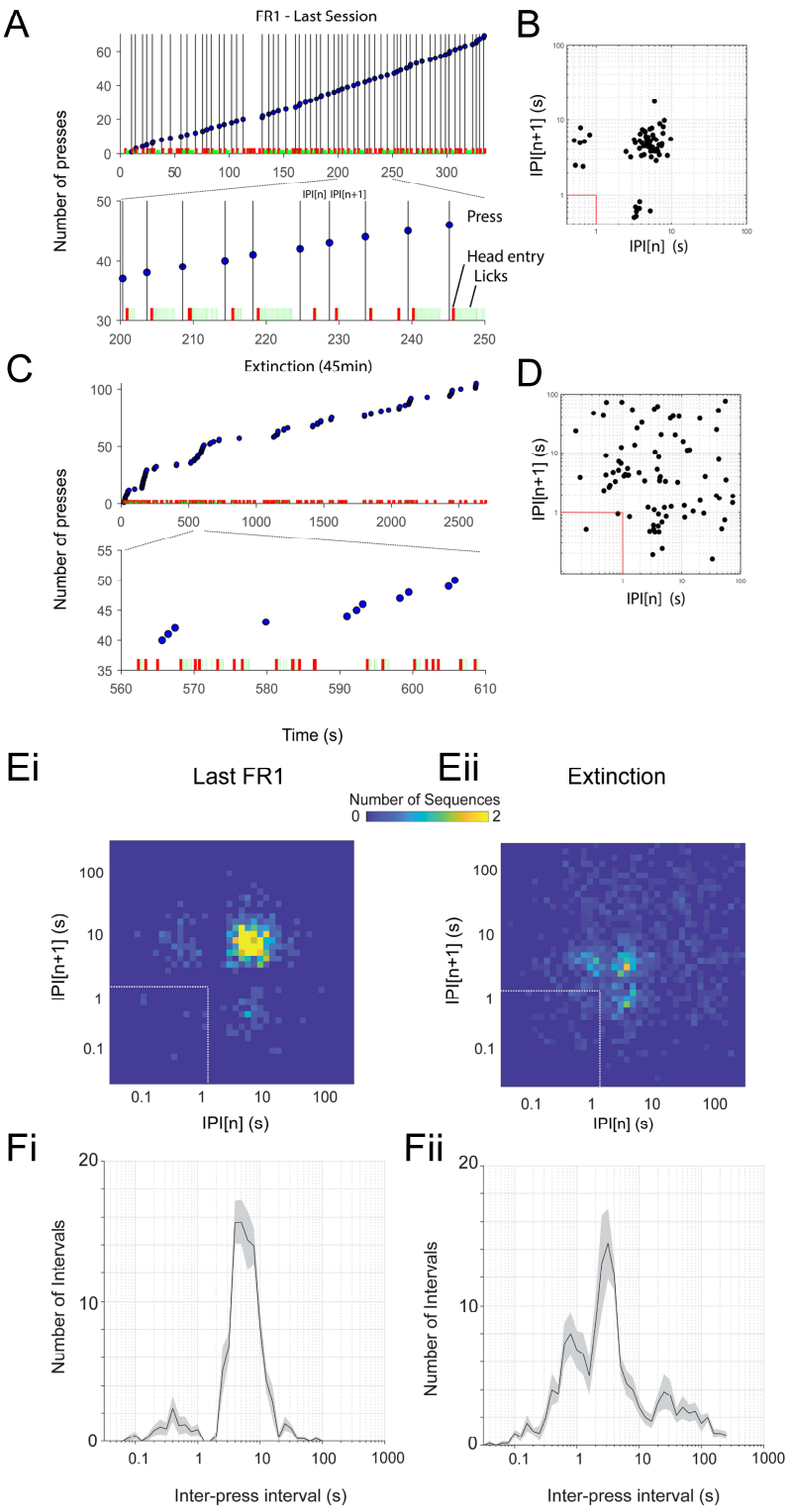



**Figure 4.2 Identifying the patterns of self-paced operant lever pressing elicited by extinction.** Mice already trained in strict fixed-ratio 1 (FR1) lever pressing undergoing extinction respond by varying the temporal pattern of lever pressing. Studying the complexity of pressing responses during extinction can be exploited to identify the maximum incremental change in sequence difficulty that most mice (at the same level) may successfully adapt to if used as a covert target for motor learning. **(A)** Single mouse

example showing pressing, head entry and lick pattern at the end of strict FR1 training (top, left) and **(C)** when subsequently exposed to 45min of extinction (bottom, left). Note the natural emergence of 3 press sequences during extinction as well as the press, head entry, lick microstructure acquired during training. **(B)** and **(D)** Associated return maps of sequential inter-press intervals (IPI) relating to panel **A** and panel **C**, showing increased motor variability in both shorter (faster) and longer (slower) directions during extinction. Each dot plots 2 temporally sequential IPIs ([n] and [n+1]), and thus requires 3 sequential lever presses to have occurred. **(Ei)** and **(Eii)** Mean histograms of the inter-press interval (IPI) return plot for each animal (n = 6 mice) showing more variable lever pressing during extinction, including an increase in sequential IPIs of < 1 s (white box; equivalent to three lever presses occurring within 2s). **(Fi)** and **(Fii)** Mean inter-press interval histograms (n = 6 mice) show an increase in absolute IPIs with a duration under 1s. As such, we targeted three presses with mean IPIs at 1s each (i.e. 2s) as our covert motor learning target for mice trained at FR1.

### 4.5 Mice covertly switched from a strict FR1 to a FR3/2s lever pressing schedule acquire it in the first test session but continue to improve efficiency over days

The ideal operant motor learning task might demonstrate that most animals i) are sufficiently motivated and capable in the pre-test stage to perform the required individual motor components (e.g. number of lever presses per session for given volume of reinforcer), ii) are capable of achieving a reasonable number of reinforcers during the first test session (to limit demotivation or unintended extinction), and iii) find the first and subsequent test sessions challenging enough that performance improvement continues to occurs over multiple training sessions (providing multiple time points for circuit manipulations and their effects to be measured). Circuit manipulations could be done in both the pre-learning, learning and stable performance stages of the task and discriminate if any impairment is due to a primary deficit in learning and/or motor control. Having identified a covert target motor sequence of three presses within 2 seconds (FR3/2s) which most mice could potentially acquire directly from FR1 training (Figure 4.2), we aimed to ensure that effort and reinforcement

remained as matched as possible between the existing and new rule to reduce the risk of motivation-related task abandonment. Since during late FR1 training each lever press would earn a 5 µl reinforcer, we reasoned that in this new FR3/2s schedule, which required three-fold greater actions, every correct sequence should earn a 15 µl reinforcer and mice could earn up to 15 reinforcers in minimum of 45 lever presses and a maximum session duration of 90 minutes. When this paradigm was used (Figure 4.3), we found that, as predicted, mice could acquire the task on the first test session (Fig 4.3A; single mouse example), and refined their pressing strategy over subsequent sessions to become more efficient (Fig 4.3A vs C; B vs D; single mouse example), and this improvement was associated with a new cluster of 3 presses occurring within 2 s (Fig 4.3Ei-iii, Fi-iii; n = 12 mice). Individual mouse trajectories for total lever presses and percentage of bouts with ≥ 3 lever presses show skill refinement over training sessions (Figure 4.4).

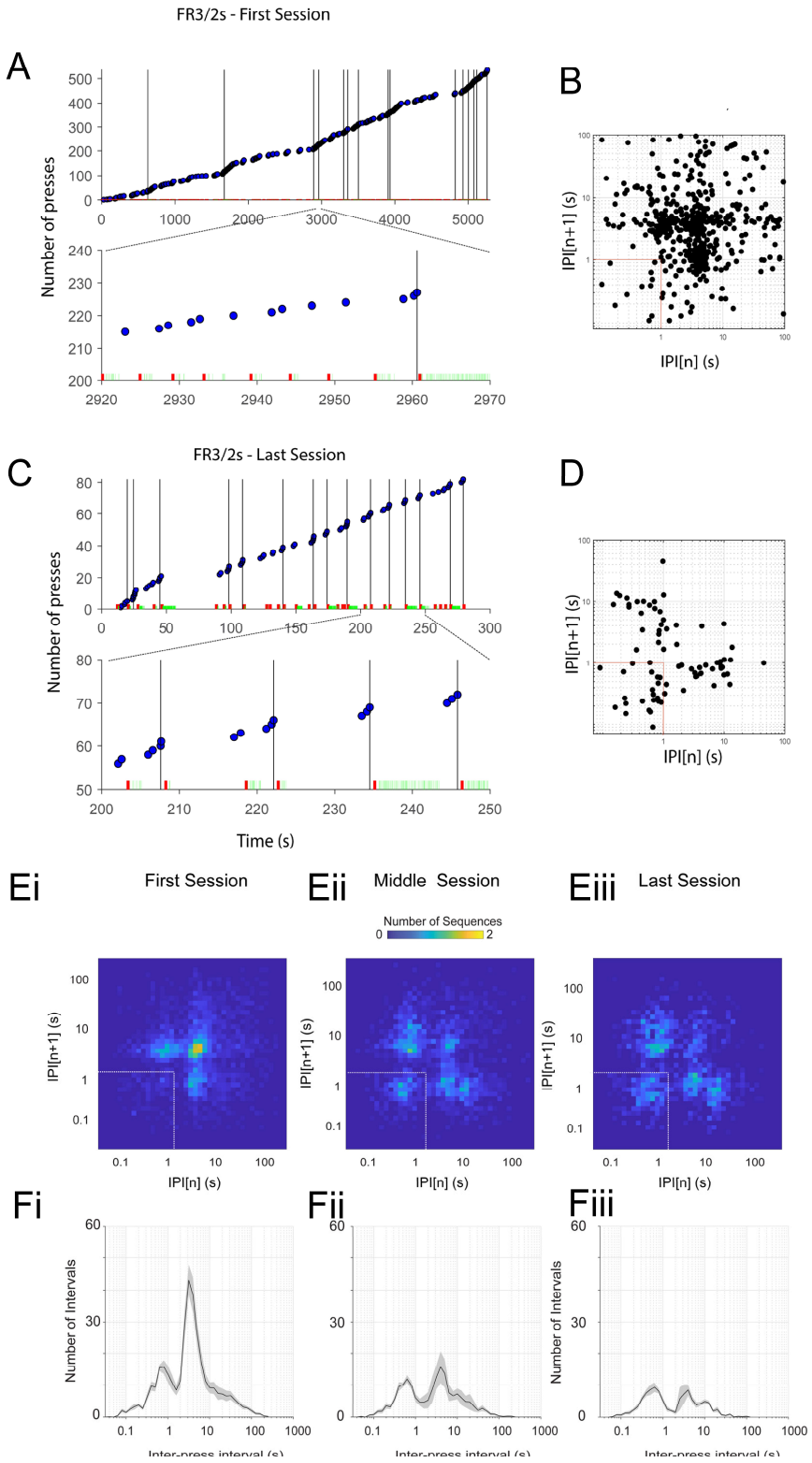



**Figure 4.3 A novel self-paced motor refinement task encouraging mice to acquire a ballistic pattern of lever pressing.** Mice that had competently learned to perform self-paced (uncued) lever presses under a fixed-ratio 1 (FR1) schedule to earn 60 sucrose reinforcers twice daily were covertly introduced to a new schedule where only a three-fold larger reinforcer could be earnt if they performed a burst of three

lever presses within any two second window (FR3/2s). If they gained a minimum of 10 reinforcers successfully during the first session of this new schedule, they were trained on it twice daily and for 7 days (14 sessions). All 15 reinforcers available during the session can be gained in a minimum of 45 presses if mice learn to refine pressing into groups of 3 at ≥ 1.5 Hz. Distinct bouts of pressing were identified in real-time during the session as being separated by licking, magazine head entry, or 2 seconds of no pressing. Single mouse example showing pressing, head entry and lick pattern in the first covert FR3/2s training session (**A**) and last session in training on day 7 (**C**). **(B)** and **(D)** associated return maps of inter-press intervals (IPI) showing an increased variability of lever press timing initially **(B)** which refines with practice **(D)** by the end of training. **(Ei-iii)** 2D histograms of the mean IPI return plot across animals (n = 12 mice) as they progress through early (session 1), middle and last session of training showing a transition in structure of IPI clusters towards the new covert target. **(Fi-iii)** Corresponding IPI histograms show an increase in the proportion of IPIs below 1s required to continue earning the reinforcer. All mice that were able to get > 10 rewards on the first FR3/2s sessions continued to gain reinforcers on all subsequent sessions.

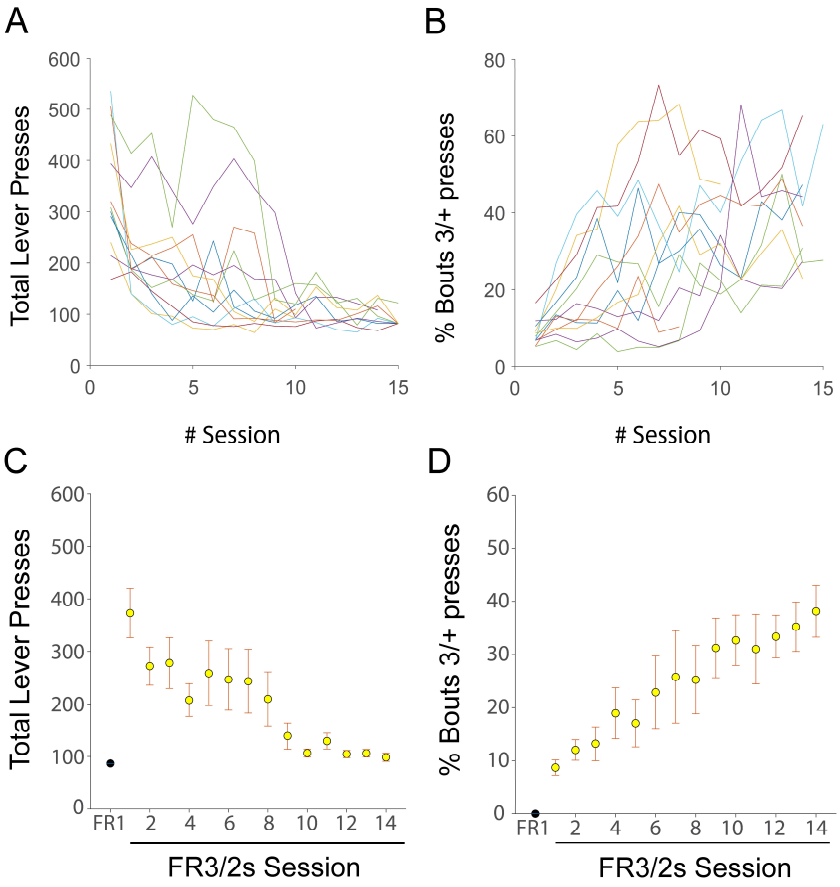



**Figure 4.4 Individual self-paced learning trajectories during acquisition of FR3/2s lever pressing.** Individual learning curves in control mice (n = 12) show **(A)** a convergent decrease in total lever presses required to gain all reinforcers and **(B)** an increase the percentage of pressing bouts with ≥ 3 lever presses over sessions. Mean (± SEM) curves for **(C)** total lever presses and **(D)** percentage of bouts with ≥ 3 presses for all FR3/2s sessions for the same mice (n = 12). Note that the plots include one mouse who only had 8 sessions of training and another who only had 10. Error bars not included for mean value of final FR1 session.

As mice can acquire FR3/2s from FR1 and show consolidation over days we next analysed key parameters which may facilitate this change (Figure 4.5). One-way ANOVA analysis of all control mice who learned the task on the first attempt and also had accelerometer data available for all training sessions (n = 7) was performed for several task parameters using data from session 1 (S1), session 5 (S5), session 9 (S9) and session 13 (S13). This was done by considering the differences

between specific pairs of training sessions (S1 vs S5, S1 vs S9, S1 vs S13, S5 vs S9, S5 vs S13, and S9 vs S13). Total lever presses ($F(3,24) = 7.28$, $p = 0.0012$; post-hoc testing showed this was significant at the $p < 0.01$ level for S1 > S9 and S1 > S13), percentage of bouts with three or more presses ($F(3,24) = 6.41$, $p = 0.0024$), rate of reinforcer delivery ($F(3,24) = 10.43$, $p = 0.0001$; post-hoc testing showed this was significant at the $p < 0.01$ level for S1 < S9, S5 < S9 and S1 < S13), and total session time ($F(3,24) = 6.67$, $p = 0.002$; post-hoc testing showed this was significant at the $p < 0.01$ level for S1 > S9 and S1 > S13) all showed significant differences between training sessions. Magazine head entry rate did not significantly differ between sessions and neither did the mean duration of individual lever presses in bouts with either 1, 2 or ≥ 3 presses.

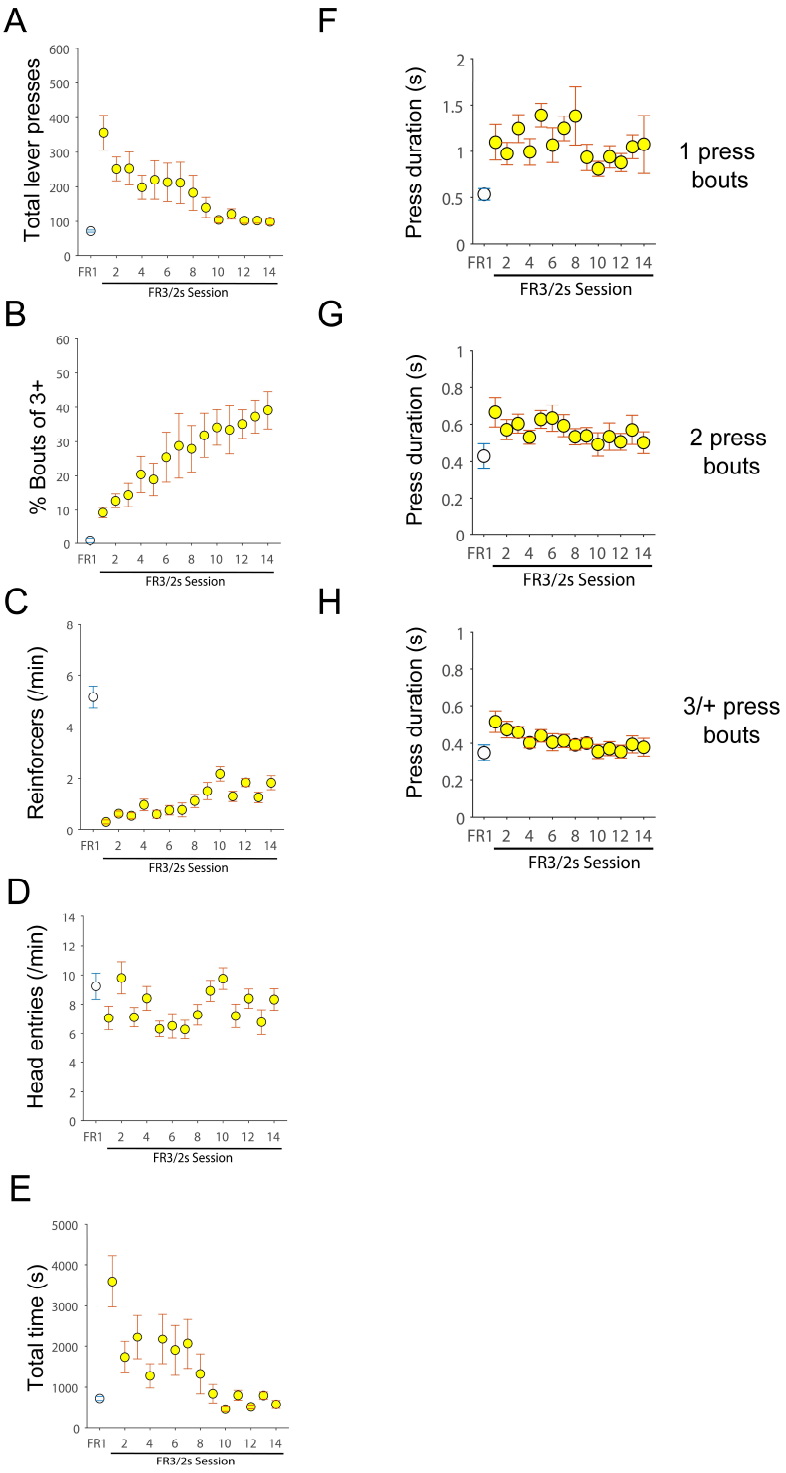



**Figure 4.5 Refinement of multiple task parameters during self-paced acquisition of a FR3/2s lever press sequence in control mice.** Mean group plots of **(A)** total lever presses to gain all reinforcers, **(B)** percentage of pressing bouts which had three or more presses, **(C)** rate of reinforcer delivery, **(D)** frequency of magazine head entry, **(E)** total time taken to gain all reinforcers, and **(F-H)** duration of lever presses for bouts where there was either **(F)** only one lever press, **(G)** two lever presses, or **(H)** three or

more lever presses, are shown for last FR1 and FR3/2s sessions 1-14 (n = all 7 mice with simultaneous lever accelerometer recording). Error bars for each the solid dot (mean value) on each plot represent ± SEM.

### 4.6 Real-time accelerometer data can capture lever dynamics during acquisition of FR3/2s lever pressing

Accelerometers have been increasingly utilised in behavioural neuroscience, often by placing them on head stages or microdrives to give fine grain detail of movements and position during *in vivo* electrophysiology recordings. Alternatively, they can be placed in response devices to obtain information about the vigour of motor responses (Yttri and Dudman, 2016). Commercially available Med Associates operant chambers are fitted with levers for mice which can register presses with a minimum weight of 2 grams (i.e. a force of 0.0196N). A press is registered when the lever is sufficiently pressed over halfway in its full range of motion (~2 mm by the mouse) to break an infrared beam for at least 10 ms. Subsequently, once the beam is re-established for at least 10 ms the pressing event is considered over and another one can be recorded. If a mouse press fails to break the beam from the resting position, or if the mouse presses the lever while it is already breaking the beam (and has not reset), these events will not be recorded by Med Associates equipment – even though the mouse may have perceived to have performed them. Capturing these sub-threshold events may be important in providing more detailed explanations for variability in task performance or response to on-line circuit manipulations. A light weight (< 0.1 g) z-axis accelerometer was retrofitted to the lever (Analog Devices ADXL326) and connected with fine copper enamel wire to avoid altering lever kinematics to a custom circuit board and amplifier and output the signal to our acquisition system.

As accelerometers do not capture position in space like gyroscopes or potentiometers, we analysed high speed video tracking of the actual lever position with the simultaneously recorded lever press and accelerometer signal to determine if it responded to most lever pressing events captured by Med-

PC software (Figure 4.6). Briefly, as mice pressed the lever downward the accelerometer (on the opposite end of the pivoted lever) would move upwards and produce a negative deflection on the accelerometer voltage trace. The trough (most negative) value of this negative deflection corresponds to the peak within-press lever acceleration generated by the mouse (Fig 4.6Eii, immediately to the left of zero timestamp). When the accelerometer end of the lever hits the housing roof, a sudden deceleration produces a much larger upwards deflection on the accelerometer trace (Fig 4.6Eii, immediately to the right of zero timestamp). Large negative deflections in the accelerometer trace (Fig 4.6A) occur when the mouse lets a lever fall from fully pressed and hits its base. Because the dynamics of each press the mouse made differed, the lever did not always experience a sudden deceleration event. As such, every press registered on Med-PC software had a preceding negative accelerometer deflection but not always followed by a large upward deflection.

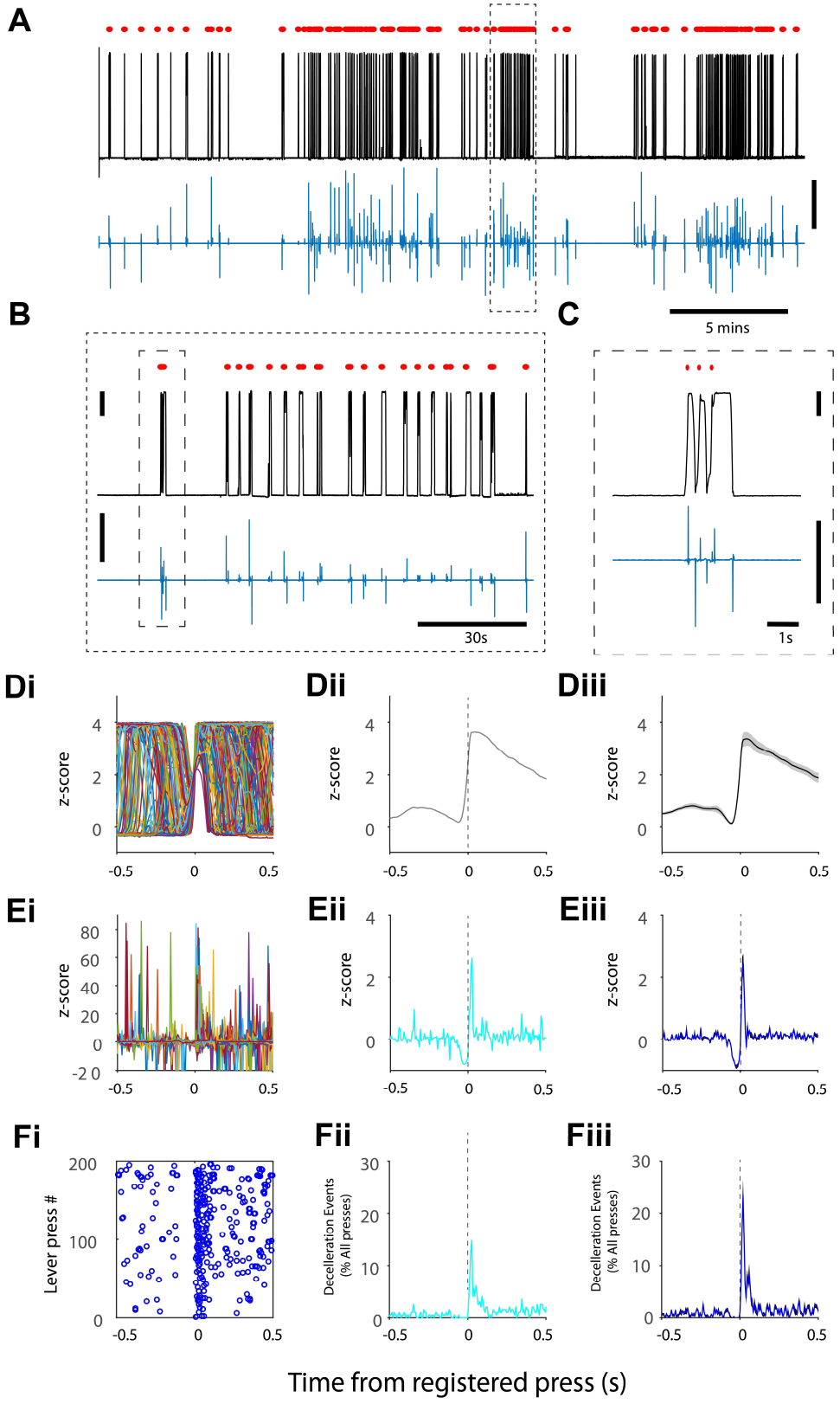



**Figure 4.6 Accelerometer recordings from the lever allow detailed analysis of lever-pressing movement kinematics. (A-C)** Raw traces of lever presses registered by Med-PC (red circles), lever position based on high speed video tracking (black trace, median-filtered difference between x and y positions) and the lever-attached accelerometer (blue trace). **(A)** An entire FR3/2s recording session. **(B)**

A magnified trace corresponding to the data in the closely dashed box in **A**. Note that the accelerometer captures each lever press. **(C)** A magnified trace of the widely spaced box in **B** showing a bout of 3 lever presses. All traces were z-scored across the entire recording. Scale bars show a z-score of 1 for each trace. **(Di)** Individual video tracked lever position traces for each lever press in **A**. **(Dii)** The mean for all the traces in **Di**. The time of the registered lever press (time zero) is highlighted with a dotted line. **(Diii)** The mean (black line) and SEM video-position traces for 8 sessions recorded in 3 different animals. **(Ei)** Individual lever accelerometer traces for each lever press in **A**. **(Eii)** The mean for all the traces in Ei. **(Eiii)** The mean and SEM of the lever accelerometer traces for 8 sessions recording in 3 different male mice. Note that in **Eii** and **Eiii** a registered lever press is preceded by a downward deflection, corresponding to lever acceleration during downward pressing by the mouse, and usually followed by a much larger upward deflection corresponding to sudden lever deceleration as it hits the roof of its plastic enclosure. **(Fi)** Raster plot of deceleration events (upward deflections of the accelerometer traces exceeding a threshold of 0.1) in relation to each lever press (y-axis) in recording **A**. All lever presses are followed by a deceleration event within around 100 ms. **(Fii)** Histogram of the proportion of presses where the deceleration events shown in **F** occur in relation to the lever presses (time zero, dotted line) in **Fi**. **(Fiii)** The mean histogram across 8 recordings in 3 animals.

We thus analysed the greatest acceleration (i.e. most negative value, or trough value) occurring in a 100 ms window before each registered press (Figure 4.7). To see if peak press acceleration changed with learning, we focussed our analysis on only those lever presses in bouts of ≥ 3 presses across all 14 sessions of training (Fig 4.7B). This showed that a significantly positive correlation over training occurred suggesting control mice began to use lower peak within-press acceleration as other learning parameters improved (Spearman's $R = 0.7389$, $p = 0.0025$).

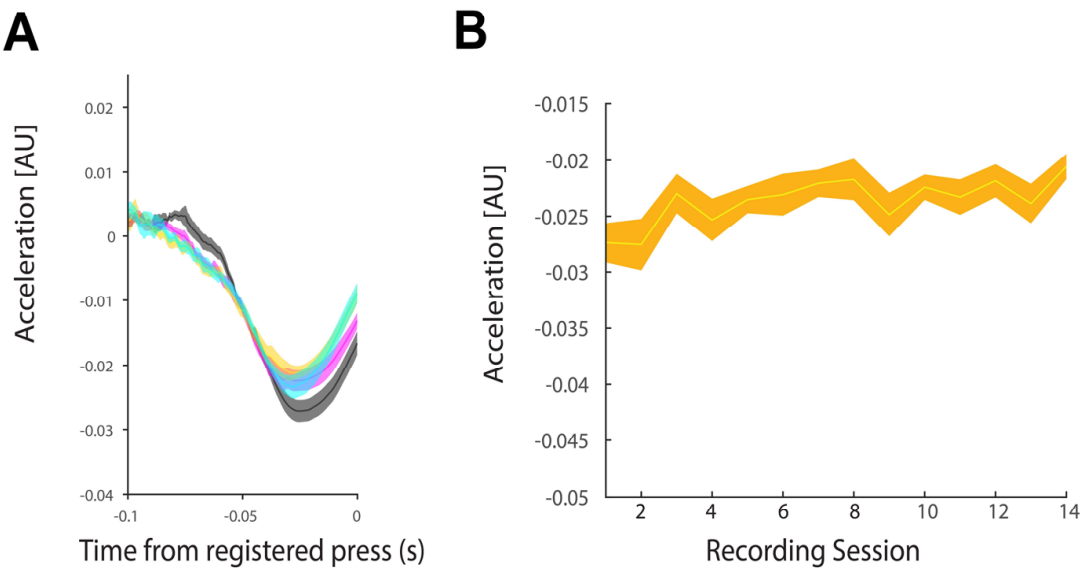



**Figure 4.7 Lever accelerometer recordings during press-initiation from bouts with ≥ 3 presses in control mice. (A)** Median-adjusted accelerometer recordings of lever presses within ≥ 3 press bouts from recordings sessions 1 (black trace), 3 (magenta trace), 7 (yellow trace) and 13 (cyan trace) in control (n = 7) mice. A bigger (more negative) trough in the mean accelerometer trace corresponds to greater peak lever accelerations during press-initiation for all registered presses in that session. Note that in the control mice the trough becomes shallower with training. **(B)** The mean trough values of median-adjusted acceleration in recording sessions 1-14 for untethered control (n = 7, yellow) mice. Shaded areas in all plots show ± SEM around the mean (solid line).

## 4.7 Discussion

Training animals to acquire complex behaviours is generally both time and labour intensive with the further caveat that the more effort required the less reproducible it may be. Due to current trends, much time and expense may already have been invested in an animal (e.g. virus injections, optic fibre or microdrive implantation) even prior to behavioural testing meaning that training paradigms need a high success rate while also addressing novel experimental questions. Nonetheless, both learning ability and motivation varies between subjects making the study of complex, non-innate behaviour challenging. More recently, there has been an expansion in the number of head-fixed tasks

in mice which aim to address motor learning via lever pull (Peters et al., 2014; Tanaka et al., 2018), skilled reaching (Guo et al., 2015a), or joystick manipulation (Yttri and Dudman, 2016). Although head-fixed tasks make simultaneous recording of neural activity more practical, it is currently unclear what effect it may have on sequence learning.

The standard operant training approach to ensure rodents acquire a particular pattern of motor output is through small increments in difficulty and/or a graded reward landscape. Difficulty can be adjusted by imposing numerical, order, or temporal constraints. Interestingly, the focus of most causal or intervention studies using this kind of behavioural paradigm is to show that a treatment of brain lesion somehow affects or retards a rodents progression through stages requiring increasing motor output while reinforcer volume remains fixed (French et al., 2019). As such, performance in such tasks may be more susceptible to motivational as well as learning deficits. While such task design is valid when aiming to push animals to the limit of their performance prior to testing the effect of drugs or lesions, their utility in studying motor learning is less clear. Is it possible to use non-dextrous lever pressing tasks to monitor learning while attempting to control for motivation? If rodents are already performing a certain motor output to gain a certain volume of reinforcer per session, then one way of isolating and testing the learning component is to ask mice to reorganise this motor output in a different pattern to continue receiving the same reinforcer volume per action, while ensuring the reinforcer volume is suitably higher to match the difficulty of the new pattern which must be learnt. For the study of motor learning processes, the main advantage of this approach is that the mice which do gain sufficient reinforcers in the first transition session should refine their actions over subsequent sessions to reach asymptotic performance as seen for dextrous motor learning tasks (Whishaw et al., 1998; Alaverdashvili and Whishaw, 2008; Guo et al., 2015a; Galinanes et al., 2018). The main disadvantages of introducing these constraints is the much greater risk that not all mice will make the sudden skill transition (either due to motivation or attention factors), even with repeat attempts, and may become demotivated and need to be removed from the dataset. Task design must thus balance the need to maximise the difficulty of this single motor learning demand (so that refinement occurs over longer periods of time), but that the rule needs to

be achievable by most mice. In summary, objectives for our operant lever press task were that it i) involve a self-paced action sequence; ii) involve learning of a covert pre-specified minimum vigour (i.e. frequency of presses within an action sequence) by applying a time window; iii) ensure each mouse has already demonstrated the ability to perform the total individual motor components for a given total reinforcer volume prior to the learning phase; and iv) learning phase lasts several training sessions before plateau allowing circuit manipulations.

Frustration is known to increase motor variability and exploration in rodents and leads to opportunities for coincidental learning (Dhawale et al., 2017). We exploited early frustration-induced patterns of mouse lever pressing behaviour to identify a potential covert target sequence which can be utilised in a novel non-dextrous motor skill learning task. Mice who had already been trained to asymptotic performance on a strict fixed-ratio 1 task showed increased variability in the lever IPIs, with both longer and shorter intervals occurring. In particular, a new peak of IPIs <1s apart arose, as well as spontaneous bursts of 3 presses uninterrupted by magazine checking or licking. As three press sequences were likely responsible for the increase in sub-second IPIs, we chose a covert motor learning target of 3 presses within 2 seconds. Although we identified a covert target for motor learning, implementing it to ensure mice would reliably acquire it required further adjustments. During our strict FR1, mice were discouraged from over-pressing as (unlike in other studies) a lever press must be preceded by licking if it is to trigger reinforcer delivery. As such, every press is associated with a fixed reinforcer volume. Given that we were asking mice to reorganise these single presses into bursts of 3 presses within 2 seconds, to preserve the lever press to reinforcer volume ratio we ensured every correct 3-press sequence resulted in a 15 µl reinforcer (i.e. three-fold larger than that for previous single presses). We combined this with reducing the overall minimum motor activity per training session required to gain all reinforcers such that the perfect performance in our task allows could gain all reinforcers in 45 presses organised into 15 sequences of 3 presses at > 1.5 Hz press frequency. What performance level mice will eventually achieve with exhaustive behavioural training (e.g. several months) on task performance is unknown. Nevertheless, our user-

defined level of expert performance at 7 days (14 sessions) is robust and stable enough to effectively probe the neural representations of movement using a variety of recording strategies.

### *4.7.1 Technical considerations*

Not all mice will acquire FR3/2s pressing on the index session despite previously identical FR1 pressing patterns and level of food restriction to their successful peers. This is likely to be due to an interaction between learning ability and motivation, though may also be due to the fact that in general behaviour is typically ambiguous as to the underlying learning strategy (Skatova et al., 2013). Future versions of the task may benefit from a more sophisticated or personalised challenging target, but this will introduce problems in comparing data. Furthermore, some of these same mice were able to learn the task successfully at the second attempt but have not been analysed in this thesis. This proportion could be increased by utilising water restricted mice, and/or by training mice in automated home cages (although the latter limits the use of optogenetics). Another issue is that our task is novel and despite having features similar to tasks shown to be encoded by basal ganglia and motor cortex we have not yet demonstrated this dependency either using *in vivo* electrophysiology or lesions of these important upstream or downstream sites.

We only analysed the simplest metric available to us from the accelerometer, and ignored captured events not simultaneously recorded as lever presses by Med-PC software. Further analysis of this, or other parameters of the accelerometer trace could also be used, such as area under the curve or progression of the accelerometer slope. In future, the accelerometer trace itself could be used to trigger reinforcer delivery if a certain threshold or trace pattern is produced by the mouse and may enable finer grain control (e.g. even of single presses in an FR1 task).

We limited our monitoring of learning to a 7-day period and it is still unclear whether mice, if trained on this task for much longer periods (e.g. several months) do further refine their behaviour to get close to the 45 press minimum. The use of automated home cages may facilitate this type of longer-

term analysis. It is reasonable to assume that once mice are comfortably earning all reinforcers in a greatly reduced number than in session 1 of FR3/2s, rather than specifically focussing on continuing to reduce the total number of presses used they may focus on instead ensuring that every bout of pressing (irrespective of the number of presses they have to execute) successfully earns a reinforcer. This is as it is currently unclear how mice value the relative cost of extra lever presses verses the cost of extra magazine checks – which may vary on a subject to subject basis.

Lastly, whether mice require different neural circuits to acquire the bursts of pressing (Jin and Costa, 2010; Jin et al., 2014) during FR3/2s training as they do for sequence tasks involving two levers and a specific order of pressing (Ostlund et al., 2009; Martiros et al., 2018), or others with more specific timing requirements (Kawai et al., 2015) is not known. If the burst lever pressing action can eventually be generated in large part by brainstem or spinal cord pattern generators without conscious monitoring it may become less susceptible to disruption by circuit manipulations (Hwang et al., 2019). As such, studying their early learning or acquisition may represent the most likely period where local interventions may have a behavioural effect.

### *4.7.2 Summary*

Self-initiated (internally cued) movement sequences are commonly disrupted in movement disorders, such as Parkinson's disease, and the use of external cues can often rescue motor deficits. Information flow between the basal ganglia, cerebellum, thalamus, and motor cortex is thought to be critical for their learning and execution of self-paced actions. We have designed a task which lets us monitor a discrete learning event in response to the covert introduction of a new target motor sequence derived from population level analysis of behavioural responses to extinction – an established trigger for increased motor variability which can be exploited for incidental learning of new sequences. Mice performing our task shown refinement of motor output over days making it suitable for testing the effect of circuit perturbations on motor skill learning.

# 5. Acute and chronic silencing of motor thalamus during behaviour

## 5.1 Introduction

A core goal of neuroscience is to explain how behaviour emerges from patterns of neural activity and, by extension, utilise this understanding to restore normal function(s) in the context of brain injury or disease. Ideally, neural recordings providing descriptions of brain dynamics could first be used to reveal correlations with important behaviours or symptoms and subsequently, a model could be built and its predictions tested by monitoring the behavioural effect of local activity manipulations (Wolff and Olveczky, 2018). However, as is increasingly becoming clear, the extent to which local neural activity correlations reflect causal or necessary contributions to ongoing behaviour is difficult to predict.

Firstly, although optogenetics and other recently developed circuit manipulation tools are making it possible to control the activity of circuits with cell-type and/or temporal specificity, experimentally activating or silencing a set of neurons may result in local and downstream circuits being driven or deprived of activity in ways that i) do not occur endogenously *in vivo*, ii) are unintended and iii) potentially unknown to the experimenter (Allen et al., 2015). Secondly, acute and chronic manipulations of neural activity can lead to different behavioural effects and conclusions regarding the role of the targeted neurons irrespective of whether they are genuinely instructive (essential) or permissive (non-essential) (Table 5.1) (Wolff and Olveczky, 2018). Chronic lesion studies aim to gleaning the functionality of a brain area by studying the behavioural deficit produced, but this is complicated by the ability for other brain areas to compensate for the functions initially carried by the lesioned area. By contrast, although acute manipulations do not allow time for compensation they potentially force the brain into an altered dynamical state with unclear consequences for overall network function (Wolff and Olveczky, 2018). As such, a better approach may be to use both acute

and chronic manipulations in identical tasks with careful behavioural and network-wide activity monitoring (Allen et al., 2015; Wolff and Olveczky, 2018).

| **Computational importance of brain region X to behaviour A** | **Lesion type in brain region X** | **Explanation for no effect on behaviour A** | **Explanation for effect on behaviour A** |
|---|---|---|---|
| **Permissive (non-essential)** | Acute | Expected | Unlikely. Downstream effects on instructive areas |
| | Chronic | Expected | Unlikely. Connectional diaschisis. |
| **Instructive (essential)** | Acute | Unlikely | Expected |
| | Chronic | Structural and functional reorganisation. Experience-dependent plasticity (especially for innate behaviours). Redundancy. Degeneracy. | Expected but may only be present in the acute period after induction of a chronic lesion. |

**Table 5.1 Complex relationship between role of brain areas and observed behavioural effects of their manipulation.**

Motor thalamus activity has been to shown to encode multiple aspects of task-related events in rodents (Gaidica et al., 2018). *In vivo* recordings in primates have shown that motor thalamus activity codes internally generated movements more than externally triggered or passive joint movements in subregions (Vitek et al., 1994). Two-photon calcium imaging of thalamocortical axon activity in the motor cortex of head fixed mice learning a self-initiated lever pull task show differential patterns of layer 1 and layer 3 activity, with contributions from substantia nigra and cerebellum respectively (Tanaka et al., 2018). Although we do not know the exact timing of peak motor thalamus activity in our own task to select a specific time point for manipulations, it seems probable that there will be neurons in the motor thalamus encoding various stages of task execution and reward. As such, in mice undergoing motor thalamus manipulations we need to balance i) the need to manipulate motor thalamus neurons during the majority of behaviour to have a chance at showing an overall effect during the session, but must also ii) capture similar behavioural events with and without ongoing

circuit manipulation to detect differences in microstructure. As such, we aimed to utilise chronic silencing to understand if motor thalamus was an instructive (i.e. essential) structure in learning our task in general and utilised acute optogenetic silencing to see if it is part of a network which may modulate within training session motor skill learning.

### 5.2 Experimental aims

1) Validate a chronic motor thalamus silencing strategy using *in vitro* electrophysiology

2) Validate acute optogenetic silencing of motor thalamus using *in vivo* recordings

3) Monitor the impact of (i) chronic motor thalamus silencing and (ii) acute optogenetic silencing of VM or VL thalamus on the acquisition and consolidation of FR3/2s lever pressing

### 5.3 Kir2.1 expression in the motor thalamus of Vglut2-Cre mice causes chronic hyperpolarisation

To chronically silence motor thalamus, we opted for a genetically targeted approach in Vglut2-Cre mice so that a comparison of results with the optogenetic silencing group might be justified. Although genetically targeted approaches are available to ablate neurons (e.g. diptheria toxin, caspase-3) or block synaptic signalling (e.g. tetanus toxin), we delivered a viral vector which results in the overexpression of the delayed inward-rectifier potassium channel Kir2.1 causing hyperpolarisation of the resting membrane potential of neurons and increasing the threshold required for action potential firing (Burrone et al., 2002). Over-expression of Kir2.1 has been shown to impair thalamocortical neuron firing *in vitro* (Yamada et al., 2010). AAVDJ-CMV-DIO-Kir2.1-ZsGreen was injected bilaterally into motor thalamus of male mice and > 6 weeks expression allowed before experiments. To validate its function, *in vitro* recordings (Figure 5.1) were performed and showed that Kir2.1-expressing neurons in motor thalamus were significantly more hyperpolarised than and adjacent Kir2.1-negative neurons controls (Fig 5.1C; n = 6 and 7 neurons respectively from 3 mice,

Mann-Whitney U test, p = 0.013). Although further statistical analysis on evoked-firing has not yet been done, example responses of Kir2.1-expressing and control neurons to depolarising current steps are as expected (Fig 5.1D). The bilateral Kir2.1 expression pattern shown (Fig 5.1E) used only the native fluorescence of Kir2.1-Zs-Green combined with immunostaining for Calbindin 1.

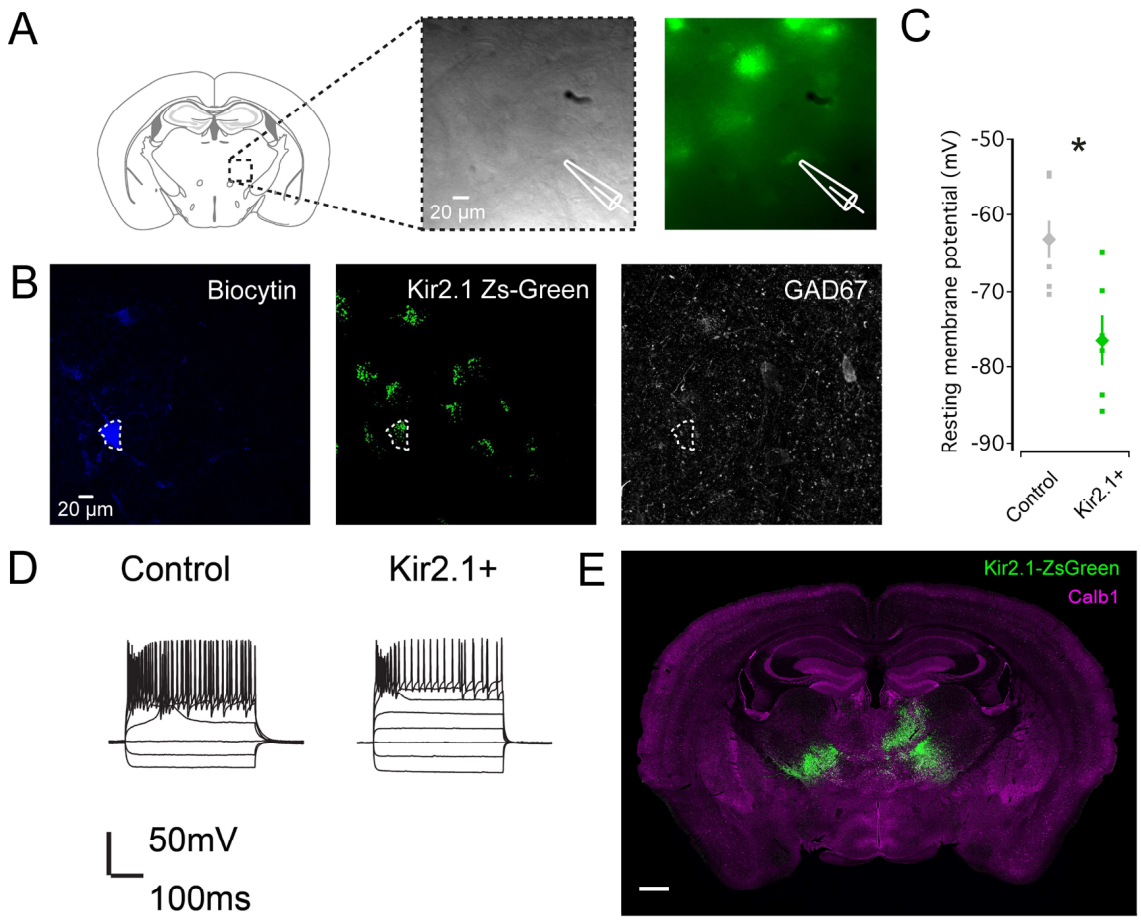



**Figure 5.1 Kir2.1-ZsGreen expression results in hyperpolarization of motor thalamus neurons. (A)** Targeted whole-cell patch-clamp recordings were performed in acute brain slices from Vglut2-Cre mice with bilateral motor thalamus Kir2.1-ZsGreen expression after they had undergone training on the FR3/2s task. Motor thalamus (left) neurons were visualized with Dodt-contrast imaging (middle) and Kir2.1 positive neurons were identified by expression of Kir2.1-ZsGreen (right). **(B)** Neurons were labelled during recordings with biocytin, which was revealed using streptavidin-405, and further processed to confirm the expression of Kir2.1-ZsGreen and the absence of expression of GAD-67. **(C)** Overexpression

of Kir2.1 led to a significant hyperpolarization of thalamic neurons (Control: -63.2 ± 2.4 mV vs. Kir2.1: -76.5 ± 3.3 mV, p=0.013, Mann-Whitney U test, n = 7 and 6 neurons). **(D)** Representative example traces of the response of control and Kir2.1+ thalamic neurons to hyperpolarizing and depolarizing current steps. **(E)** Representative bilateral injection of AAVDJ-CMV-DIO-Kir2.1-ZsGreen in motor thalamus of Vglut2-Cre mice used for behaviour (MThal-Kir2.1 group). Only native fluorescence of Zs-Green was imaged. Scale bars: **(A) and (B)** 20 µm; **(E)** 500 µm.

### 5.4 Light-induced ArchT silencing of VM or VL thalamus does not disrupt learned operant lever pressing

Compared to electrical stimulation, drug infusion or physical lesions, optogenetic tools offer both cell type specific activation or silencing of neuronal populations or circuits with temporal specificity. Although sub-second manipulations are important in many areas of neuroscience, the general ability to control temporal activity has benefits relative to other genetically defined/cell type specific acute interventions such as chemogenetics which are at risk of effect spill over into non-training periods, especially when task duration is determined by self-paced achievement of a fixed target (as in our case). As such, they may have effects on offline processes rather than strictly during task engagement. By contrast, light delivery can be controlled instantaneously and occurs only during training sessions. Ideally, experiments using optogenetic tools would involve light-induced endogenous patterns of local activity to induce expected behavioural effects *de novo*, or time-locked silencing of task-related neuronal activity to disrupt existing behavioural competency. This goal is made somewhat more challenging if, in the brain area of interest, neurons are known to encode one (or more) aspects of task-related activity and are intermingled with those encoding other aspects of the same task. In a nose poke decision making task, motor thalamus neurons in rats were shown to respond to action onset, delay period and reward consumption (Gaidica et al., 2018). In a head-fixed lever pull task in mice, thalamocortical boutons in L1 and L3 of cortex showed increased activity in both lever pull and reward consumption (licking) (Tanaka et al., 2018). As combinations, rather than specific subsets, of these neurons may be most important for modulating motor learning we felt that

silencing information flow from motor thalamus during entire behavioural routines where reinforcer was successfully earnt (approach to lever, pressing, magazine approach, licking) had the best chance of interfering with learning trajectories. These routines can be 10 or more seconds in length (Fig 4.3A and C) and triggering light delivery only on initiation of these sequences was not feasible for several reasons. Firstly, as we were interested in studying the inherently variable process of skill acquisition rather than execution of an already well learnt behaviour, we could not rely on pre-existing stereotyped patterns of movements which others have exploited to trigger light delivery immediately prior to the first lever press (Tecuapetla et al., 2016; Diaz-Hernandez et al., 2018). Secondly, triggering light delivery off the first action in a behavioural sequence may not be sufficiently early enough to cause a behavioural effect (Tecuapetla et al., 2016). Thirdly, the total session time can vary between early and late FR3/2s training sessions from over an hour to only a few minutes to earn all reinforcers (Fig 4.3A and C) and since we only wanted to effect this period of time, without hangover into rest periods where offline processes relevant to the behaviour may be active, we could not use chemogenetic silencing approaches (e.g. DREADDs).

Although there has been a massive expansion in the number of inhibitory optogenetic tools, one of the most commonly used is archaerhodopsin. Although third generation versions with better membrane targeting (and thus photocurrent) are available, they have poorer stability of inhibition over 60s periods (Mattis et al., 2011). Given that we wished to stably silence over prolonged periods, we opted to use a first generation ArchT (Han et al., 2011). We used yellow (561 nm) light delivered as 30s long continuous pulses with probabilistic inter-pulse intervals of 5-20 s (i.e. light on accounts for approximately 60% of each training session), similar to recent studies in other brain areas (Trouche et al., 2019) and adjusted laser power to achieve approximately 20 mW power at each tip of a 200 μm fibre located bilaterally in either VM or VL thalamus. Longer light durations may also limit the frequency of ArchT-related rebound excitation seen on light termination (Allen et al., 2015; Wiegert et al., 2017), which could potentially mimic thalamic burst firing. Validation of differential cortical targeting when ArchT expression is targeted to different motor thalamus territories (VM vs VL) in Vglut2-Cre mice was shown in Chapter 3.

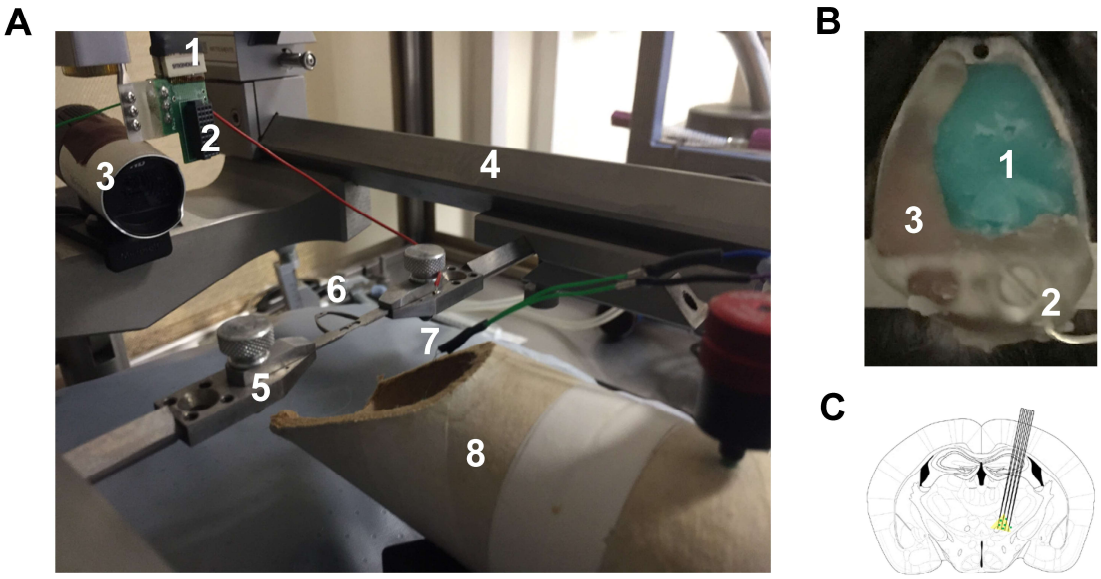



**Figure 5.2 Custom setup for quiescent head-fixed electrophysiological recordings. (A)** Basic recording setup (without mouse. 1, Intan headstage; 2, Silicone probe adaptor (with holding arm); 3, Webcam; 4, stereotactic frame; 5, Mounting bars; 6, Head plate; 7, piezoelectric motion sensor; 8, cardboard tunnel. **(B)** Top view of implanted full access head plate. 1, silicone covering skull/craniotomy site; 2, cerebellar reference screw and connector wire; 3, dental cement. **(C)** Schematic showing standard angled silicone probe orientation for thalamic recordings.

As we planned to use optogenetic silencing of motor thalamus in behaving mice, we wished to first confirm that we could consistently achieve 30s of silencing in motor thalamus neurons expressing ArchT in awake mice. To record from thalamus in awake mice, we adapted a previously described headplate and mounting bar design to suit out purposes (Guo et al., 2014). Briefly, custom headplate design courtesy of Dr Zengcai Guo (personal communication) was adapted to allow cerebellar screw placement, while mounting bar designs (courtesy of Svoboda Lab, Howard Hughes Medical Institute) were adapted to allow use within a Kopf stereotactic frame (Figure 5.2). Custom designs were used by a CNC machine milling company (Get It Made Ltd, London, UK) to produce titanium headplates and steel mounting bars. After viral injection and subsequent head plate implantation, mice were habituated to head fixation with ad-hoc 20% sucrose reinforcers for several days until

they could sit comfortably for 1h. Cardboard tunnels used by mice used during quiescent head fixed recording were kept in the home cage at all other times. At this point, a craniotomy was fashioned and awake silicone probe recordings performed > 24 h later. ArchT silencing recordings under isoflurane anaesthesia were also performed in the same rig. *In vivo* silicone probe recordings (Fig 5.2C; Figure 5.3) showed that multi-unit activity was reliably silenced over 30s of light delivery in mice injected with ArchT.

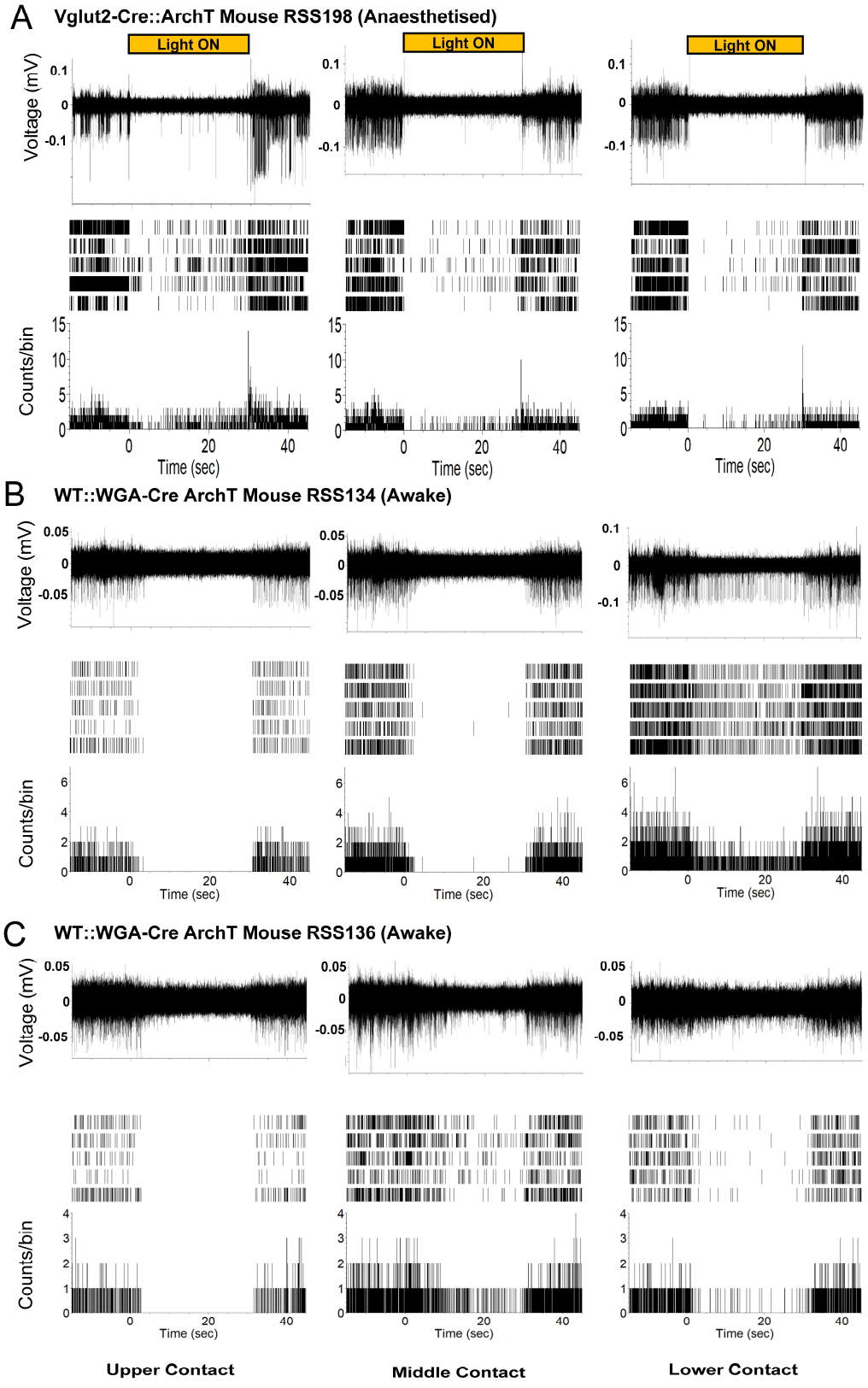



**Figure 5.3 Sustained light-induced *in vivo* silencing of motor thalamus neurons expressing ArchT in mice. (A)** Multi-unit recordings from three adjacent contacts on the same shank of a 4-shank silicone optrode in an anaesthetised Vglut2-Cre mouse injected with AAV-CAG-Flex-ArchT-GFP. Light power

at the tip of a 100 µm-core (0.22 NA) fibre was 10 mW which gives an irradiance similar to that used in our optogenetic behavioural experiments utilising 20 mW tip powers via a 200 µm core fibre. Multi-unit activity (MUA) is reduced for the entire period of light delivery (30s). High pass filtered voltage traces (top) are shown for the lowest row of sweeps in the raster plot. A peri-event histogram (bottom) shows the average effect of all sweeps. **(B) and (C)** Multi-unit recordings from three adjacent contacts on the same shank of a 4-shank silicone optrode in awake head-fixed quiescent wild-type mice expressing ArchT in motor thalamus secondary to WGA-Cre delivery from substantia nigra. Light power at the tip of the fibre was 20 mW in both cases. Histogram bin size = 1 ms.

If there is a significant gross motor effect of silencing VM or VL thalamus, we may expect that mice redistribute or bias their already well learnt operant lever pressing into light-off periods or terminate it altogether. In mice already trained in FR1 operant lever pressing, there was no significant difference in the rate of lever pressing between light-on and light-off periods, although in light-off periods VL-ArchT mice showed significantly higher rate of head entries (magazine checks) during light-off periods and tethered controls reached signficance for higher rate of licking (Table 5.2). Multi-way ANOVA was performed to test the effect of experimental group (tethered control vs. VM-ArchT vs. VL-ArchT) and light condition (on vs. off) on the rate of lever pressing, rate of head entry and rate of licking. There were significant effect of experimental group but not light condition for both lever press rate ($F(2,60) = 3.58$, $p = 0.04$) and licking rate ($F(2,60) = 5.55$, $p = 0.0075$). In both cases post-hoc testing suggested this was driven by higher rates of pressing ($p = 0.033$) and licking ($p = 0.0075$) in VL-ArchT mices compared to VM-ArchT mice. Overall, this suggests that there was no absolute motor deficit or action inhibition induced by bilateral optogenetic sliencing of motor thalamus, consistent with other recent studies utilising unilateral optogenetic motor thalamus silencing (Guo et al., 2017; Tanaka et al., 2018).

| Rate (per min) | Light-on | Light-off | Wilcoxon rank sum test (p value) |
|---|---|---|---|
| ***Tethered Controls*** | | | |
| Head entry | 8.4 | 8.3 | 0.68 |
| Lick | 118.57 | 125.68 | 0.05 |
| Lever | 5.7 | 6.3 | 0.2 |
| ***VL-ArchT*** | | | |
| Head entry | 9.742 | 10.9077 | 0.03 |
| Lick | 162.133 | 161.1023 | 0.825 |
| Lever | 6.84 | 7.111 | 0.4688 |
| ***VM-ArchT*** | | | |
| Head entry | 8.74 | 8.4 | 0.3 |
| Lick | 113 | 111.1 | 0.7 |
| Lever | 5.4 | 5.3 | 0.5 |

**Table 5.2 Within group comparison of mean rates of head entries, licks and lever presses in light-on versus light-off periods during well learnt fixed-ratio 1 lever pressing.** Mean rates are shown for last 4 sessions of FR1 training immediately before VM-ArchT (n = 7 mice) or VL-ArchT (n = 5 mice) were transitioned to FR3/2s. Yellow (561 nm) light was delivered as 30s long continuous pulses with probabilistic inter-pulse intervals of 5-20 s such that light-on periods account for ~60% of the training session.

### 5.5 MThal-Kir2.1 and VM-ArchT mice show faster self-paced FR3/2s sequence acquisition without significantly different performance endpoints

Next, we compared how chronic silencing of the motor thalamus (MThal-Kir2.1; n = 4 mice) or acute optogenetic silencing of either VM (VM-ArchT; n = 7 mice) or VL (VL-ArchT; n = 5 mice) thalamus affected selected task parameters during acquisition of FR3/2s lever pressing relative to their respective controls (Figures 5.4, 5.6 and 5.7; optic fibre tip position and thalamic ArchT expression pattern in shown in Figure 5.5). Task parameters considered per training session were (i) total lever presses, (ii) the percentage of lever pressing bouts with three or more presses, (iii) rate of reinforcer delivery, (iv) rate of head entries, (v) total time taken to complete the training session, and mean lever press duration in pressing bouts with either a (vi) single lever press, (vii) two lever presses or (viii) ≥3 presses. Kruskal-Wallis testing of between group differences (untethered control vs MThal-Kir2.1; tethered control vs VM-ArchT; tethered control vs VL-ArchT; and VM-ArchT vs VL-ArchT) in all aforementioned task parameters on either Session 1, Session 7 or session 13 were

not statistically significant. Subsequently, we used a multi-way ANOVA analysis to test the influence of experimental group (untethered control vs MThal-Kir2.1; tethered control vs. VM-ArchT vs. VL-ArchT) and between-session differences (S1 vs S5, S1 vs S9, S1 vs S13, S5 vs S9, S5 vs S13, and S9 vs S13) on each task parameter.

Total lever presses to gain all reinforcers for the untethered control vs MThal-Kir2.1 comparison (Fig 5.4Ai-ii) was significantly influenced by between-session differences ($F(3,36) = 12.4$, $p < 0.01$; post-hoc testing was significant at $p < 0.01$ for S1 > S5 and at $p < 0.0001$ for S1 > S9 and S1 > S13) but not by experimental group. For the optogenetic experiments (Fig 5.6Ai-iii), total lever presses were significantly influenced by experimental group ($F(2,60) = 3.82$, $p = 0.0275$; post-hoc testing showed VL-ArchT mice had significantly higher presses than VM-ArchT, $p = 0.049$) and between-session differences ($F(3,60) = 29.08$, $p < 0.0001$; post-hoc testing was significant at $p < 0.0001$ for S1 > S5, S1 > S9 and S1 > S13), and there was a significant interaction between them ($F(6,60) = 2.56$, $p = 0.0283$). This interaction is likely due to VL-ArchT mice having significantly more lever presses in S1 than any other group on any other session ($p < 0.05$).

Percentage of bouts with ≥ 3 presses (PB3) for the untethered control vs MThal-Kir2.1 comparison (Fig 5.4Bi-ii) was significantly influenced by between-session differences ($F(3,36) = 8.4$, $p < 0.0001$; post-hoc testing was significant at $p = 0.03$ for S1 < S5 and at $p < 0.01$ for S1 < S9 and S1 < S13) but not by experimental group. For the optogenetic experiments (Fig 5.6Bi-iii), PB3 was significantly influenced by between session differences ($F(3,60) = 20.67$, $p < 0.0001$; post-hoc testing was significant at $p = 0.02$ for S1 < S5, and $p = 0.0002$ for S5 < S13, and $p < 0.0001$ for S1 < S9 and S1 < S13) but not by experimental group.

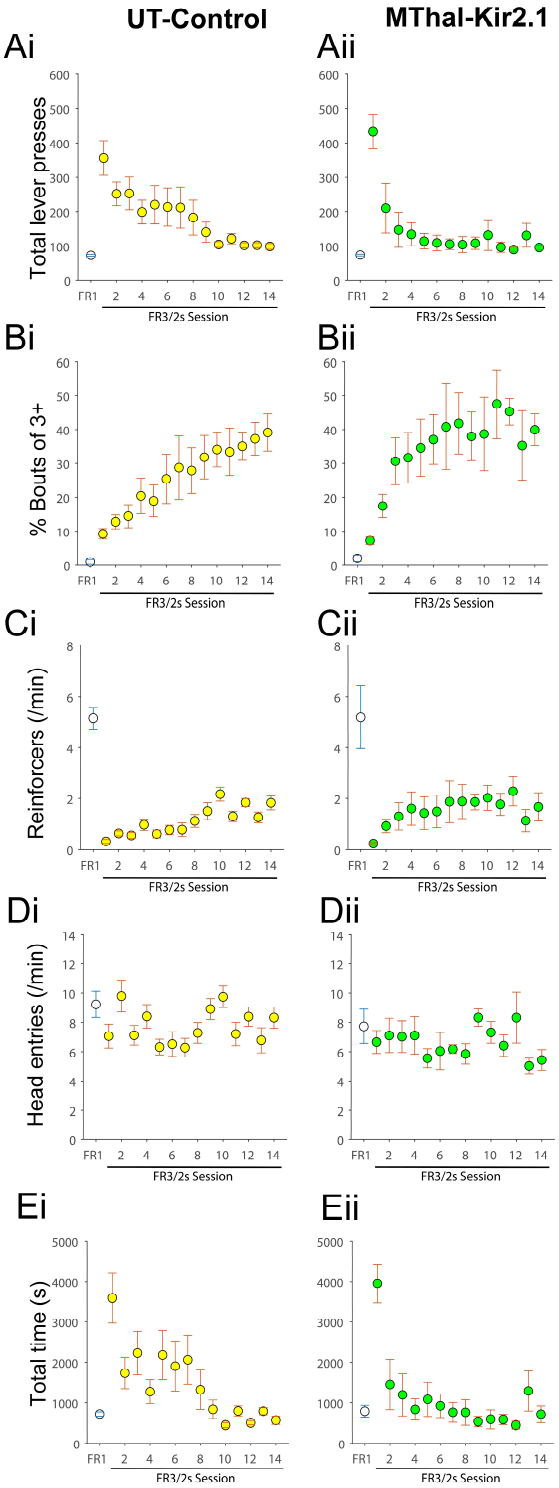



**Figure 5.4 Refinement of multiple task parameters during self-paced acquisition of a FR3/2s lever press sequence in untethered control and MThal-Kir2.1 mice**. Mean group plots of **(Ai-ii)** total lever presses to gain all reinforcers, **(Bi-ii)** percentage of pressing bouts which had three or more presses, **(Ci-ii)** rate of reinforcer delivery, **(Di-ii)** frequency of magazine head entry, and **(Ei-ii)** total time taken to gain all reinforcers are shown for the last FR1 session and FR3/2s sessions 1-14 for controls (n = 7 mice,

yellow plots; **Ai, Bi, Ci, Di, Ei**) and MThal-Kir2.1 (n = 4 mice, green plots; **Aii, Bii, Cii, Dii, Eii**) mice. Error bars for each solid dot (mean value) on each plot represent ± SEM.

Rate of reinforcer delivery for the untethered control vs MThal-Kir2.1 comparison (Fig 5.4Ci-ii) was significantly influenced by between-session differences ($F(3,36) = 7.43$, $p < 0.0001$; post-hoc testing was significant at $p < 0.001$ for S1 < S9 and at $p = 0.02$ for S1 < S13) but not by experimental group. For the optogenetic experiments (Fig 5.6Ci-iii), rate of reinforcer delivery was significantly influenced by both experimental group ($F(2,60) = 3.29$, $p = 0.0469$; post-hoc testing showed tethered controls had significantly higher reinforcer rate than VM-ArchT mice, $p = 0.04$) and between-session differences ($F(3,60) = 9.78$, $p < 0.0001$; post-hoc testing was significant at $p = 0.008$ for S1 < S9 and S5 < S13, and $p < 0.0001$ for S1 < S13).

Rate of head entry for the untethered control vs MThal-Kir2.1 comparison (Fig 5.4Di-ii) was significantly influenced by experimental group ($F(1,36) = 6.49$, $p = 0.015$; higher in controls than MThal-Kir2.1) and between-session differences ($F(3,36) = 3.8$, $p = 0.018$; post-hoc testing was significant at $p = 0.0315$ for S5 < S9). For the optogenetic experiments (Fig 5.6Di-iii), rate of head entry was significantly influenced by experimental group ($F(2,60) = 6.85$, $p = 0.0021$; post-hoc testing showed this was driven by tethered controls having significantly higher head entry rate than VM-ArchT mice, $p = 0.0014$) but not by between-session differences.

Total session time for the untethered control vs MThal-Kir2.1 comparison (Fig 5.4Ei-ii) was significantly influenced by between-session differences ($F(3,36) = 10.15$, $p < 0.0001$; post-hoc testing was significant at $p = 0.04$ for S1 > S5, at $p < 0.0001$ for S1 > S9 and $p = 0.0004$ for S1 > S13) but not by experimental group. For the optogenetic experiments (Fig 5.6Ei-iii), total session time was significantly influenced between-session differences ($F(3,60) = 23.8$, $p < 0.0001$; post-hoc testing was significant at $p = 0.00001$ for S1 > S5, S1 > S9 and S1 > S13) but not by experimental group.

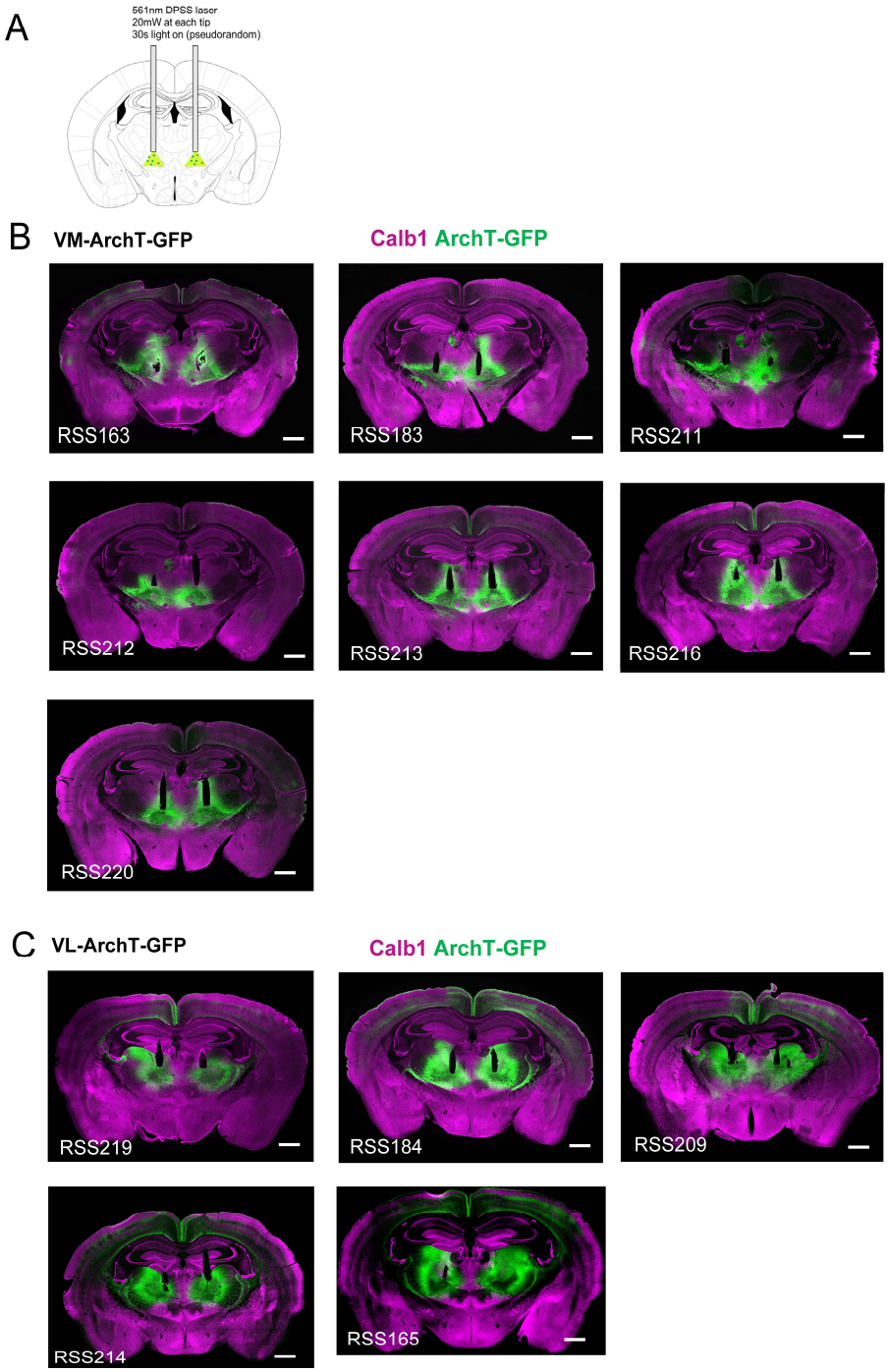



**Figure 5.5 Optic fibre sites for all VM-ArchT and VL-ArchT mice used for opto-behaviour experiments. (A)** Schematic of bilateral optic fibre implantation for behaviour. All mice received bilateral AAV5-CAG-Flex-ArchT-GFP in either VM (AP -1.3 mm, ML 0.8 mm, DV 4.0) or VL (AP -1.1 mm, ML, 1.1 mm, DV 3.5 mm). Fibre tips were implanted to a depth 700 µm above the virus injection centre coordinates. **(B)** ArchT expression and optic fibre tip locations in all VM-ArchT mice (n = 7) analysed. **(C)** ArchT expression and optic fibre tip locations in all VL-ArchT mice (n = 5) analysed. Scale bars all represent 600 µm.

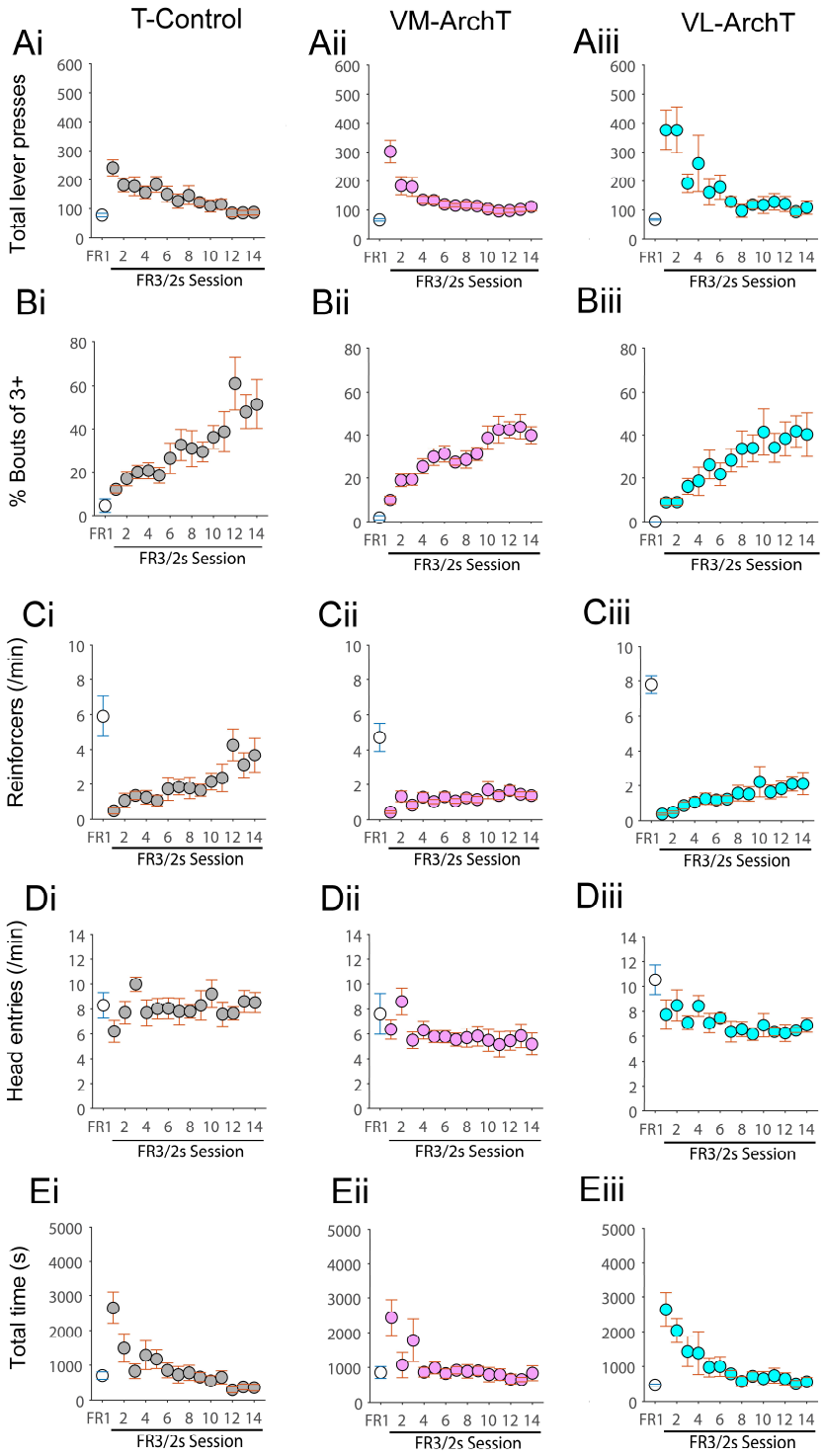



**Figure 5.6 Refinement of multiple task parameters during self-paced acquisition of a FR3/2s lever press sequence in VM-ArchT, VL-ArchT and tethered control mice.** Mean group plots of **(Ai-iii)** total lever presses to gain all reinforcers, **(Bi-iii)** percentage of pressing bouts which had three or more presses, **(Ci-iii)** rate of reinforcer delivery, **(Di-iii)** frequency of magazine head entry, and **(Ei-iii)** total time taken to gain all reinforcers are shown for sessions 1-14 for tethered controls (n = 6 mice, grey plots; **Ai, Bi, Ci,**

**Di, Ei**), VM-ArchT (n = 7 mice, pink plots; **Aii, Bii, Cii, Dii, Eii**) and VL-ArchT (n = 5 mice, blue plots; **Aiii, Biii, Ciii, Diii, Eiii**) mice. Error bars around the solid dot (mean value) on each plot represent ± SEM.

Lastly, we considered the mean lever press duration in pressing bouts with either a single lever press, two lever presses or ≥ 3 presses (Figure 5.7). Multi-way ANOVA testing did not show any statistically significant differences in press duration in 1 press, 2 press or 3 press bouts between session 1, 5, 9 or 13 for any experimental group (untethered control vs MThal-Kir2.1; tethered control vs VM-ArchT; tethered control vs VL-ArchT; VM-ArchT vs VL-ArchT).

Given that total lever presses, PB3, and total session time showed significant differences between S1 and S5 we refocussed our multi-way ANOVA to only early training sessions by looking at between-session differences for sessions 1-4 (S1 vs S2, S1 vs S3, S1 vs S4, S2 vs S3, S2 vs S4, and S3 vs S4). In the untethered control vs MThal-Kir2.1 comparison (Fig 5.4E) total lever presses (post-hoc $p = 0.029$ for S1 > S3, at $p < 0.0142$ for S1 > S4) and total session time ($F(3,36) = 3.19$, $p = 0.035$) remained significantly influenced by between-session differences but not experimental group. By contrast, PB3 was now significantly influenced by experimental group ($F(1,36) = 5.31$, $p = 0.271$; post-hoc testing showed MThal-Kir2.1 significantly higher than untethered control) and differences between early sessions ($F(3,36) = 4.47$, $p < 0.0069$; post-hoc showed S1 > S4 at $p = 0.0054$). Reinforcer rate was significantly influenced by experimental group (post-hoc test $p = 0.0133$, MThal-Kir2.1 > untethered control) but not differences between early sessions.

In the optogenetic group comparison, total lever presses was influenced by both experimental group ($F(2,60) = 3.96$, $p = 0.0242$; post-hoc testing showed this was driven by VL-ArchT being significantly higher than VM-ArchT, $p = 0.027$) and differences between early sessions ($F(3,60) = 12.27$, $p < 0.0001$; post-hoc $p < 0.01$ for S1 > S2, and $p < 0.0001$ for S1 > S3 and S1 > S4). BP3 was only significantly influenced by differences between early sessions ($F(3,60) = 10.22$, $p < 0.0001$; post-hoc $p < 0.01$ for S1 < S3, $p < 0.0001$ for S1 < S4, and $p = 0.02$ for S2 < S4) but not experimental

group. Head entry rate was significantly influenced by experimental group (post-hoc testing showed this was due to tethered controls having significantly higher rate than VM-ArchT mice, $p = 0.0019$) but not differences between early sessions. Differences between early sessions but not experimental group significantly influenced total session time (post-hoc $p = 0.013$ for S1 > S2, $p < 0.0001$ for S1 > S3 and S1 > S4) and rate of reinforcer delivery (post-hoc $p = 0.0074$ for S1 < S4).

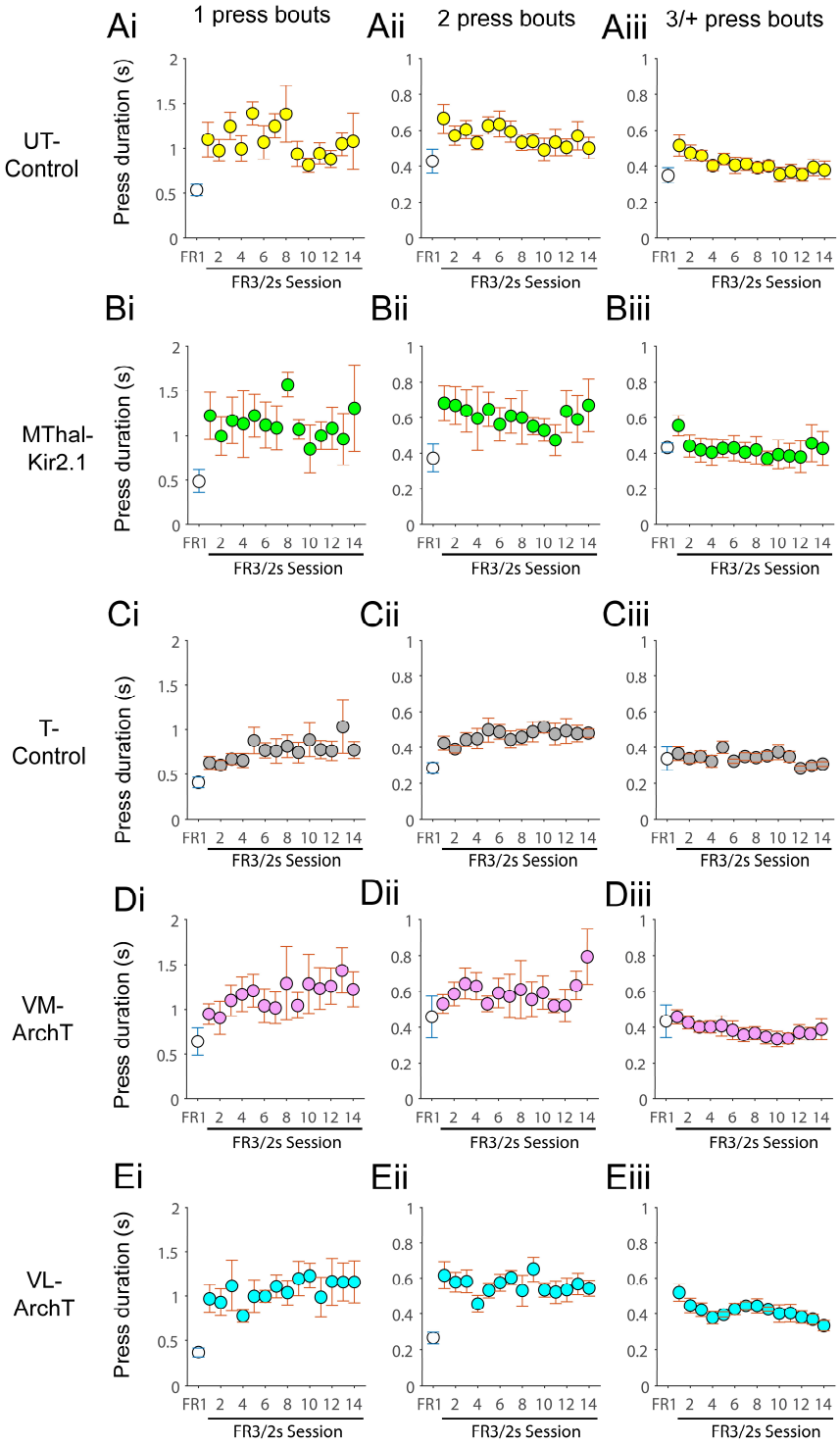



**Figure 5.7 Refinement of lever press duration for bouts with 1, 2, or ≥ 3 presses during self-paced acquisition of a FR3/2s lever press sequence in MThal-Kir2.1, VM-ArchT, VL-ArchT, and respective control mice.** Group plots of mean press duration for bouts where there was either **(Ai, Bi, Ci, Di, Ei)** one lever press, **(Aii, Bii, Cii, Dii, Eii)** two lever presses, or **(Aiii, Biii, Ciii, Diii, Eiii)** three or more lever presses are shown for sessions 1-14 for untethered controls (n = 7 mice, yellow plot; **Ai-**

**iii**), MThal-Kir2.1 (n = 4 mice, green plots; **Bi-iii**), tethered controls (n = 6 mice, grey plots; **Ci-iii**), VM-ArchT (n = 7 mice, pink plots; **Diii**) and VL-ArchT (n = 5 mice, blue plots; **Ei-iii**) mice. Multi-way ANOVA did not show any significant difference in mean press durations of 1, 2 or 3 press bouts between sessions 1, 5, 9 and 13 for untethered control vs MThal-Kir2.1 mice or for tethered controls vs VL-ArchT vs VM-ArchT groups. Error bars for each solid dot (mean value) on each plot represent ± SEM.

### 5.6 Refinement of accelerometer profile during sequence learning only occurs in untethered control mice

Next, we analysed how peak acceleration during press initiation (i.e. in the preceding 100 ms before a lever press was registered via an infra-red beam break) for those lever presses occurring within ≥ 3 press bouts varies across training sessions in the different groups (Figure 5.8 and 5.9). Spearman's rank correlation of mean trough values of median adjusted accelerometer traces across sessions 1-4 (Fig 5.8B and 5.9B) showed significantly positive correlations for untethered controls (n = 7, R = 0.74, p= 0.0025) but no significant correlations for MThal-Kir2.1, tethered control, VM-ArchT or VL-ArchT mice. This suggests that untethered control mice tend to reduce the peak acceleration within presses with sequence acquisition whereas mice with motor thalamus lesions or implants do not. To check if this lack of effect was due to highly variable responses within MThal-Kir2.1, tethered controls, VM-ArchT and VL-ArchT groups we then computed means of all R-values and calculated an $R^2$-values to assess correlation irrespective of sign. Comparison of Spearmans's rank correlation was significant between untethered control vs Mthal-Kir2.1 (Mann-Whitney U, p = 0.042) but not tethered controls vs VM-ArchT, tethered controls vs VL-ArchT, or VM-ArchT vs VL-ArchT. Comparison of Spearman $R^2$ values showed no significant difference between untethered control vs Mthal-Kir2.1 (Mann-Whitney U, p = 0.5) or tethered control vs VM-ArchT (Mann-Whitney U, p = 0.8), but did show a significant difference between VL-ArchT vs tethered controls (Mann-Whitney U, p = 0.014), and between VL-ArchT and VM-ArchT (Mann-Whitney U, p = 0.0025). This was supplemented by performing individual correlations on each animal within each group to understand if individual mice had significant positive, significant negative or no clear

correlation. This showed that 2/7 untethered controls showed a significant positive correlation, 1/4 MThal-Kir2.1 mice showed a significant negative correlation; 2/6 tethered controls showed a significant positive correlation; 2/7 and 1/7 VM-ArchT showed significant positive and negative correlations respectively, while no VL-ArchT mice show any correlation.

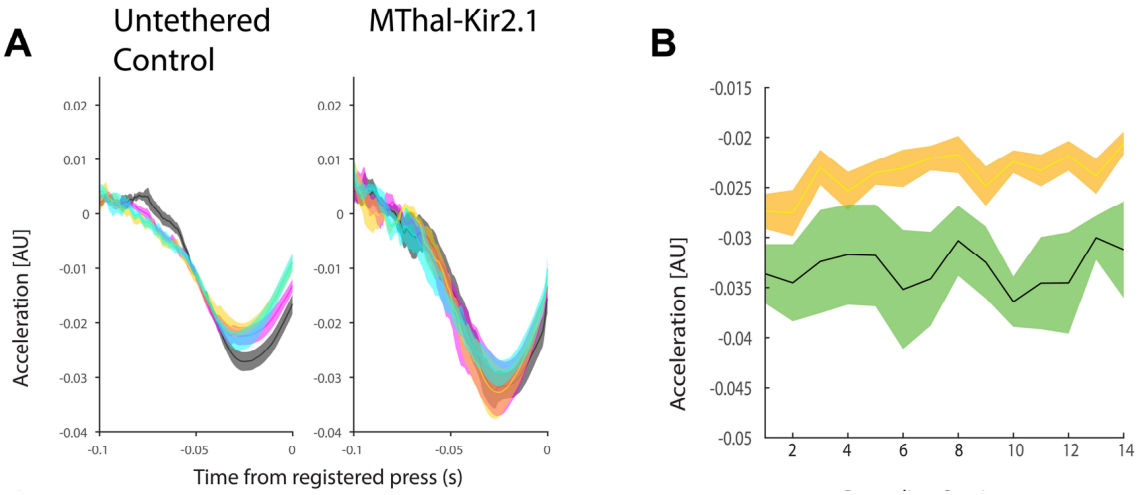



**Figure 5.8 Accelerometer recordings from bouts of ≥ 3 presses in untethered control and MThal-Kir2.1 mice. (A)** Median-adjusted accelerometer recordings of lever presses within ≥ 3 press bouts from recordings sessions 1 (black trace), 3 (magenta trace), 7 (yellow trace) and 13 (cyan trace) in untethered control (n = 7) and MThal-Kir2.1 (n = 4) mice. A bigger (more negative) trough in the accelerometer trace corresponds to a higher mean peak acceleration of the lever during all registered presses in that session. Note that in the control mice the trough becomes shallower with training, whereas MThal-Kir2.1 mice do not adjust this parameter during learning across session. **(B)** The mean trough values of median-adjusted acceleration in recording sessions 1-14 for untethered control (n = 7, yellow) and MThal-Kir2.1 (n = 4, green) mice. Shaded areas in all plots show ± SEM around the mean (solid line).

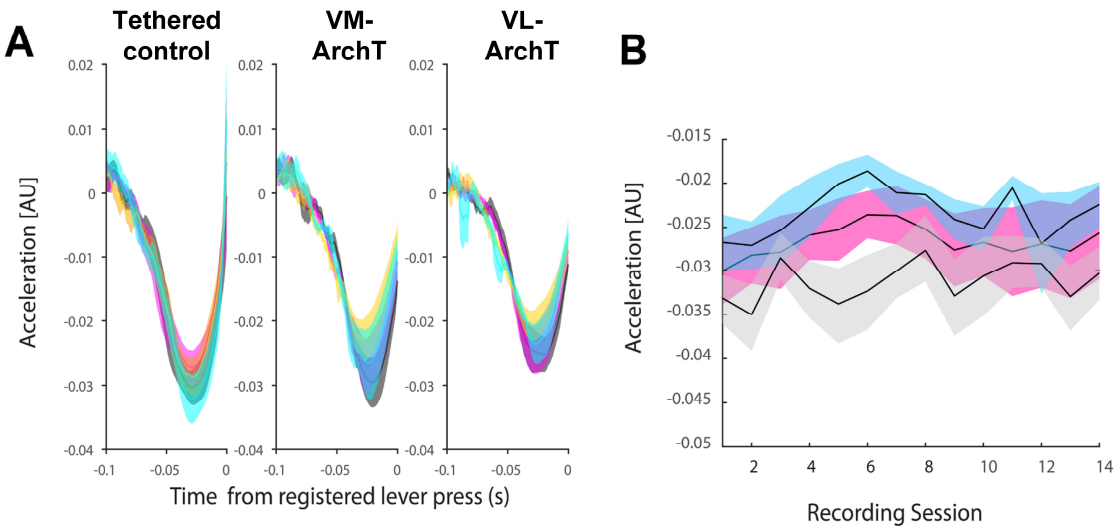



**Figure 5.9 Accelerometer recordings from bouts of ≥ 3 presses in tethered control, VM-ArchT and VL-ArchT mice. (A)** Median-adjusted accelerometer recordings of lever presses within ≥ 3 press bouts from recordings sessions 1 (black trace), 3 (magenta trace), 7 (yellow trace) and 13 (cyan trace) in tethered control (n = 6, left), VM-ArchT (n = 7, middle) and VL-ArchT-expressing (n = 5, right) mice. A bigger (more negative) trough in the accelerometer trace corresponds to a higher mean peak acceleration of the lever during all registered presses in that session. Note that in the VM-ArchT and VL-ArchT mice the biggest troughs in mean-adjusted accelerometer traces are in the middle sessions, but even in tethered controls there is no clear separation of the traces as learning progresses. **(B)** The mean trough values of median-adjusted acceleration in recording sessions 1-14 for tethered control (n = 6, grey), VM-ArchT (n = 7, pink) and VL-ArchT -expressing (n = 5, blue) mice. Shaded areas in all plots show ± SEM around the mean (solid line).

## 5.7 Manipulating motor thalamus alters the pattern of within-day and between-day performance gains during early FR3/2s sequence acquisition

### *5.7.1 Effect of recording day, daily session and experimental group on the absolute percentage of ≥ 3 press bouts*

Although there was no statistically significant separation in task parameters in session 1, 7 or 13 between any of the experimental groups, early session ANOVA showed that MThal-Kir2.1 mice showed significant PB3 performance gains compared to untethered controls, and VM-ArchT had significantly lower total lever presses than VL-ArchT mice. As such, we considered these early sessions further by testing the influence of recording day (first session of Day 1 [session 1] or Day 2 [session 3]), daily recording session (first or second session of the day) and experimental group (untethered control [n = 7) vs MThal-Kir2.1 [n = 4]) on the percentage of ≥ 3 bouts using a multi-way ANOVA (MATLAB function: ANOVAN). There were significant effects of both experimental group ($F(1,18) = 6.28$, $p = 0.0168$) and recording day ($F(1,18) = 17.65$, $p = 0.0002$) in the percentage of ≥ 3 bouts and a significant interaction between the two ($F(1,18) = 4.26$, $p = 0.046$). Post-hoc Dunn-Šidák testing revealed that this was driven by the percentage of ≥ 3 press bouts being significantly larger in MThal-Kir2.1 mice on day 2 than all other conditions.

We performed similar analysis using multi-way ANOVAs to compare task acquisition on the first two recording days for optogenetic silencing groups. Given that we had 3 experimental groups (VM-ArchT [n = 7], VL-ArchT [n = 5], tethered controls [n = 6]), we computed separate ANOVAs for percentage of ≥ 3 press bouts for recording days 1 (S1) and 2 (S3), with daily recording session (first or second session of the day) as the second factor. On day 1, but not day 2, there was as significant effect of experimental group ($F(2,30) = 3.37$, $p = 0.048$) and daily session ($F(1,30) = 5.76$, $p = 0.023$) on the percentage of ≥ 3 press bouts. There was no significant difference in the absolute percentage of ≥ 3 press bouts between experimental groups between days.

*5.7.2 Significant differences for within-day and between-day performance gains exist within each experimental group during early sessions*

We next considered the temporal profile of performance improvement between the early sessions. Performance improvement was measured as the increase in the percentage of ≥ 3 press bouts (P3B) between two sequential early training sessions (mice received 14 sessions overall during the entirety of FR3/2s training). These were either (i) within day 1 (comparing session 1 and session 2 of FR3/2s training), (ii) within day 2 (comparing session 3 and session 4), (iii) between the last session of day 1 and first session of day 2 (comparing session 2 and session 3), or (iv) between the last session of day 2 and first session of day 3 ( comparing session 4 and session 5). PB3 performance change for each experimental group was analysed for both types of interval (2-factor ANOVA, across sessions 'within days' (factor 1) or 'between days' (factor 2)).

MThal-Kir2.1 mice (n = 4) showed significantly higher within first day (S1-S2) and between session S2-S3 performance gains compared to either within second day (S3-S4) or between sessions S4-S5 ($F(1,24) = 15.13$, $p = 0.002$; post-hoc Dunn-Šidák tests). Untethered control mice (n = 7) showed significantly higher performance improvement within-days (S1-S2 and S3-S4) than between-days (S2-S3 and S4-S5) ($F(1,24) = 8.87$, $p = 0.0065$; post-hoc Dunn-Šidák tests). There was no significant difference in within-day or between-day performance gains for tethered controls (Fig 5.10A), but there was a significant effect of interval, reflecting that there was a larger improvement in the earlier (S1-S2 and S2-S3) than the latter (S3-4 and S4-5) sessions. For both VM-ArchT (n = 7 mice, $F(1,30) = 7.51$, $p = 0.01$) and VL-ArchT (n = 5 mice, $F(1,30) = 6.89$, $p = 0.018$) animals there was a significant effect of interval. However, for VM-ArchT mice, improvement in performance was greater for the interval across sessions within days, whereas for VL-ArchT animals, it was greater across sessions between days (Fig 5.10B-C).

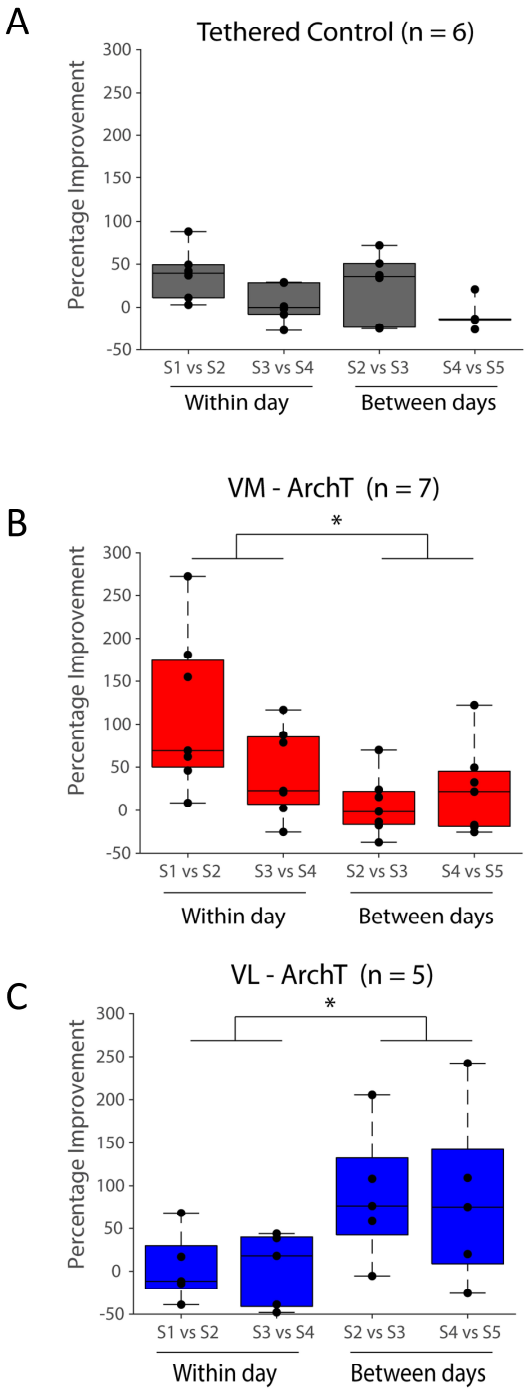



**Figure 5.10 Within group comparisons of early task performance improvement within days and between days for VM-ArchT, VL-ArchT and tethered control mice. (A)** Tethered control mice (n = 6) do not show any significant difference in mean performance improvements seen within days versus those seen between days (multi-way ANOVA, $p > 0.05$). **(B)** VM-ArchT mice (n = 7) showed significantly higher performance improvement within days than between days (multi-way ANOVA, $p < 0.05$). **(C)** VL-ArchT mice (n = 5) showed significantly higher performance improvement between

days than within days (multi-way ANOVA, $p < 0.05$). Note that during FR3/2s training mice underwent 2 identical training sessions per day (with a 90 minute rest period in between) for 7 consecutive days.

### *5.7.3 Significant differences in within-day and between-day performance gains exist between each experimental group during early sessions*

To further test the effect of Kir2.1-expression on early improvement in performance (i.e. the increase in the percentage of ≥ 3 press bouts between sessions), we computed separate ANOVAs for the percentage *change* in the number of ≥ 3 press bouts across sessions *within* one of the first two training days (i.e. between session 1 and 2 [the two sessions on training day one] or 3 and 4 [the two sessions on training day 2]) and across sessions between training days (i.e. between session 2 and 3 [the last session on training day 1 and the first session on training day 2], or session 4 and 5 [the last session on training day 2 and the first session on training day 3]). Both of these models thus had the *interval* between sessions (either in the within or between days) as one factor and the experimental group (untethered control vs MThal-Kir2.1) as the other.

For the ANOVA analysing improvement between sessions *within* training days (Fig 5.11A), there a significant effect of interval ($F(1,18) = 9.46$, $p = 0.0065$) and an interaction between interval and experimental group ($F(1,18) = 9.08$, $p = 0.0075$). Post-hoc Dunn-Šidák testing revealed that the increase in performance of the MThal-Kir2.1 mice across sessions within training day 1 was greater than that of control animals across sessions within day 1 or day 2, and greater than MThal-Kir2.1 animals across sessions within day 2 (Fig 5.11A). For the ANOVA analysing improvement across sessions *between* training days (last session of one day and first session of the next, Fig 5.11B) there were significant effects of both interval ($F(1,18) = 5.23$, $p = 0.0345$) and experimental group ($F(1,18) = 8.13$, $p = 0.01$). These results were driven by a larger improvement in the performance of the MThal-Kir2.1 mice between days 1 and 2 (i.e. S2-S3) than in untethered controls between

both days 1 and 2 (S2-S3), and days 2 and 3 (S4-S5) (post-hoc Dunn-Šidák tests). Overall, there was a greater increase in performance across the two sessions on Day 1 and between the last session of Day 1 and the first session of Day 2 than any of the intervals in controls animals. These results suggest that chronic inhibition of the motor thalamus increases the speed of learning the FR3/2s task, although it does not change the final performance level relative to controls at Day 7 (Figure 5.4 and 5.6).

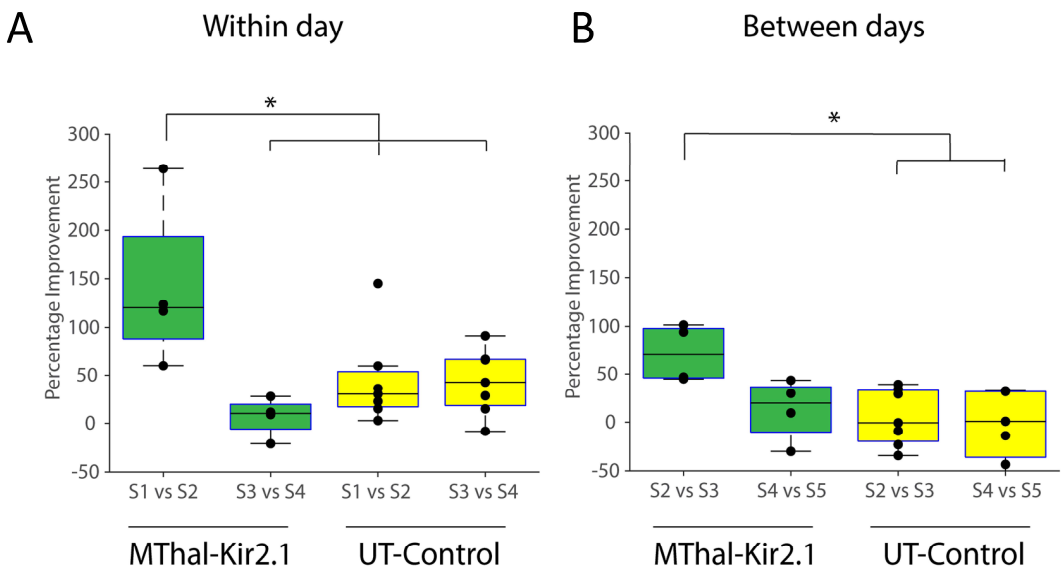



**Figure 5.11 Between group comparisons of early task performance improvement within days and between days for MThal-Kir2.1 and control groups. (A)** Within-day analysis showed that the MThal-Kir2.1 group (n = 4) showed significantly greater improvement within the first day (S1 vs S2) compared to the second day of training, and compared to control mice (n = 7) on both the first and second days of training (multi-way ANOVA, $p < 0.05$). **(B)** Between-day analysis showed that the MThal-Kir2.1 group showed superior improvement between the last session of day 1 (i.e. S2) and the first session of the next day (S3) relative to that shown by control mice between Day 1 and day 2 (i.e. S2 vs S3) or Day 2 vs Day3 (S4 vs S5) (multi-way ANOVA, $p < 0.05$). Note that during FR3/2s training mice underwent 2 identical training sessions per day (with a 90 minute rest period in between) for 7 consecutive days.

We then computed equivalent models to analyse whether optogenetic inhibition of VM or VL thalamus had comparable effects on the improvement in performance across sessions within and between training days. Within days (i.e. change in ≥ 3 press bouts between session 1 and 2) there was a significant effect of experimental group on improvement in performance, but no significant effect of interval or interaction between interval and group (Fig 5.12A). Post-hoc Dunn-Šidák testing showed that improvement across sessions within a recording day (irrespective of which recording day) was larger in VM-ArchT mice than either VL-ArchT mice or controls (Fig 5.12A). There was also a significant effect of experimental group, but not interval or interaction with interval, in the improvement of FR3/2s performance between days ($F(2,30) = 6.28$, $p = 0.0053$, Fig 5.12B). However, in contrast to performance change across sessions within days, this effect was driven by a larger increase in performance in the VL-ArchT group than either VM-ArchT animals or controls (Fig 5.12A).

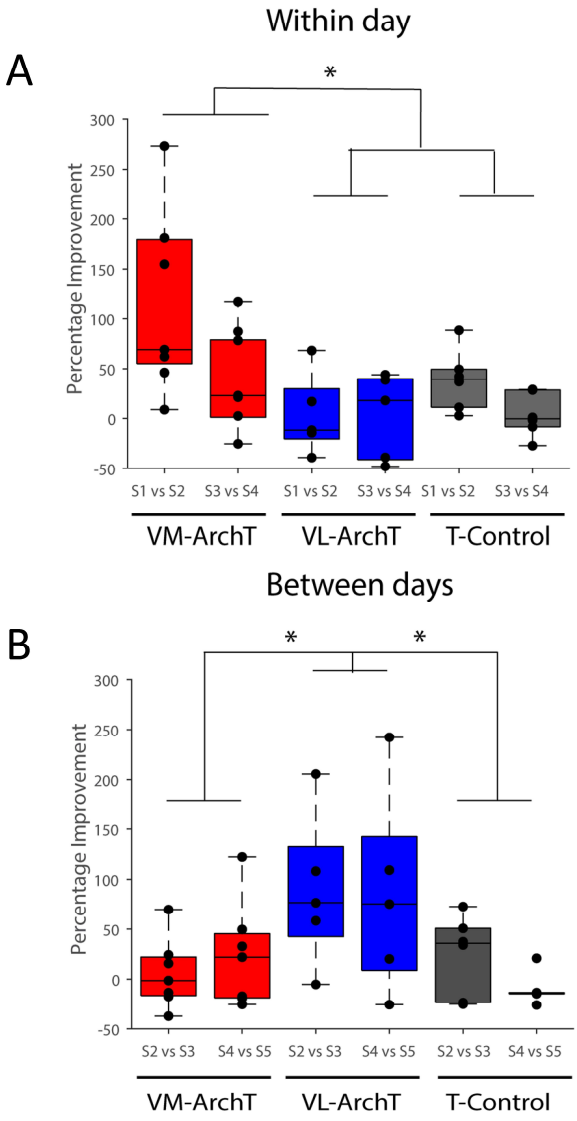



**Figure 5.12 Between group comparisons of early task performance improvement within days and between days for VM-ArchT, VL-ArchT and tethered control groups. (A)** Comparing the mean within day improvements for D1 and D2 of training showed that the VM-ArchT group (n = 7) showed superior improvement compared to VL-ArchT (n = 5) or tethered control mice (n = 6) (multi-way ANOVA, $p < 0.05$). **(B)** Comparing the mean between day improvements for Day 1-3 showed significantly greater improvement in the VL-ArchT group compared to either the VM-ArchT group or tethered controls (multi-way ANOVA, $p < 0.05$). Note that during FR3/2s training mice underwent 2 identical training sessions per day (with a 90 minute rest period in between) for 7 consecutive days.

Overall, these results suggest that inhibition of motor thalamus changed the pattern of early skill acquisition. In VM-ArchT mice, acute optogenetic inhibition improved the gain in performance

between sessions within the same day (S1-S2 and S3-S4) compared to tethered controls. In contrast, in VL-ArchT mice acute inhibition improved the gain in performance between training days (S2-S3 and S4-S5), but not between sessions within the same day. In chronically silenced MThal-Kir2.1 mice, performance gains were significantly higher within day 1 (S1-S2) and between the first and second days (S2-S3), than within day 2 (S3-S4) or between the second and third days (S4-S5). Despite these early session differences performance gain in mice receiving acute or chronic motor thalamus inhibition, absolute performance (percentage of 3 press bouts) at the end of the training period was not significantly different to respective controls.

### 5.8 Discussion

Neuroimaging studies in humans show motor thalamus activity is intimately related to learning of sequences of increasing frequency and complexity, yet paradoxically lesions of it can improve focal dystonia allowing professional musicians to return to playing (Lehericy et al., 2005; Horisawa et al., 2019). Motor thalamus neuron activity has been shown to encode activity in a range of motor tasks, including during internally generated and externally (visually triggered) movements (van Donkelaar et al., 2000), skilled reaching (Bosch-Bouju et al., 2014), learning of lever pressing tasks (Tanaka et al., 2018), as well as reward consumption (Gaidica et al., 2018). Acute lesions of the motor thalamus in primates cause transient motor deficits, and while these disappear in the chronic state other functions related to performance monitoring (e.g. after thalamic stroke) may be impaired. In mice, optogenetic perturbations of motor thalamus have so far shown to impair correct lick direction decisions (Guo et al., 2017) and the ability of mice to press a lever for a minimum duration (Tanaka et al., 2018). Furthermore, it receives significant input from the basal ganglia and cerebellum, and projects heavily to the motor cortex – structures which have been implicated in motor learning, action selection and movement timing. As such, we hypothesised that silencing motor thalamus during the acquisition of a challenging, time-dependent sequence execution task would be impaired relative to controls.

To examine this, we utilised acute and chronic silencing of thalamocortical neurons in Vglut2-Cre mice. Vglut2 is ubiquitously expressed in thalamocortical neurons, ensuring sufficient expression of Cre-dependent viral constructs. Expression of Kir2.1-ZsGreen in the motor thalamus caused hyperpolarisation of the membrane potential of neurons measured *in vitro*, making them less likely to respond to depolarising events (Figure 5.1). Equally, *in vivo* recordings of motor thalamus neurons expressing the light sensitive proton pump inhibitor ArchT showed sustained silencing of neuronal firing for 30s at light powers used during our behavioural studies (Figure 5.3). Light delivery bilaterally into VL or VM motor thalamus did not affect well learnt lever pressing routines – there was no evidence that mice redistributed task related activity into light-off periods, suggesting silencing did not cause a gross motor deficit (Table 5.2). Equally, mice with bilateral motor thalamus Kir2.1-expression did not show any impairment in learning simple (fixed ratio 1 schedule) operant lever pressing.

Mice in acute and chronic lesion groups were able to successfully acquire FR3/2s on the first attempt, with a similar failure rate to controls at this transition (Table 2.1). As failure, or non-engagement, with the task demands also occurred in controls and is highly likely to be influenced by multiple factors (e.g. motivation, attention) we focused our analysis on the patterns of learning and performance in the majority of mice who were able to acquire the task at first attempt. Contrary to our original hypothesis, we found that some motor thalamus manipulations (MThal-Kir2.1 and VM-ArchT groups) showed slightly accelerated sequence acquisition compared to their respective controls as evidenced by earlier between session performance gains in task parameters such as total lever presses required to gain all reinforcers and the percent of ≥ 3 press bouts (Table 5.2; Figures 5.4 and 5.6). Interestingly, despite faster acquisition during early sessions the overall task performance did not differ significantly from controls on the last day of training (Session 13) despite there still being significant scope for optimisation toward the theoretical goal of earning all reinforcers in 45 presses.

To understand if this accelerated early learning came at any discernible cost to motor control, we analysed the correlation between peak within-press acceleration (in bouts with ≥ 3 presses) over training sessions. This showed that while untethered control mice showed a significant correlation in the direction of reducing peak acceleration with skill acquisition, mice with acute or chronic motor thalamus inhibition or tethered controls did not. Were the untethered control mice unnecessarily devoting resources to refining aspects of motor control in an otherwise non-dextrous task? If so, was the motor thalamus lesion impairing this parallel process allowing resources to be reattributed to the core sequence learning aspect of the FR3/2s task? Closer analysis showed that ~30% of mice in untethered control, tethered control and VM-ArchT groups did at least show significant positive correlation in reducing peak acceleration (one VM-ArchT mouse showed a significantly negative correlation) whereas VL-ArchT mice did not show any correlation and MThal-Kir2.1 only showed a significantly negative correlation in one mouse. Training mice for longer periods of time (e.g. several weeks or months) may allow this to influence further development of lever pressing kinematics, such as the frequency of bouts where tighter oscillation of the lever movements around the middle of its arc where the infrared beam break is located.

To better clarify the nature of the learning processes that may have been enhanced in these groups, we looked at within day learning for the first two training days and between day learning for the first three days of training on FR3/2s. Briefly, we either calculated the difference in the percentage of ≥ 3 press bouts recorded for the first and second sessions within a given day, or between the second session of one day and the first session of the next day. Within group analysis showed that untethered control mice showed a significantly higher within-day than between-day performance gain, but this was still significantly lower than the within- or between-day performance gains in MThal-Kir2.1 mice (Figure 5.11). In contrast to untethered controls, tethered control mice did not show a significant difference in performance improvements occurring within-day vs. between-days. However, VM-ArchT mice showed significantly higher within-day than between-day performance gains while VL-ArchT mice showed the opposite pattern (Figure 5.10). Subsequent between group comparisons confirmed that VM-ArchT mice showed significantly higher within-day learning than

either VL-ArchT or tethered control mice, while VL-ArchT mice showed significantly higher between-day performance gains than VM-ArchT or tethered control mice (Figure 5.12). Interestingly, MThal-Kir2.1 mice showed both features but compacted into the first within-day and first between-day gains (Figure 5.11). Overall, these findings suggest that inhibition of motor thalamus is associated with alterations in the temporal pattern of performance improvements during skill acquisition relative to controls. It is unclear if these are network-wide compensatory changes which aim to ensure that overall task competency (i.e. percentage of 3 press bouts) is not significantly worse overall between inhibition and control groups, or a potential beneficial effect of motor thalamus inhibition on reducing competition with parallel systems also supporting sequence learning (e.g. mediodorsal to prefrontal pathway, or hippocampal networks). Although MThal-Kir2.1 mice show earlier learning, this appears to be at the cost of refining kinematic parameters.

These results are dichotomous with respect to our original prediction that silencing motor thalamus will cause an impairment in acquisition of FR3/2s and this could be due to several reasons. Firstly, motor thalamus may not be causally driving the movements or is simply permissive for the rest of the circuit to generate the movement which may explain (i) the longstanding difficulty in understanding how basal ganglia-thalamic communication relates to movement production (Goldberg et al., 2013), (ii) why non-physiological stimulation of motor thalamus may be able to evoke movements via downstream structures (Miall et al., 1998) but (iii) silencing does not abolish movement generation (van Donkelaar et al., 2000; Guo et al., 2017; Lalive et al., 2018; Tanaka et al., 2018; Sauerbrei et al., 2020). Secondly, thalamic nuclei have projection patterns with overlapping terminal fields at the level of cortex, hence silencing of one nucleus may potentially be compensated by increased activity in other nuclei (potentially in a task-dependent manner) projecting to the same target given the complex arrangement of open and closed cortico-basal ganglia-thalamocortical loops (Guo et al., 2018; Aoki et al., 2019; Halassa and Sherman, 2019; Nakajima et al., 2019). Thirdly, if motor thalamus is mostly important for movement kinematics then in our non-dextrous FR3/2s task silencing may not significantly impair lever manipulation. Fourthly, although we have identified our optic fibre tip positions in implanted animals, systematic

assessment of the spread of virus in each brain and retrospective grouping into VM-ArchT or VL-ArchT groups will be required to confidently attribute effects to silencing of specific thalamic zones. Lastly, as motor thalamus projects densely to cortical areas thought to control the balance of exploitation of learned ruled versus exploration (Schreiner and Gremel, 2018) but targets both excitatory and inhibitory neurons (Duan et al., 2020), silencing certain zones may modulate activity in a complex manner to favour earlier exploitation and hence earlier performance gains.

### *5.8.1 Technical considerations*

Due to significant difficulties in breeding enough male Vglut2-Cre mice and because not all injected or implanted mice successfully acquire the FR3/2s paradigm (thus cannot be included in our analysis), our control groups are mixed and need optimising. The untethered control group includes wild type C57/BL6J mice (who have not undergone surgery for bilateral AAV-CAG-Flex-GFP injections). Although our Vglut2-Cre line is on a C57/BL6 genetic background and we only use heterozygous males for experiments, we did not have sufficient animals to compare the Vglut2-MThal-Kir2.1 group to a true Vglut2-MThal-GFP control group. Equally, our tethered control group includes 3 VM-GFP injected and implanted mice who received light delivery as per VL-ArchT and VM-ArchT mice, but also includes 3 implanted mice (bilaterally expressing AAV-CAG-Flex-ArchT-GFP in motor thalamus via SNr injection of AAV-Ef1a-mCherry-IRES-WGA-Cre virus) which did not receive light stimulation during FR3/2s sessions. In both cases, however, if anything this should have improved their performance relative to the VM-ArchT or MThal-Kir2.1 groups which nonetheless showed faster early acquisition of the task. Another issue is the small number of mice in the Mthal-Kir2.1 group (n = 4) as only 4 out of 7 injected mice acquired FR3/2s sufficiently to be included. As such, further experiments are required to perfectly match the inhibition groups. Greater numbers of mice in each group may also allow the correlation of behaviour with virus expression pattern and fibre tip position. Using an even smaller viral load, or AAV serotype with less spread may also help limit mixed behavioural effects. It is unclear why, within group analysis showed a significant bias toward within day learning in untethered controls but not in tethered

controls. Nonetheless, within day learning was still significantly higher in MThal-Kir2.1 versus untethered controls and VM-ArchT relative to tethered controls, suggesting that this is still facilitated.

We did not induce the chronic lesion of motor thalamus after the mouse had already learnt lever pressing behaviour as others have (Kawai et al., 2015), hence there is a possibility in our chronically lesioned mice that an alternative or parallel learning circuit independent of motor thalamus was utilised for initial operant learning and hence mice were able to be successful overall in the task despite the lesion. Other thalamic nuclei which may compensate include intralaminar and mediodorsal and laterodorsal, as well as lesser known direct input from GPe to cortex (Saunders et al., 2015). Given that we waited a minimum of 6 weeks for Kir2.1 expression prior to undertaking behaviour, this is a conceivable timescale for circuit plasticity to occur. Other potential issues were insufficient number of neurons silenced, or that sufficient cortical excitation of Kir2.1 expressing neurons was still possible *in vivo* (despite hyperpolarization) for signals to be transmitted.

A consequence of our pseudorandom light stimulation pattern meant all mice are getting a slightly different pattern of silencing in relation to task-events. Although previous studies have been able to use stereotyped patterns of movement in over trained mice to trigger laser prior to lever press onset, in our task rule transition during early FR3/2s disrupts the stereotyped movements between magazine and lever seen at the end of FR1. Mice are more likely to approach the lever from elsewhere in the chamber and so triggering the laser from an infra-red beam break situated between lever and magazine may not have been practical. An alternative option would have been to utilise laser triggered by real time position tracking through a commercially available (expensive) system, or by building our own version (time consuming). Alternatively, newer optogenetic tools are becoming available that allow sustained silencing over periods of tens of seconds and minutes in response to intermittent short light pulses, and thus could give better silencing throughout the entire training session without fear of heat related effects (tissue damage or non-cell type specific inhibition) (Owen et al., 2019). However, our *in vivo* recordings with 30s light delivery do not show

non-specific thermal silencing – contacts immediately (~100 μm) adjacent to those showing silencing of multi-unit activity show preserved spiking activity (Figure 5.3) and spiking is preserved even in contacts closer to the optic fibre where intensity would be the highest. In future, other patterns of silencing linked specifically to lever press or reward consumption using more sophisticated triggers could be utilised to determine a critical time point for intervention during learning. Optimal silencing at a critical window of motor thalamus activity may have a much more dramatic behavioural effect rather than 30s long pulses but may still either impair or improve performance.

We only trained the animals to 7 days (session 14), and although learning grossly improved at early time points there could be a detrimental effect on automatization later on in training after several weeks. The analysis presented here could be significantly augmented by methods looking at the pattern of learning *within* individual training sessions, and how this pattern affects the performance or learning pattern within the next session. This would provide much more reliable insight regarding any potential effect motor thalamus inhibition on online versus offline motor learning. This may also help explain whether the significantly higher performance gain between days in VL-ArchT mice is due to augmented offline processes, or due to significantly slower within-day learning that only accelerates at the end of the second daily training session. Whether the frequency and duration of within session rest periods affects learning and whether the pattern of number of lever presses between each reinforcer delivery, or whether a reduction in the overall number of bouts is the key priority of learning (or some ratio between the two as mice may show variation in strategy) remains unclear and was not dissociated in the analysis presented. Furthermore, we did not analyse other aspects of acceleration such as the total time between initiation of the press and beam break, or the gradients of the acceleration curve.

*5.8.2 Summary*

Although the cerebellum (Ito, 1993) and basal ganglia (Graybiel et al., 1994) are known to support many aspects of motor control, their contributions to acquired skills are often presumed to be mediated through interactions with motor cortex (Hikosaka et al., 2002; Doyon et al., 2009). Other subcortical motor structures, such as the reticular formation (Baker, 2011; Esposito et al., 2014), red nucleus (Massion, 1988), and superior colliculus (Philipp and Hoffmann, 2014), are thought to encode species-specific movements and action patterns or serve as intermediaries for cortical commands (Esposito et al., 2014). Recent evidence suggests that movements generated by subcortical controllers can be shaped, sequenced, and coordinated during skill learning to yield complex task-specific motor patterns that can be stored and produced independently of motor cortex (Kawai et al., 2015). The limits of subcortical plasticity and the extent to which lower-level motor circuits can support other forms of complex learned motor behaviours remains to be understood. It has been reported by various groups that lesions of motor cortex impair skill learning, but do not disrupt performance of already well learnt skills. The major inputs to pyramidal neurons in motor cortex are from sensory cortex (~65%), followed by (~8%) motor thalamus (Zhang et al., 2016). Motor cortex also receives dopaminergic projections from the VTA and lesions here also impair acquisition of skilled grasp but have no detrimental effect once acquired (Hosp et al., 2011). Furthermore, given that corticostriatal signalling is important for temporal chunking of lever press sequences (Jin and Costa, 2010; Jin et al., 2014; Santos et al., 2015) and basal ganglia feedback to motor cortex is thought to be routed primarily through motor thalamus, and that learning of temporally-specified lever pressing involves signalling to motor cortex (Tanaka et al., 2018) it may be expected that inhibiting the activity in motor cortex causes severe deficits in acquiring temporally constrained sequences of lever presses.

Surprisingly, we found that chronic or acute pseudorandom inhibition of motor thalamus regions can facilitate early sequence acquisition and alter the relative contributions of within day versus between day performance improvements, supporting the idea that motor thalamus is connected to

downstream networks that may modulate aspects of motor skill learning. We also found that this may come at the cost of associated changes in motor control of lever acceleration, which, though not critical to the efficiency of earning reinforcers in our task *per se*, could feasibly affect longer term refinement of motor kinematics relative to control mice.

# 6. Discussion

## 6.1 Summary of Main Findings

Motor thalamus is highly interconnected with brain regions important for movement and cognition, and is a common target for movement disorder surgery in humans. Despite this, how its computations affect the scope of motor behaviour during health remains uncertain. Although motor thalamus lesioning experiments in rodents and primates have produced acute motor side effects, these resolved over time (Starr and Summerhayes, 1983b; Canavan et al., 1989). Though this is in contrast to long-held assumptions by circuit models of motor control, it is consistent with more recent evidence suggesting that in rodents motor cortex is required for online dextrous movements and motor learning rather than all voluntary movement (Kawai et al., 2015). Given that motor thalamus is the largest subcortical input to motor cortex, one may predict that its roles may also primarily contribute to these two functions. Discriminating effects on motor learning and motor control within dextrous tasks (e.g. skilled reaching and grasp) is difficult as manipulations causing impairment in motor dexterity may secondarily impair motor learning (Olveczky, 2011). As such, for practical purposes many have divided skilled behavioural tasks into those focussing on motor adaptation (e.g. skilled reaching for pellets) or non-dextrous tasks involving motor sequence learning (e.g. lever press sequences with specific numerical and/or temporal properties). Although evidence suggests a role for the motor thalamus in the former (van Donkelaar et al., 2000), its role in the latter is less clear - as is the specific contribution of its basal ganglia- and cerebellar-receiving subregions.

We found that in mice, as previously identified in rats, motor thalamus neurons can be segregated based on their input from either basal ganglia or cerebellar output nuclei and do have a slightly differing distribution within motor thalamus and distinct laminar targeting profiles identified by anatomical and electrophysiological means (Chapter 3). Subsequently, we

developed a task aimed at monitoring how mice acquire and consolidate a challenging novel lever pressing pattern (FR3/2s) requiring chunking of already learnt actions (Chapter 4). Control mice consolidated this pattern over sessions and days, allowing sufficient opportunities to monitor and manipulate activity, and showed adaptation of peak within-press lever accelerometer traces. Next, we explored how either chronic silencing of the motor thalamus, or within session optogenetic silencing of VM or VL thalamic nuclei bilaterally affected skill acquisition trajectories in the FR3/2s task (Chapter 5). In mice where motor thalamus is chronically silenced (MThal-Kir2.1) during training, to our surprise, the self-paced acquisition of the novel pattern is faster than in control mice both between sessions in the same day and between the second session of one day and the first session of the next day. Despite this improvement, MThal-Kir2.1 mice do not show the same refinement of accelerometer traces as untethered control mice. We next looked at whether online (within session) optogenetic silencing of either VM or VL thalamus using ArchT could partially or wholly reproduce this effect on skill acquisition. We found that acute within-session VM silencing enhanced acquisition between sessions within the same day relative to tethered controls but did not affect performance gains between consecutive sessions on different days. By contrast, acute within-session VL silencing had the opposite effect - performance gains between days were significantly enhanced relative to those within the same day, and compared to tethered controls and VM-ArchT mice. We will now discuss these findings, their implications and possible mechanisms in more detail.

### 6.2 Anatomically distinct motor thalamus neuron populations are conserved in mice

At present there no reliable way of selectively targeting only either basal ganglia-receiving or cerebellar-receiving motor thalamus neurons through transgenic mouse lines (Gerfen et al., 2013), through recent transcriptomic analysis of thalamic neurons may aid this in future (Phillips et al., 2019). Despite the anatomical difficulty of targeting these pathways selectively within the thalamus, we leveraged the non-reciprocal connections with its subcortical input

nuclei by attempting to anterogradely, transsynaptically tag motor thalamus neurons from a presynaptic starting site in either SNr or DCN. Our data has shown that the bicistronic AAV-Ef1a-mCherry-IRES-WGA-Cre virus is reliably expressed in the SNr and DCN, and that WGA-Cre travelling anterogradely in nigrothalamic and cerebellothalamic projections can cross into the postsynaptic thalamic neuron to activate expression of a Cre-dependent channelrhodopsin-eYFP. This approach did confirm both that, i) despite overlapping axonal projections from basal ganglia and cerebellum in motor thalamus, they target relatively segregated neuron populations as in other species and ii) at a population level their anatomical targets are conserved across species – namely that basal ganglia recipient neurons in VM target neocortical layer 1 while cerebellar-recipient neurons in VL target lower neocortical layers (McFarland and Haber, 2000; McFarland and Haber, 2002; Kuramoto et al., 2009; Hintzen et al., 2018).

Unfortunately, the low proportion of thalamic neurons tagged postsynaptically using commercially available virus combinations meant it was unlikely to be a robust approach to selectively manipulate BZ or CZ neuron activity during a behavioural task. Furthermore, we could not restrict opsin in the area immediately below VM thalamus, the zona incerta, which has reciprocal connections to SNr – demonstrating one of the challenges of a purely connectivity-based targeting approach in wild type animals. A conceptually similar strategy utilising very high titre ($10^{13}$-$10^{14}$ vg/ml) AAV1-Cre and AAV9-Cre viruses to target postsynaptic neurons has also been reported recently (Zingg et al., 2017). Although other strategies for anterograde transsynaptic tagging of postsynaptic neurons are being developed, they are yet to be widely available (Beier et al., 2011; Saleeba et al., 2019). Although terminal fibre silencing has its own technical issues (Mahn et al., 2016), it is being used more frequently and may also be able to provide meaningful cessation of basal ganglia and cerebellar information streams in the motor thalamus(Guo et al., 2017).

The approach of segregating motor thalamus neurons based on known basal ganglia or cerebellar input assumes that this dichotomy is the most functionally relevant. Divergence of

these neurons occurs at the level of cortex too. For example, Layer 1 projecting motor thalamus neurons likely synapse onto layer 1 interneurons, but also onto the apical dendrites of layer 2/3 and layer 5 pyramidal neurons which exist here. Given that there is growing evidence that superficial vs deep pyramidal neurons have functionally distinct roles, silencing motor thalamus neurons across BG and cerebellar territories which converge onto either of these populations may be more relevant given their proximity to motor output. Transgenic lines do exist for targeting subsets of cortical neurons, such as *Ndnf* (layer 1), *Wfs1* (layer 2/3), *Rorb* (functional 'layer 4'), *Rbp5* (layer 5 in general), *Sim1* (layer 5 pyramidal tract neurons), *Tlx3* (layer 5 intratelencephalic neurons), and *Ntsr1* (layer 6 corticothalamic neurons) (Zariwala et al., 2012; Gerfen et al., 2013; Abs et al., 2018). Coupled with newer tools for retrograde monosynaptic delivery of optogenetic constructs via a self-inactivating modified-rabies virus (Ciabatti et al., 2017), these may parcellate motor thalamus in a different way which may be just as functionally relevant. However, even these strategies will likely need combining with intersectional strategies to ensure that tools are only expressed in presynaptic populations of interest (Fenno et al., 2014), until strategies for achieving similar selectivity in wild type animals through promoter-specific viral constructs has become possible (Nathanson et al., 2009; Gompf et al., 2015). For example, in our case both glutamatergic thalamic neurons in VM thalamus (McFarland and Haber, 2000; McFarland and Haber, 2002; Kuramoto et al., 2009; Kuramoto et al., 2015) and GABAergic zona incerta neurons immediately below (Bourane et al., 2015) project to layer 1 of neocortex and would still need to be segregated in activity manipulations .

### 6.3 Discrete acquisition of a demanding non-dextrous motor sequence shows refinement in multiple behavioural domains in mice

Operant lever pressing has classically been used to study self-paced behaviour, but mice are usually encouraged to adopt a target behaviour via small increments in difficulty (Jin et al., 2014; Santos et al., 2015) or a graded reward landscape (Kawai et al., 2015). Multiple small adjustments or using scaled reinforcer size make it harder to detect motor learning in response

to any single change in motor demands of the task. Another route is to utilise a single more difficult rule change, where a novel minimum performance level must be met to gain any reinforcement. The main disadvantage of this approach is that mice who are unable to meet this predetermined performance level may become demotivated and abandon pressing altogether. We thus set out to see if some of these difficulties could be overcome and still reliably drive motor learning, to characterise how mice increasingly adopt the correct motor sequences as a proportion of all motor output. This approach has not been used in mice previously, and only infrequently in rats learning a novel sequence (Ostlund et al., 2009; Martiros et al., 2018).

Motor variability, or exploration of motor parameter space, is known to increase the likelihood of incidental learning of new rules or task contingencies (Dhawale et al., 2017). One method of increasing motor variability in mice who have already acquired operant responding is by inducing uncertainty and/or a frustration response through unexpected non-reward (Burokas et al., 2012). We hypothesised that analysing the repertoire of lever pressing responses during early extinction can be exploited to identify more challenging sequence targets that mice can adopt directly from a fixed-ratio 1 (FR1) schedule. We exploited this phenomenon in mice who had already acquired FR1 operant lever pressing to capture, at a group level, the common motor parameter space (i.e. variations in number and timing of lever presses within individual bouts of pressing) most mice were willing to explore when faced with unexpected non-reward. Using this approach, we found that many mice would increase the proportion of bouts where 3 presses would occur with each inter-press interval being less than 1s. We then trained another group of mice on FR1 and covertly introduced this new rule (FR3/2s) with a matched (three-fold) increase in reinforcer volume balanced to that in FR1. We found that most mice (~ 60-70%), through motor exploration and incidental reinforcer delivery, could acquire this new FR3/2s pattern of lever pressing in the first session of exposure and refined their pressing pattern over subsequent sessions and days so that fewer unreinforced lever presses were performed.

Concomitantly, we measured the peak within-press acceleration generated and found that, despite not being task relevant *per se*, mice showed a significant correlation between training sessions and reducing peak within-press acceleration. As such, mice showed elements of both sequence learning and motor adaptation in the same task but reinforcer delivery was not contingent on the latter. Although this data is not commonly collected, and assumed not to be relevant in a non-dextrous task, it justifies the additional monitoring of other parameters such as paw trajectory tracking or lever potentiometers in future (Kawai et al., 2015; Yttri and Dudman, 2016).

It remains unclear why some mice with identical performance during FR1 fail to acquire the FR3/2s task at the first attempt but do so on a second attempt after further training on the original FR1 schedule. If this is purely motivational, it may be improved by using water restriction rather than food restriction in future (Goltstein et al., 2018). However, it also remains plausible that identically performing mice are still using different strategies, or relative amounts of them, such as the ratio between model free and model based approach (Skatova et al., 2013).

### 6.4 Silencing of motor thalamus may facilitate motor sequence learning in mice

Recording or predicting the full downstream (i.e. nervous system wide) activity effects of localised manipulations of brain activity is currently not possible. The development of new *in vivo* technologies such as high-density neural recordings, genetic reporters of activity, or optogenetic manipulations that are even more precise or drive more naturalistic patterns of activity may aide us in approaching this goal (Allen et al., 2015). We found that manipulation of motor thalamus activity can affect the rate of early learning but not the end skill level, at least not at the end point tested in this thesis. Within this, we saw differential effects of VM and VL biased manipulations on the timing of performance gains in our task (across sessions within the same day vs across consecutive sessions between days).

VM-ArchT mice showed improved learning within days compared to VL-ArchT and tethered controls, but no difference in the performance gain between days relative to tethered control. These larger within-day performance gains may have obviated the need or motivation for additional processes responsible for producing offline gains. Indeed, larger within-day gains may have occurred secondary to reduced competition with hippocampal dependent sequence learning or by reducing non-task relevant information getting to cortex in a manner that did not impair motor output (Lee et al., 2008). Human studies of cognitive enhancement induced by neuromodulation is hypothesised as being either due to (i) direct modulation of a cortical region or network that leads to more efficient processing, and/or (ii) addition-by-subtraction, which is the disruption of processing which competes or distracts from task performance (Luber and Lisanby, 2014). Since thalamocortical neurons are known to project to both excitatory and inhibitory neurons in both cortex and striatum (Wall et al., 2010; Guo et al., 2015b; Duan et al., 2020), inhibiting motor thalamus also has the potential to influence excitatory/inhibitory balance. Another possibility is that silencing VM reduces reticular thalamus mediated silencing of other nuclei (e.g. mediodorsal thalamus, anterior nuclei) to allow relevant information transmission to the cortex, or that direct silencing suppresses transmission of task irrelevant information. This may improve the relative function of MD thalamus or anterior thalamic nuclei, or direct hippocampal-cortical information flow.

In contrast, VL-ArchT mice showed the majority of their performance gains in the FR3/2s task between days. That within session optogenetic silencing could lead to such a pattern is counterintuitive. It could a be product of overall poor learning throughout the day except for at the end of the second session, giving the appearance that performance gains all occurred offline between days. Further detailed analysis of within session progression of learning parameters may help clarify if this was the case. Alternatively, consistently poor performance within both sessions during the day may prioritise the experience for offline replay, and how experiences are tagged or prioritised during online behaviour for offline replay is an active field of research (Momennejad et al., 2018). MThal-Kir2.1 mice show features of both VM-ArchT and VL-ArchT groups, and hence may concentrate their performance gains within and between the earliest training sessions and not require

larger gains at later phases unlike VM-ArchT and VL-ArchT mice. Learning can occur via multiple parallel systems (Jocham et al., 2016), and while in general this may work to support acquisition of complex task contingencies it may also serve to delay potential gains in task performance if exploration is prioritised over exploitation (Lee et al., 2008; Dhawale et al., 2017). Motor thalamus is known to project to cortical areas involved in regulating exploitation of learned rules (Schreiner and Gremel, 2018) and thus may play a complex role in modulating this during motor sequence learning.

### 6.5 Future directions

The experiments described in this thesis provide only a starting point for investigating the role of the motor thalamus in the self-paced acquisition of motor sequences. Other important experiments which need addressing include:

1) Further analysis of existing behavioural data to ascertain the immediate effect of silencing on ongoing motor output (timing of next press, duration of presses, accelerometer profile and success of earning a reinforcer) in all instances where light onset occurs during an already self-initiated bout of pressing (rather than prior to initiation). This may inform us about potential differences in the role of motor thalamus in cued versus self-initiated non-dextrous motor output.

2) *In vivo* freely moving multi-site electrophysiology to identify the thalamic, cortical and striatal biomarkers underlying or predicting acquisition and refinement of the FR3/2s task. Concurrent electrophysiology during optogenetic silencing experiments may help us understand how motor thalamus modulates these underlying phenomena to enhance online or offline learning processes. For example, does motor thalamus silencing disrupt how these phenomena develop during learning or does it enhance them? Is there evidence of increased inhibition in cortex in mice who learn faster? Can we use this information to move away from pseudorandom silencing protocols of motor

thalamus to intervene at particular task points or in a closed loop fashion to bidirectionally control task acquisition rate? Does driving rather than silencing these neurons using excitatory opsins have the same or different effect on task acquisition?

3) Understanding whether acquisition of the FR3/2s task requires cortex (e.g. primary motor cortex, secondary motor cortex, prefrontal cortex), striatum and cerebellum through lesion studies or local optogenetic perturbations (e.g. terminal fibre silencing of either basal ganglia or cerebellar inputs to motor thalamus) in either wild type or appropriate transgenic mouse lines.

4) Detailed monitoring of sleep-wake activity outside of the task environment may identify behavioural changes induced by within session motor thalamus silencing to affect online and offline performance gains. Furthermore, within task paw tracking may also be useful in clarifying if there are other motor control related effects of motor thalamus silencing.

### 6.6 Conclusion

The motor thalamus is a hub of input from basal ganglia and cerebellar output nuclei and provides the major subcortical projection to motor cortical areas. The role of motor thalamus in self-paced skill learning is largely inferred by its large input from the basal ganglia and cerebellum, though conceivably it may equally need to receive this information to play a global modulatory role affecting various parallel subcortico-cortical processing streams. Although our findings do not demonstrate necessity of motor thalamus in the acquisition of a self-paced motor sequence task requiring characteristics thought to be encoded in the basal ganglia and cerebellum, we do find evidence that it may modulate downstream networks important for the rate of sequence acquisition and support simultaneous motor adaptation.

# References


ABS, E., POORTHUIS, R. B., APELBLAT, D., MUHAMMAD, K., PARDI, M. B., ENKE, L., KUSHINSKY, D., PU, D. L., EIZINGER, M. F., CONZELMANN, K. K., SPIEGEL, I. & LETZKUS, J. J. 2018. Learning-Related Plasticity in Dendrite-Targeting Layer 1 Interneurons. *Neuron,* 100, 684-699 e6.

ALAVERDASHVILI, M. & WHISHAW, I. Q. 2008. Motor cortex stroke impairs individual digit movement in skilled reaching by the rat. *Eur J Neurosci,* 28, 311-22.

ALBIN, R. L., YOUNG, A. B. & PENNEY, J. B. 1989. The functional anatomy of basal ganglia disorders. *Trends Neurosci,* 12, 366-75.

ALBOUY, G., STERPENICH, V., BALTEAU, E., VANDEWALLE, G., DESSEILLES, M., DANG-VU, T., DARSAUD, A., RUBY, P., LUPPI, P. H., DEGUELDRE, C., PEIGNEUX, P., LUXEN, A. & MAQUET, P. 2008. Both the hippocampus and striatum are involved in consolidation of motor sequence memory. *Neuron,* 58, 261-72.

ALLEN, B. D., SINGER, A. C. & BOYDEN, E. S. 2015. Principles of designing interpretable optogenetic behavior experiments. *Learn Mem,* 22, 232-8.

ANDERSON, M. E. & TURNER, R. S. 1991. Activity of neurons in cerebellar-receiving and pallidal-receiving areas of the thalamus of the behaving monkey. *J Neurophysiol,* 66, 879-93.

ANDERSON, W. S., WEISS, N., LAWSON, H. C., OHARA, S., ROWLAND, L. & LENZ, F. A. 2011. Demonstration of motor imagery movement and phantom movement-related neuronal activity in human thalamus. *Neuroreport,* 22, 88-92.

AOKI, S., SMITH, J. B., LI, H., YAN, X., IGARASHI, M., COULON, P., WICKENS, J. R., RUIGROK, T. J. & JIN, X. 2019. An open cortico-basal ganglia loop allows limbic control over motor output via the nigrothalamic pathway. *Elife,* 8, e49995.

AZIM, E., JIANG, J., ALSTERMARK, B. & JESSELL, T. M. 2014. Skilled reaching relies on a V2a propriospinal internal copy circuit. *Nature,* 508, 357-63.

BAKER, S. N. 2011. The primate reticulospinal tract, hand function and functional recovery. *J Physiol,* 589, 5603-12.

BALLERMANN, M., METZ, G. A., MCKENNA, J. E., KLASSEN, F. & WHISHAW, I. Q. 2001. The pasta matrix reaching task: a simple test for measuring skilled reaching distance, direction, and dexterity in rats. *J Neurosci Methods,* 106, 39-45.

BEIER, K. T., SAUNDERS, A., OLDENBURG, I. A., MIYAMICHI, K., AKHTAR, N., LUO, L., WHELAN, S. P., SABATINI, B. & CEPKO, C. L. 2011. Anterograde or retrograde transsynaptic labeling of CNS neurons with vesicular stomatitis virus vectors. *Proc Natl Acad Sci U S A,* 108, 15414-9.

BIANE, J. S., TAKASHIMA, Y., SCANZIANI, M., CONNER, J. M. & TUSZYNSKI, M. H. 2016. Thalamocortical Projections onto Behaviorally Relevant Neurons Exhibit Plasticity during Adult Motor Learning. *Neuron,* 89, 1173-1179.

BIRBAUMER, N. 2007. Motor learning: passing a skill from one hand to the other. *Curr Biol,* 17, R1024-6.

BOLKAN, S. S., STUJENSKE, J. M., PARNAUDEAU, S., SPELLMAN, T. J., RAUFFENBART, C., ABBAS, A. I., HARRIS, A. Z., GORDON, J. A. & KELLENDONK, C. 2017. Thalamic projections sustain prefrontal activity during working memory maintenance. *Nat Neurosci,* 20, 987-996.

BONSTRUP, M., ITURRATE, I., THOMPSON, R., CRUCIANI, G., CENSOR, N. & COHEN, L. G. 2019. A Rapid Form of Offline Consolidation in Skill Learning. *Curr Biol,* 29, 1346-1351 e4.

BORNSCHLEGL, M. & ASANUMA, H. 1987. Importance of the projection from the sensory to the motor cortex for recovery of motor function following partial thalamic lesion in the monkey. *Brain Res,* 437, 121-30.

BOSCH-BOUJU, C., HYLAND, B. I. & PARR-BROWNLIE, L. C. 2013. Motor thalamus integration of cortical, cerebellar and basal ganglia information: implications for normal and parkinsonian conditions. *Front Comput Neurosci,* 7, 163.
BOSCH-BOUJU, C., SMITHER, R. A., HYLAND, B. I. & PARR-BROWNLIE, L. C. 2014. Reduced reach-related modulation of motor thalamus neural activity in a rat model of Parkinson's disease. *J Neurosci,* 34, 15836-50.
BOURANE, S., DUAN, B., KOCH, S. C., DALET, A., BRITZ, O., GARCIA-CAMPMANY, L., KIM, E., CHENG, L., GHOSH, A., MA, Q. & GOULDING, M. 2015. Gate control of mechanical itch by a subpopulation of spinal cord interneurons. *Science,* 350, 550-4.
BUROKAS, A., GUTIERREZ-CUESTA, J., MARTIN-GARCIA, E. & MALDONADO, R. 2012. Operant model of frustrated expected reward in mice. *Addict Biol,* 17, 770-82.
BURRONE, J., O'BYRNE, M. & MURTHY, V. N. 2002. Multiple forms of synaptic plasticity triggered by selective suppression of activity in individual neurons. *Nature,* 420, 414-8.
BUTLER, A. B. 2008. Evolution of the thalamus: a morphological and functional review. *Thalamus & Related Systems,* 4.
CAGNAN, H., DENISON, T., MCINTYRE, C. & BROWN, P. 2019. Emerging technologies for improved deep brain stimulation. *Nat Biotechnol,* 37, 1024-1033.
CANAVAN, A. G., NIXON, P. D. & PASSINGHAM, R. E. 1989. Motor learning in monkeys (Macaca fascicularis) with lesions in motor thalamus. *Exp Brain Res,* 77, 113-26.
CAO, V. Y., YE, Y., MASTWAL, S., REN, M., COON, M., LIU, Q., COSTA, R. M. & WANG, K. H. 2015. Motor Learning Consolidates Arc-Expressing Neuronal Ensembles in Secondary Motor Cortex. *Neuron,* 86, 1385-92.
CARRERA, E. & BOGOUSSLAVSKY, J. 2006. The thalamus and behavior: effects of anatomically distinct strokes. *Neurology,* 66, 1817-23.
CASTRO-ALAMANCOS, M. A. & CONNORS, B. W. 1997. Thalamocortical synapses. *Prog Neurobiol,* 51, 581-606.
CAVDAR, S., ONAT, F. Y., YANANLI, H. R., SEHIRLI, U. S., TULAY, C., SAKA, E. & GURDAL, E. 2002. Cerebellar connections to the rostral reticular nucleus of the thalamus in the rat. *J Anat,* 201, 485-91.
CEBRIAN, C., PARENT, A. & PRENSA, L. 2005. Patterns of axonal branching of neurons of the substantia nigra pars reticulata and pars lateralis in the rat. *J Comp Neurol,* 492, 349-69.
CHABROL, F. P., BLOT, A. & MRSIC-FLOGEL, T. D. 2019. Cerebellar Contribution to Preparatory Activity in Motor Neocortex. *Neuron,* 103, 506-519 e4.
CHEN, C. H., FREMONT, R., ARTEAGA-BRACHO, E. E. & KHODAKHAH, K. 2014. Short latency cerebellar modulation of the basal ganglia. *Nat Neurosci,* 17, 1767-75.
CHEN, H., HUA, S. E., SMITH, M. A., LENZ, F. A. & SHADMEHR, R. 2006. Effects of human cerebellar thalamus disruption on adaptive control of reaching. *Cereb Cortex,* 16, 1462-73.
CIABATTI, E., GONZALEZ-RUEDA, A., MARIOTTI, L., MORGESE, F. & TRIPODI, M. 2017. Life-Long Genetic and Functional Access to Neural Circuits Using Self-Inactivating Rabies Virus. *Cell,* 170, 382-392 e14.
CLAVIER, R. M. & GERFEN, C. R. 1982. Intracranial self-stimulation in the thalamus of the rat. *Brain Res Bull,* 8, 353-8.
COLLINS, D. P., ANASTASIADES, P. G., MARLIN, J. J. & CARTER, A. G. 2018. Reciprocal Circuits Linking the Prefrontal Cortex with Dorsal and Ventral Thalamic Nuclei. *Neuron,* 98, 366-379 e4.
CROSSMAN, A. R. & OBESO, J. A. 2016. Functions of the basal ganglia-paradox or no paradox? *Mov Disord,* 31, 1120-1.
CRUIKSHANK, S. J., AHMED, O. J., STEVENS, T. R., PATRICK, S. L., GONZALEZ, A. N., ELMALEH, M. & CONNORS, B. W. 2012. Thalamic control of layer 1 circuits in prefrontal cortex. *J Neurosci,* 32, 17813-23.
DESMURGET, M. & TURNER, R. S. 2010. Motor sequences and the basal ganglia: kinematics, not habits. *J Neurosci,* 30, 7685-90.
DHAWALE, A. K., SMITH, M. A. & OLVECZKY, B. P. 2017. The Role of Variability in Motor Learning. *Annu Rev Neurosci,* 40, 479-498.

DI CHIARA, G., MORELLI, M., PORCEDDU, M. L. & GESSA, G. L. 1979. Role of thalamic gamma-aminobutyrate in motor functions: catalepsy and ipsiversive turning after intrathalamic muscimol. *Neuroscience,* 4, 1453-65.
DIAZ-HERNANDEZ, E., CONTRERAS-LOPEZ, R., SANCHEZ-FUENTES, A., RODRIGUEZ-SIBRIAN, L., RAMIREZ-JARQUIN, J. O. & TECUAPETLA, F. 2018. The Thalamostriatal Projections Contribute to the Initiation and Execution of a Sequence of Movements. *Neuron,* 100, 739-752 e5.
DOYON, J., BELLEC, P., AMSEL, R., PENHUNE, V., MONCHI, O., CARRIER, J., LEHERICY, S. & BENALI, H. 2009. Contributions of the basal ganglia and functionally related brain structures to motor learning. *Behav Brain Res,* 199, 61-75.
DOYON, J. & BENALI, H. 2005. Reorganization and plasticity in the adult brain during learning of motor skills. *Curr Opin Neurobiol,* 15, 161-7.
DUAN, Z., LI, A., GONG, H. & LI, X. 2020. A Whole-brain Map of Long-range Inputs to GABAergic Interneurons in the Mouse Caudal Forelimb Area. *Neurosci Bull,* 36, 493-505.
DUDMAN, J. T. & KRAKAUER, J. W. 2016. The basal ganglia: from motor commands to the control of vigor. *Curr Opin Neurobiol,* 37, 158-166.
DUNHAM, N. W. & MIYA, T. S. 1957. A note on a simple apparatus for detecting neurological deficit in rats and mice. *J Am Pharm Assoc Am Pharm Assoc,* 46, 208-9.
ESPOSITO, M. S., CAPELLI, P. & ARBER, S. 2014. Brainstem nucleus MdV mediates skilled forelimb motor tasks. *Nature,* 508, 351-6.
EVANGELIO, M., GARCIA-AMADO, M. & CLASCA, F. 2018. Thalamocortical Projection Neuron and Interneuron Numbers in the Visual Thalamic Nuclei of the Adult C57BL/6 Mouse. *Front Neuroanat,* 12, 27.
FENNO, L. E., MATTIS, J., RAMAKRISHNAN, C., HYUN, M., LEE, S. Y., HE, M., TUCCIARONE, J., SELIMBEYOGLU, A., BERNDT, A., GROSENICK, L., ZALOCUSKY, K. A., BERNSTEIN, H., SWANSON, H., PERRY, C., DIESTER, I., BOYCE, F. M., BASS, C. E., NEVE, R., HUANG, Z. J. & DEISSEROTH, K. 2014. Targeting cells with single vectors using multiple-feature Boolean logic. *Nat Methods,* 11, 763-72.
FERSTER, C. B. & SKINNER, B. F. 1957. *Schedules of reinforcement,* New York, Appleton-Century-Crofts.
FITTS, P. M. & POSNER, M. I. 1967. *Human performance,* California, Brooks/Cole.
FRENCH, C. A., VINUEZA VELOZ, M. F., ZHOU, K., PETER, S., FISHER, S. E., COSTA, R. M. & DE ZEEUW, C. I. 2019. Differential effects of Foxp2 disruption in distinct motor circuits. *Mol Psychiatry,* 24, 447-462.
GAIDICA, M., HURST, A., CYR, C. & LEVENTHAL, D. K. 2018. Distinct Populations of Motor Thalamic Neurons Encode Action Initiation, Action Selection, and Movement Vigor. *J Neurosci,* 38, 6563-6573.
GALINANES, G. L., BONARDI, C. & HUBER, D. 2018. Directional Reaching for Water as a Cortex-Dependent Behavioral Framework for Mice. *Cell Rep,* 22, 2767-2783.
GALVAN, A., DEVERGNAS, A. & WICHMANN, T. 2015. Alterations in neuronal activity in basal ganglia-thalamocortical circuits in the parkinsonian state. *Front Neuroanat,* 9, 5.
GALVAN, A., HU, X., SMITH, Y. & WICHMANN, T. 2016. Effects of Optogenetic Activation of Corticothalamic Terminals in the Motor Thalamus of Awake Monkeys. *J Neurosci,* 36, 3519-30.
GAO, Z., DAVIS, C., THOMAS, A. M., ECONOMO, M. N., ABREGO, A. M., SVOBODA, K., DE ZEEUW, C. I. & LI, N. 2018. A cortico-cerebellar loop for motor planning. *Nature,* 563, 113-116.
GARCIA-MUNOZ, M. & ARBUTHNOTT, G. W. 2015. Basal ganglia-thalamus and the "crowning enigma". *Front Neural Circuits,* 9, 71.
GERFEN, C. R., PALETZKI, R. & HEINTZ, N. 2013. GENSAT BAC cre-recombinase driver lines to study the functional organization of cerebral cortical and basal ganglia circuits. *Neuron,* 80, 1368-83.

GOLDBERG, J. H., FARRIES, M. A. & FEE, M. S. 2012. Integration of cortical and pallidal inputs in the basal ganglia-recipient thalamus of singing birds. *J Neurophysiol,* 108, 1403-29.
GOLDBERG, J. H., FARRIES, M. A. & FEE, M. S. 2013. Basal ganglia output to the thalamus: still a paradox. *Trends Neurosci,* 36, 695-705.
GOLTSTEIN, P. M., REINERT, S., GLAS, A., BONHOEFFER, T. & HUBENER, M. 2018. Food and water restriction lead to differential learning behaviors in a head-fixed two-choice visual discrimination task for mice. *PLoS One,* 13, e0204066.
GOMPF, H. S., BUDYGIN, E. A., FULLER, P. M. & BASS, C. E. 2015. Targeted genetic manipulations of neuronal subtypes using promoter-specific combinatorial AAVs in wild-type animals. *Front Behav Neurosci,* 9, 152.
GORNATI, S. V., SCHAFER, C. B., EELKMAN ROODA, O. H. J., NIGG, A. L., DE ZEEUW, C. I. & HOEBEEK, F. E. 2018. Differentiating Cerebellar Impact on Thalamic Nuclei. *Cell Rep,* 23, 2690-2704.
GRADINARU, V., ZHANG, F., RAMAKRISHNAN, C., MATTIS, J., PRAKASH, R., DIESTER, I., GOSHEN, I., THOMPSON, K. R. & DEISSEROTH, K. 2010. Molecular and cellular approaches for diversifying and extending optogenetics. *Cell,* 141, 154-165.
GRAYBIEL, A. M. 1998. The basal ganglia and chunking of action repertoires. *Neurobiol Learn Mem,* 70, 119-36.
GRAYBIEL, A. M., AOSAKI, T., FLAHERTY, A. W. & KIMURA, M. 1994. The basal ganglia and adaptive motor control. *Science,* 265, 1826-31.
GULCEBI, M. I., KETENCI, S., LINKE, R., HACIOGLU, H., YANALI, H., VELISKOVA, J., MOSHE, S. L., ONAT, F. & CAVDAR, S. 2012. Topographical connections of the substantia nigra pars reticulata to higher-order thalamic nuclei in the rat. *Brain Res Bull,* 87, 312-8.
GUNAYDIN, L. A., GROSENICK, L., FINKELSTEIN, J. C., KAUVAR, I. V., FENNO, L. E., ADHIKARI, A., LAMMEL, S., MIRZABEKOV, J. J., AIRAN, R. D., ZALOCUSKY, K. A., TYE, K. M., ANIKEEVA, P., MALENKA, R. C. & DEISSEROTH, K. 2014. Natural neural projection dynamics underlying social behavior. *Cell,* 157, 1535-51.
GUO, J. Z., GRAVES, A. R., GUO, W. W., ZHENG, J., LEE, A., RODRIGUEZ-GONZALEZ, J., LI, N., MACKLIN, J. J., PHILLIPS, J. W., MENSH, B. D., BRANSON, K. & HANTMAN, A. W. 2015a. Cortex commands the performance of skilled movement. *Elife,* 4, e10774.
GUO, K., YAMAWAKI, N., SVOBODA, K. & SHEPHERD, G. M. G. 2018. Anterolateral Motor Cortex Connects with a Medial Subdivision of Ventromedial Thalamus through Cell Type-Specific Circuits, Forming an Excitatory Thalamo-Cortico-Thalamic Loop via Layer 1 Apical Tuft Dendrites of Layer 5B Pyramidal Tract Type Neurons. *J Neurosci,* 38, 8787-8797.
GUO, Q., WANG, D., HE, X., FENG, Q., LIN, R., XU, F., FU, L. & LUO, M. 2015b. Whole-brain mapping of inputs to projection neurons and cholinergic interneurons in the dorsal striatum. *PLoS One,* 10, e0123381.
GUO, Z. V., HIRES, S. A., LI, N., O'CONNOR, D. H., KOMIYAMA, T., OPHIR, E., HUBER, D., BONARDI, C., MORANDELL, K., GUTNISKY, D., PERON, S., XU, N. L., COX, J. & SVOBODA, K. 2014. Procedures for behavioral experiments in head-fixed mice. *PLoS One,* 9, e88678.
GUO, Z. V., INAGAKI, H. K., DAIE, K., DRUCKMANN, S., GERFEN, C. R. & SVOBODA, K. 2017. Maintenance of persistent activity in a frontal thalamocortical loop. *Nature,* 545, 181-186.
HALASSA, M. M. & ACSADY, L. 2016. Thalamic Inhibition: Diverse Sources, Diverse Scales. *Trends Neurosci,* 39, 680-693.
HALASSA, M. M. & SHERMAN, S. M. 2019. Thalamocortical Circuit Motifs: A General Framework. *Neuron,* 103, 762-770.
HAN, X., CHOW, B. Y., ZHOU, H., KLAPOETKE, N. C., CHUONG, A., RAJIMEHR, R., YANG, A., BARATTA, M. V., WINKLE, J., DESIMONE, R. & BOYDEN, E. S. 2011. A

high-light sensitivity optical neural silencer: development and application to optogenetic control of non-human primate cortex. *Front Syst Neurosci,* 5, 18.
HASSLER, R. G. & RIECHERT, T. 1959. Anatomy of the thalamus. *In:* SCHALTENBRAND & BAILEY (eds.) *Introduction to stereotaxis with an atlas of the human brain.* Stuttgart: Thieme.
HEISE, C. E. & MITROFANIS, J. 2004. Evidence for a glutamatergic projection from the zona incerta to the basal ganglia of rats. *J Comp Neurol,* 468, 482-95.
HELD, R. & FREEDMAN, S. J. 1963. Plasticity in Human Sensorimotor Control. *Science,* 142, 455-62.
HIKOSAKA, O., NAKAMURA, K., SAKAI, K. & NAKAHARA, H. 2002. Central mechanisms of motor skill learning. *Curr Opin Neurobiol,* 12, 217-22.
HIKOSAKA, O., TAKIKAWA, Y. & KAWAGOE, R. 2000. Role of the basal ganglia in the control of purposive saccadic eye movements. *Physiol Rev,* 80, 953-78.
HINTZEN, A., PELZER, E. A. & TITTGEMEYER, M. 2018. Thalamic interactions of cerebellum and basal ganglia. *Brain Struct Funct,* 223, 569-587.
HIRAI, T. & JONES, E. G. 1989. A new parcellation of the human thalamus on the basis of histochemical staining. *Brain Res Brain Res Rev,* 14, 1-34.
HONJOH, S., SASAI, S., SCHIERECK, S. S., NAGAI, H., TONONI, G. & CIRELLI, C. 2018. Regulation of cortical activity and arousal by the matrix cells of the ventromedial thalamic nucleus. *Nat Commun,* 9, 2100.
HOOKS, B. M., MAO, T., GUTNISKY, D. A., YAMAWAKI, N., SVOBODA, K. & SHEPHERD, G. M. 2013. Organization of cortical and thalamic input to pyramidal neurons in mouse motor cortex. *J Neurosci,* 33, 748-60.
HOOVER, J. E. & STRICK, P. L. 1999. The organization of cerebellar and basal ganglia outputs to primary motor cortex as revealed by retrograde transneuronal transport of herpes simplex virus type 1. *J Neurosci,* 19, 1446-63.
HORISAWA, S., OCHIAI, T., GOTO, S., NAKAJIMA, T., TAKEDA, N., FUKUI, A., HANADA, T., KAWAMATA, T. & TAIRA, T. 2019. Safety and long-term efficacy of ventro-oral thalamotomy for focal hand dystonia: A retrospective study of 171 patients. *Neurology,* 92, e371-e377.
HOSP, J. A., PEKANOVIC, A., RIOULT-PEDOTTI, M. S. & LUFT, A. R. 2011. Dopaminergic projections from midbrain to primary motor cortex mediate motor skill learning. *J Neurosci,* 31, 2481-7.
HUNNICUTT, B. J., LONG, B. R., KUSEFOGLU, D., GERTZ, K. J., ZHONG, H. & MAO, T. 2014. A comprehensive thalamocortical projection map at the mesoscopic level. *Nat Neurosci,* 17, 1276-85.
HWANG, E. J., DAHLEN, J. E., HU, Y. Y., AGUILAR, K., YU, B., MUKUNDAN, M., MITANI, A. & KOMIYAMA, T. 2019. Disengagement of motor cortex from movement control during long-term learning. *Sci Adv,* 5, eaay0001.
HWANG, K., BERTOLERO, M. A., LIU, W. B. & D'ESPOSITO, M. 2017. The Human Thalamus Is an Integrative Hub for Functional Brain Networks. *J Neurosci,* 37, 5594-5607.
ILINSKY, I. A., YI, H. & KULTAS-ILINSKY, K. 1997. Mode of termination of pallidal afferents to the thalamus: A light and electron microscopic study with anterograde tracers and immunocytochemistry inMacaca mulatta. *The Journal of Comparative Neurology,* 386, 601-612.
INASE, M., BUFORD, J. A. & ANDERSON, M. E. 1996. Changes in the control of arm position, movement, and thalamic discharge during local inactivation in the globus pallidus of the monkey. *J Neurophysiol,* 75, 1087-1104.
ITO, M. 1993. Movement and thought: identical control mechanisms by the cerebellum. *Trends Neurosci,* 16, 448-50; discussion 453-4.
JELJELI, M., STRAZIELLE, C., CASTON, J. & LALONDE, R. 2003. Effects of ventrolateral-ventromedial thalamic lesions on motor coordination and spatial orientation in rats. *Neurosci Res,* 47, 309-16.

JEONG, M., KIM, Y., KIM, J., FERRANTE, D. D., MITRA, P. P., OSTEN, P. & KIM, D. 2016. Comparative three-dimensional connectome map of motor cortical projections in the mouse brain. *Sci Rep,* 6, 20072.
JIANG, X., WANG, G., LEE, A. J., STORNETTA, R. L. & ZHU, J. J. 2013. The organization of two new cortical interneuronal circuits. *Nat Neurosci,* 16, 210-8.
JIN, X. & COSTA, R. M. 2010. Start/stop signals emerge in nigrostriatal circuits during sequence learning. *Nature,* 466, 457-62.
JIN, X., TECUAPETLA, F. & COSTA, R. M. 2014. Basal ganglia subcircuits distinctively encode the parsing and concatenation of action sequences. *Nat Neurosci,* 17, 423-30.
JOCHAM, G., BRODERSEN, K. H., CONSTANTINESCU, A. O., KAHN, M. C., IANNI, A. M., WALTON, M. E., RUSHWORTH, M. F. & BEHRENS, T. E. 2016. Reward-Guided Learning with and without Causal Attribution. *Neuron,* 90, 177-90.
JONES, E. G. 2001. The thalamic matrix and thalamocortical synchrony. *Trends Neurosci,* 24, 595-601.
JONES, E. G. 2007. *The Thalamus*, Cambridge University Press.
KAKEI, S., NA, J. & SHINODA, Y. 2001. Thalamic terminal morphology and distribution of single corticothalamic axons originating from layers 5 and 6 of the cat motor cortex. *J Comp Neurol,* 437, 170-85.
KAWAI, R., MARKMAN, T., PODDAR, R., KO, R., FANTANA, A. L., DHAWALE, A. K., KAMPFF, A. R. & OLVECZKY, B. P. 2015. Motor cortex is required for learning but not for executing a motor skill. *Neuron,* 86, 800-12.
KELLER, D., ERO, C. & MARKRAM, H. 2018. Cell Densities in the Mouse Brain: A Systematic Review. *Front Neuroanat,* 12, 83.
KHA, H. T., FINKELSTEIN, D. I., POW, D. V., LAWRENCE, A. J. & HORNE, M. K. 2000. Study of projections from the entopeduncular nucleus to the thalamus of the rat. *J Comp Neurol,* 426, 366-77.
KIM, E. J., JACOBS, M. W., ITO-COLE, T. & CALLAWAY, E. M. 2016. Improved Monosynaptic Neural Circuit Tracing Using Engineered Rabies Virus Glycoproteins. *Cell Rep,* 15, 692-699.
KIM, J., KIM, Y., NAKAJIMA, R., SHIN, A., JEONG, M., PARK, A. H., JEONG, Y., JO, S., YANG, S., PARK, H., CHO, S. H., CHO, K. H., SHIM, I., CHUNG, J. H., PAIK, S. B., AUGUSTINE, G. J. & KIM, D. 2017. Inhibitory Basal Ganglia Inputs Induce Excitatory Motor Signals in the Thalamus. *Neuron,* 95, 1181-1196 e8.
KLAUS, A., ALVES DA SILVA, J. & COSTA, R. M. 2019. What, If, and When to Move: Basal Ganglia Circuits and Self-Paced Action Initiation. *Annu Rev Neurosci,* 42, 459-483.
KLAUS, A., MARTINS, G. J., PAIXAO, V. B., ZHOU, P., PANINSKI, L. & COSTA, R. M. 2017. The Spatiotemporal Organization of the Striatum Encodes Action Space. *Neuron,* 95, 1171-1180 e7.
KLOCKGETHER, T., SCHWARZ, M., TURSKI, L. & SONTAG, K. H. 1986a. The rat ventromedial thalamic nucleus and motor control: role of N-methyl-D-aspartate-mediated excitation, GABAergic inhibition, and muscarinic transmission. *J Neurosci,* 6, 1702-11.
KLOCKGETHER, T., TURSKI, L., SCHWARZ, M. & SONTAG, K. H. 1986b. Motor actions of excitatory amino acids and their antagonists within the rat ventromedial thalamic nucleus. *Brain Res,* 399, 1-9.
KRACK, P., DOSTROVSKY, J., ILINSKY, I., KULTAS-ILINSKY, K., LENZ, F., LOZANO, A. & VITEK, J. 2002. Surgery of the motor thalamus: problems with the present nomenclatures. *Mov Disord,* 17 Suppl 3, S2-8.
KULTAS-ILINSKY, K., ILINSKY, I. A. & VERNEY, C. 2011. Glutamic acid decarboxylase isoform 65 immunoreactivity in the motor thalamus of humans and monkeys: gamma-aminobutyric acidergic connections and nuclear delineations. *J Comp Neurol,* 519, 2811-37.
KULTAS-ILINSKY, K., SIVAN-LOUKIANOVA, E. & ILINSKY, I. A. 2003. Reevaluation of the primary motor cortex connections with the thalamus in primates. *J Comp Neurol,* 457, 133-58.

KURAMOTO, E., FUJIYAMA, F., NAKAMURA, K. C., TANAKA, Y., HIOKI, H. & KANEKO, T. 2011. Complementary distribution of glutamatergic cerebellar and GABAergic basal ganglia afferents to the rat motor thalamic nuclei. *Eur J Neurosci,* 33, 95-109.
KURAMOTO, E., FURUTA, T., NAKAMURA, K. C., UNZAI, T., HIOKI, H. & KANEKO, T. 2009. Two types of thalamocortical projections from the motor thalamic nuclei of the rat: a single neuron-tracing study using viral vectors. *Cereb Cortex,* 19, 2065-77.
KURAMOTO, E., OHNO, S., FURUTA, T., UNZAI, T., TANAKA, Y. R., HIOKI, H. & KANEKO, T. 2015. Ventral medial nucleus neurons send thalamocortical afferents more widely and more preferentially to layer 1 than neurons of the ventral anterior-ventral lateral nuclear complex in the rat. *Cereb Cortex,* 25, 221-35.
LALIVE, A. L., LIEN, A. D., ROSEBERRY, T. K., DONAHUE, C. H. & KREITZER, A. C. 2018. Motor thalamus supports striatum-driven reinforcement. *Elife,* 7, e34032.
LAM, Y. W. & SHERMAN, S. M. 2015. Functional topographic organization of the motor reticulothalamic pathway. *J Neurophysiol,* 113, 3090-7.
LANCIEGO, J. L., LUQUIN, N. & OBESO, J. A. 2012. Functional neuroanatomy of the basal ganglia. *Cold Spring Harb Perspect Med,* 2, a009621.
LARKUM, M. E. 2013. The yin and yang of cortical layer 1. *Nat Neurosci,* 16, 114-5.
LEE, A. J., WANG, G., JIANG, X., JOHNSON, S. M., HOANG, E. T., LANTE, F., STORNETTA, R. L., BEENHAKKER, M. P., SHEN, Y. & JULIUS ZHU, J. 2015. Canonical Organization of Layer 1 Neuron-Led Cortical Inhibitory and Disinhibitory Interneuronal Circuits. *Cereb Cortex,* 25, 2114-26.
LEE, A. S., DUMAN, R. S. & PITTENGER, C. 2008. A double dissociation revealing bidirectional competition between striatum and hippocampus during learning. *Proc Natl Acad Sci U S A,* 105, 17163-8.
LEE, H. J., WEITZ, A. J., BERNAL-CASAS, D., DUFFY, B. A., CHOY, M., KRAVITZ, A. V., KREITZER, A. C. & LEE, J. H. 2016. Activation of Direct and Indirect Pathway Medium Spiny Neurons Drives Distinct Brain-wide Responses. *Neuron,* 91, 412-24.
LEHERICY, S., BARDINET, E., TREMBLAY, L., VAN DE MOORTELE, P. F., POCHON, J. B., DORMONT, D., KIM, D. S., YELNIK, J. & UGURBIL, K. 2006. Motor control in basal ganglia circuits using fMRI and brain atlas approaches. *Cereb Cortex,* 16, 149-61.
LEHERICY, S., BENALI, H., VAN DE MOORTELE, P. F., PELEGRINI-ISSAC, M., WAECHTER, T., UGURBIL, K. & DOYON, J. 2005. Distinct basal ganglia territories are engaged in early and advanced motor sequence learning. *Proc Natl Acad Sci U S A,* 102, 12566-71.
LIBBRECHT, S., VAN DEN HAUTE, C., MALINOUSKAYA, L., GIJSBERS, R. & BAEKELANDT, V. 2017. Evaluation of WGA-Cre-dependent topological transgene expression in the rodent brain. *Brain Struct Funct,* 222, 717-733.
LISMAN, J. 1997. Bursts as a unit of neural information: making unreliable synapses reliable. *Trends in Neurosciences,* 20, 38-43.
LUBER, B. & LISANBY, S. H. 2014. Enhancement of human cognitive performance using transcranial magnetic stimulation (TMS). *Neuroimage,* 85 Pt 3, 961-70.
LUO, M. & PERKEL, D. J. 1999. A GABAergic, strongly inhibitory projection to a thalamic nucleus in the zebra finch song system. *J Neurosci,* 19, 6700-11.
MAAROUF, M., NEUDORFER, C., EL MAJDOUB, F., LENARTZ, D., KUHN, J. & STURM, V. 2016. Deep Brain Stimulation of Medial Dorsal and Ventral Anterior Nucleus of the Thalamus in OCD: A Retrospective Case Series. *PLoS One,* 11, e0160750.
MAHN, M., PRIGGE, M., RON, S., LEVY, R. & YIZHAR, O. 2016. Biophysical constraints of optogenetic inhibition at presynaptic terminals. *Nat Neurosci,* 19, 554-6.
MARTIROS, N., BURGESS, A. A. & GRAYBIEL, A. M. 2018. Inversely Active Striatal Projection Neurons and Interneurons Selectively Delimit Useful Behavioral Sequences. *Curr Biol,* 28, 560-573 e5.
MASSION, J. 1988. Red nucleus: past and future. *Behav Brain Res,* 28, 1-8.

MASTRO, K. J., ZITELLI, K. T., WILLARD, A. M., LEBLANC, K. H., KRAVITZ, A. V. & GITTIS, A. H. 2017. Cell-specific pallidal intervention induces long-lasting motor recovery in dopamine-depleted mice. *Nat Neurosci,* 20, 815-823.
MATAMALES, M., SKRBIS, Z., BAILEY, M. R., BALSAM, P. D., BALLEINE, B. W., GOTZ, J. & BERTRAN-GONZALEZ, J. 2017. A corticostriatal deficit promotes temporal distortion of automatic action in ageing. *Elife,* 6, e29908.
MATTIS, J., TYE, K. M., FERENCZI, E. A., RAMAKRISHNAN, C., O'SHEA, D. J., PRAKASH, R., GUNAYDIN, L. A., HYUN, M., FENNO, L. E., GRADINARU, V., YIZHAR, O. & DEISSEROTH, K. 2011. Principles for applying optogenetic tools derived from direct comparative analysis of microbial opsins. *Nat Methods,* 9, 159-72.
MCFARLAND, N. R. & HABER, S. N. 2000. Convergent inputs from thalamic motor nuclei and frontal cortical areas to the dorsal striatum in the primate. *J Neurosci,* 20, 3798-813.
MCFARLAND, N. R. & HABER, S. N. 2002. Thalamic relay nuclei of the basal ganglia form both reciprocal and nonreciprocal cortical connections, linking multiple frontal cortical areas. *J Neurosci,* 22, 8117-32.
MEASE, R. A., KUNER, T., FAIRHALL, A. L. & GROH, A. 2017. Multiplexed Spike Coding and Adaptation in the Thalamus. *Cell Rep,* 19, 1130-1140.
MIALL, R. C., PRICE, S., MASON, R., PASSINGHAM, R. E., WINTER, J. L. & STEIN, J. F. 1998. Microstimulation of movements from cerebellar-receiving, but not pallidal-receiving areas of the macaque thalamus under ketamine anaesthesia. *Exp Brain Res,* 123, 387-96.
MITCHELL, S. J., RICHARDSON, R. T., BAKER, F. H. & DELONG, M. R. 1987. The primate globus pallidus: neuronal activity related to direction of movement. *Exp Brain Res,* 68, 491-505.
MOLYNEAUX, B. J., ARLOTTA, P., MENEZES, J. R. & MACKLIS, J. D. 2007. Neuronal subtype specification in the cerebral cortex. *Nat Rev Neurosci,* 8, 427-37.
MOMENNEJAD, I., OTTO, A. R., DAW, N. D. & NORMAN, K. A. 2018. Offline replay supports planning in human reinforcement learning. *Elife,* 7, e32548.
MURAKAMI, T. C., MANO, T., SAIKAWA, S., HORIGUCHI, S. A., SHIGETA, D., BABA, K., SEKIYA, H., SHIMIZU, Y., TANAKA, K. F., KIYONARI, H., IINO, M., MOCHIZUKI, H., TAINAKA, K. & UEDA, H. R. 2018. A three-dimensional single-cell-resolution whole-brain atlas using CUBIC-X expansion microscopy and tissue clearing. *Nat Neurosci,* 21, 625-637.
NAKAJIMA, M., SCHMITT, L. I. & HALASSA, M. M. 2019. Prefrontal Cortex Regulates Sensory Filtering through a Basal Ganglia-to-Thalamus Pathway. *Neuron,* 103, 445-458 e10.
NAKAMURA, K. C., SHAROTT, A. & MAGILL, P. J. 2014. Temporal coupling with cortex distinguishes spontaneous neuronal activities in identified basal ganglia-recipient and cerebellar-recipient zones of the motor thalamus. *Cereb Cortex,* 24, 81-97.
NATHANSON, J. L., JAPPELLI, R., SCHEEFF, E. D., MANNING, G., OBATA, K., BRENNER, S. & CALLAWAY, E. M. 2009. Short Promoters in Viral Vectors Drive Selective Expression in Mammalian Inhibitory Neurons, but do not Restrict Activity to Specific Inhibitory Cell-Types. *Front Neural Circuits,* 3, 19.
NUDO, R. J. 2013. Recovery after brain injury: mechanisms and principles. *Front Hum Neurosci,* 7, 887.
O'SHEA, D. J., KALANITHI, P., FERENCZI, E. A., HSUEH, B., CHANDRASEKARAN, C., GOO, W., DIESTER, I., RAMAKRISHNAN, C., KAUFMAN, M. T., RYU, S. I., YEOM, K. W., DEISSEROTH, K. & SHENOY, K. V. 2018. Development of an optogenetic toolkit for neural circuit dissection in squirrel monkeys. *Sci Rep,* 8, 6775.
OLDENBURG, I. A. & SABATINI, B. L. 2015. Antagonistic but Not Symmetric Regulation of Primary Motor Cortex by Basal Ganglia Direct and Indirect Pathways. *Neuron,* 86, 1174-81.
OLSZEWSKI, J. 1952. *The Thalamus of the Macaca Mulatta: An Atlas for Use with the Stereotaxic Instrument,* Basel, Karger.
OLVECZKY, B. P. 2011. Motoring ahead with rodents. *Curr Opin Neurobiol,* 21, 571-8.

OSTLUND, S. B., WINTERBAUER, N. E. & BALLEINE, B. W. 2009. Evidence of action sequence chunking in goal-directed instrumental conditioning and its dependence on the dorsomedial prefrontal cortex. *J Neurosci,* 29, 8280-7.
OWEN, S. F., LIU, M. H. & KREITZER, A. C. 2019. Thermal constraints on in vivo optogenetic manipulations. *Nat Neurosci,* 22, 1061-1065.
PARKER, P. R., LALIVE, A. L. & KREITZER, A. C. 2016. Pathway-Specific Remodeling of Thalamostriatal Synapses in Parkinsonian Mice. *Neuron,* 89, 734-40.
PATEL, S. R. & LIEBER, C. M. 2019. Precision electronic medicine in the brain. *Nat Biotechnol,* 37, 1007-1012.
PAXINOS, G. & FRANKLIN, K. B. J. 2012. *The Mouse Brain in Stereotaxic Coordinates,* San Diego, Academic Press.
PAXINOS, G. & WATSON, C. 1996. *The Rat Brain in Stereotaxic Coordinates,* San Diego, Academic Press.
PEREZ-ESCUDERO, A., VICENTE-PAGE, J., HINZ, R. C., ARGANDA, S. & DE POLAVIEJA, G. G. 2014. idTracker: tracking individuals in a group by automatic identification of unmarked animals. *Nat Methods,* 11, 743-8.
PEREZ, M. A., TANAKA, S., WISE, S. P., SADATO, N., TANABE, H. C., WILLINGHAM, D. T. & COHEN, L. G. 2007. Neural substrates of intermanual transfer of a newly acquired motor skill. *Curr Biol,* 17, 1896-902.
PERSON, A. L. & PERKEL, D. J. 2005. Unitary IPSPs drive precise thalamic spiking in a circuit required for learning. *Neuron,* 46, 129-40.
PETERS, A. J., CHEN, S. X. & KOMIYAMA, T. 2014. Emergence of reproducible spatiotemporal activity during motor learning. *Nature,* 510, 263-7.
PHILIPP, R. & HOFFMANN, K. P. 2014. Arm movements induced by electrical microstimulation in the superior colliculus of the macaque monkey. *J Neurosci,* 34, 3350-63.
PHILLIPS, J. W., SCHULMANN, A., HARA, E., WINNUBST, J., LIU, C., VALAKH, V., WANG, L., SHIELDS, B. C., KORFF, W., CHANDRASHEKAR, J., LEMIRE, A. L., MENSH, B., DUDMAN, J. T., NELSON, S. B. & HANTMAN, A. W. 2019. A repeated molecular architecture across thalamic pathways. *Nat Neurosci,* 22, 1925-1935.
PINSARD, B., BOUTIN, A., GABITOV, E., LUNGU, O., BENALI, H. & DOYON, J. 2019. Consolidation alters motor sequence-specific distributed representations. *Elife,* 8, e39324.
PIRON, C., KASE, D., TOPALIDOU, M., GOILLANDEAU, M., ORIGNAC, H., N'GUYEN, T. H., ROUGIER, N. & BORAUD, T. 2016. The globus pallidus pars interna in goal-oriented and routine behaviors: Resolving a long-standing paradox. *Mov Disord,* 31, 1146-54.
REDGRAVE, P., RODRIGUEZ, M., SMITH, Y., RODRIGUEZ-OROZ, M. C., LEHERICY, S., BERGMAN, H., AGID, Y., DELONG, M. R. & OBESO, J. A. 2010. Goal-directed and habitual control in the basal ganglia: implications for Parkinson's disease. *Nat Rev Neurosci,* 11, 760-72.
ROSEBERRY, T. K., LEE, A. M., LALIVE, A. L., WILBRECHT, L., BONCI, A. & KREITZER, A. C. 2016. Cell-Type-Specific Control of Brainstem Locomotor Circuits by Basal Ganglia. *Cell,* 164, 526-37.
ROVO, Z., ULBERT, I. & ACSADY, L. 2012. Drivers of the primate thalamus. *J Neurosci,* 32, 17894-908.
RUBIO-GARRIDO, P., PEREZ-DE-MANZO, F., PORRERO, C., GALAZO, M. J. & CLASCA, F. 2009. Thalamic input to distal apical dendrites in neocortical layer 1 is massive and highly convergent. *Cereb Cortex,* 19, 2380-95.
SAKAYORI, N., KATO, S., SUGAWARA, M., SETOGAWA, S., FUKUSHIMA, H., ISHIKAWA, R., KIDA, S. & KOBAYASHI, K. 2019. Motor skills mediated through cerebellothalamic tracts projecting to the central lateral nucleus. *Mol Brain,* 12, 13.
SALEEBA, C., DEMPSEY, B., LE, S., GOODCHILD, A. & MCMULLAN, S. 2019. A Student's Guide to Neural Circuit Tracing. *Front Neurosci,* 13, 897.
SANCHEZ-GONZALEZ, M. A., GARCIA-CABEZAS, M. A., RICO, B. & CAVADA, C. 2005. The primate thalamus is a key target for brain dopamine. *J Neurosci,* 25, 6076-83.

SANTOS, F. J., OLIVEIRA, R. F., JIN, X. & COSTA, R. M. 2015. Corticostriatal dynamics encode the refinement of specific behavioral variability during skill learning. *Elife,* 4, e09423.
SAUERBREI, B. A., GUO, J. Z., COHEN, J. D., MISCHIATI, M., GUO, W., KABRA, M., VERMA, N., MENSH, B., BRANSON, K. & HANTMAN, A. W. 2020. Cortical pattern generation during dexterous movement is input-driven. *Nature,* 577, 386-391.
SAUNDERS, A., OLDENBURG, I. A., BEREZOVSKII, V. K., JOHNSON, C. A., KINGERY, N. D., ELLIOTT, H. L., XIE, T., GERFEN, C. R. & SABATINI, B. L. 2015. A direct GABAergic output from the basal ganglia to frontal cortex. *Nature,* 521, 85-9.
SAWYER, S. F., YOUNG, S. J., GROVES, P. M. & TEPPER, J. M. 1994. Cerebellar-responsive neurons in the thalamic ventroanterior-ventrolateral complex of rats: in vivo electrophysiology. *Neuroscience,* 63, 711-24.
SCHMITT, L. I., WIMMER, R. D., NAKAJIMA, M., HAPP, M., MOFAKHAM, S. & HALASSA, M. M. 2017. Thalamic amplification of cortical connectivity sustains attentional control. *Nature,* 545, 219-223.
SCHREINER, D. C. & GREMEL, C. M. 2018. Orbital Frontal Cortex Projections to Secondary Motor Cortex Mediate Exploitation of Learned Rules. *Sci Rep,* 8, 10979.
SEEGER-ARMBRUSTER, S., BOSCH-BOUJU, C., LITTLE, S. T., SMITHER, R. A., HUGHES, S. M., HYLAND, B. I. & PARR-BROWNLIE, L. C. 2015. Patterned, but not tonic, optogenetic stimulation in motor thalamus improves reaching in acute drug-induced Parkinsonian rats. *J Neurosci,* 35, 1211-6.
SEIFERT, S., VON CRAMON, D. Y., IMPERATI, D., TITTGEMEYER, M. & ULLSPERGER, M. 2011. Thalamocingulate interactions in performance monitoring. *J Neurosci,* 31, 3375-83.
SHERMAN, S. M. 2016. Thalamus plays a central role in ongoing cortical functioning. *Nat Neurosci,* 19, 533-41.
SHERMAN, S. M. & GUILLERY, R. W. 1996. Functional organization of thalamocortical relays. *J Neurophysiol,* 76, 1367-95.
SIEVERITZ, B., GARCIA-MUNOZ, M. & ARBUTHNOTT, G. W. 2019. Thalamic afferents to prefrontal cortices from ventral motor nuclei in decision-making. *Eur J Neurosci,* 49, 646-657.
SKATOVA, A., CHAN, P. A. & DAW, N. D. 2013. Extraversion differentiates between model-based and model-free strategies in a reinforcement learning task. *Front Hum Neurosci,* 7, 525.
SKINNER, B. F. 1938. *The Behaviour of organisms: An experimental analysis. ,* New York, Appleton-Century.
STARR, M. S. & SUMMERHAYES, M. 1983a. Role of the ventromedial nucleus of the thalamus in motor behaviour--I. Effects of focal injections of drugs. *Neuroscience,* 10, 1157-69.
STARR, M. S. & SUMMERHAYES, M. 1983b. Role of the ventromedial nucleus of the thalamus in motor behaviour--II. Effects of lesions. *Neuroscience,* 10, 1171-83.
TANAKA, Y. H., TANAKA, Y. R., KONDO, M., TERADA, S. I., KAWAGUCHI, Y. & MATSUZAKI, M. 2018. Thalamocortical Axonal Activity in Motor Cortex Exhibits Layer-Specific Dynamics during Motor Learning. *Neuron,* 100, 244-258 e12.
TECUAPETLA, F., JIN, X., LIMA, S. Q. & COSTA, R. M. 2016. Complementary Contributions of Striatal Projection Pathways to Action Initiation and Execution. *Cell,* 166, 703-715.
TECUAPETLA, F., MATIAS, S., DUGUE, G. P., MAINEN, Z. F. & COSTA, R. M. 2014. Balanced activity in basal ganglia projection pathways is critical for contraversive movements. *Nat Commun,* 5, 4315.
TERVO, D. G., HWANG, B. Y., VISWANATHAN, S., GAJ, T., LAVZIN, M., RITOLA, K. D., LINDO, S., MICHAEL, S., KULESHOVA, E., OJALA, D., HUANG, C. C., GERFEN, C. R., SCHILLER, J., DUDMAN, J. T., HANTMAN, A. W., LOOGER, L. L., SCHAFFER, D. V. & KARPOVA, A. Y. 2016. A Designer AAV Variant Permits Efficient Retrograde Access to Projection Neurons. *Neuron,* 92, 372-382.
THORNDIKE, E. L. 1898. Animal intelligence: An experimental study of the associative processes in animals. *The Psychological Review: Monograph Supplements,* 2, i-109.

THURA, D. & CISEK, P. 2017. The Basal Ganglia Do Not Select Reach Targets but Control the Urgency of Commitment. *Neuron,* 95, 1160-1170 e5.
TROUCHE, S., KOREN, V., DOIG, N. M., ELLENDER, T. J., EL-GABY, M., LOPES-DOS-SANTOS, V., REEVE, H. M., PERESTENKO, P. V., GARAS, F. N., MAGILL, P. J., SHAROTT, A. & DUPRET, D. 2019. A Hippocampus-Accumbens Tripartite Neuronal Motif Guides Appetitive Memory in Space. *Cell,* 176, 1393-1406 e16.
TROUCHE, S., PERESTENKO, P. V., VAN DE VEN, G. M., BRATLEY, C. T., MCNAMARA, C. G., CAMPO-URRIZA, N., BLACK, S. L., REIJMERS, L. G. & DUPRET, D. 2016. Recoding a cocaine-place memory engram to a neutral engram in the hippocampus. *Nat Neurosci,* 19, 564-7.
TURNER, R. S. & ANDERSON, M. E. 1997. Pallidal discharge related to the kinematics of reaching movements in two dimensions. *J Neurophysiol,* 77, 1051-74.
TURNER, R. S. & DESMURGET, M. 2010. Basal ganglia contributions to motor control: a vigorous tutor. *Curr Opin Neurobiol,* 20, 704-16.
UNGERLEIDER, L. G., DOYON, J. & KARNI, A. 2002. Imaging brain plasticity during motor skill learning. *Neurobiol Learn Mem,* 78, 553-64.
VAN DONKELAAR, P., STEIN, J. F., PASSINGHAM, R. E. & MIALL, R. C. 2000. Temporary inactivation in the primate motor thalamus during visually triggered and internally generated limb movements. *J Neurophysiol,* 83, 2780-90.
VITEK, J. L., ASHE, J., DELONG, M. R. & ALEXANDER, G. E. 1994. Physiologic properties and somatotopic organization of the primate motor thalamus. *J Neurophysiol,* 71, 1498-513.
VITEK, J. L., ASHE, J., DELONG, M. R. & KANEOKE, Y. 1996. Microstimulation of primate motor thalamus: somatotopic organization and differential distribution of evoked motor responses among subnuclei. *J Neurophysiol,* 75, 2486-95.
WALL, N. R., DE LA PARRA, M., SOROKIN, J. M., TANIGUCHI, H., HUANG, Z. J. & CALLAWAY, E. M. 2016. Brain-Wide Maps of Synaptic Input to Cortical Interneurons. *J Neurosci,* 36, 4000-9.
WALL, N. R., WICKERSHAM, I. R., CETIN, A., DE LA PARRA, M. & CALLAWAY, E. M. 2010. Monosynaptic circuit tracing in vivo through Cre-dependent targeting and complementation of modified rabies virus. *Proc Natl Acad Sci U S A,* 107, 21848-53.
WALLACE, M. L., SAUNDERS, A., HUANG, K. W., PHILSON, A. C., GOLDMAN, M., MACOSKO, E. Z., MCCARROLL, S. A. & SABATINI, B. L. 2017. Genetically Distinct Parallel Pathways in the Entopeduncular Nucleus for Limbic and Sensorimotor Output of the Basal Ganglia. *Neuron,* 94, 138-152 e5.
WANG, X., LIU, Y., LI, X., ZHANG, Z., YANG, H., ZHANG, Y., WILLIAMS, P. R., ALWAHAB, N. S. A., KAPUR, K., YU, B., ZHANG, Y., CHEN, M., DING, H., GERFEN, C. R., WANG, K. H. & HE, Z. 2017. Deconstruction of Corticospinal Circuits for Goal-Directed Motor Skills. *Cell,* 171, 440-455 e14.
WHISHAW, I. Q., FARAJI, J., KUNTZ, J. R., MIRZA AGHA, B., METZ, G. A. S. & MOHAJERANI, M. H. 2017. The syntactic organization of pasta-eating and the structure of reach movements in the head-fixed mouse. *Sci Rep,* 7, 10987.
WHISHAW, I. Q., GORNY, B. & SARNA, J. 1998. Paw and limb use in skilled and spontaneous reaching after pyramidal tract, red nucleus and combined lesions in the rat: behavioral and anatomical dissociations. *Behav Brain Res,* 93, 167-83.
WIEGERT, J. S., MAHN, M., PRIGGE, M., PRINTZ, Y. & YIZHAR, O. 2017. Silencing Neurons: Tools, Applications, and Experimental Constraints. *Neuron,* 95, 504-529.
WILLINGHAM, D. B. 1998. A neuropsychological theory of motor skill learning. *Psychol Rev,* 105, 558-84.
WOLFF, S. B. & OLVECZKY, B. P. 2018. The promise and perils of causal circuit manipulations. *Curr Opin Neurobiol,* 49, 84-94.
WULLNER, U., KLOCKGETHER, T., SCHWARZ, M. & SONTAG, K. H. 1987. Behavioral actions of baclofen in the rat ventromedial thalamic nucleus: antagonism by delta-aminovalerate. *Brain Res,* 422, 129-36.

XIAO, L., BORNMANN, C., HATSTATT-BURKLE, L. & SCHEIFFELE, P. 2018. Regulation of striatal cells and goal-directed behavior by cerebellar outputs. *Nat Commun,* 9, 3133.
XU, T., YU, X., PERLIK, A. J., TOBIN, W. F., ZWEIG, J. A., TENNANT, K., JONES, T. & ZUO, Y. 2009. Rapid formation and selective stabilization of synapses for enduring motor memories. *Nature,* 462, 915-9.
XU, W. & SUDHOF, T. C. 2013. A neural circuit for memory specificity and generalization. *Science,* 339, 1290-5.
YAMADA, A., UESAKA, N., HAYANO, Y., TABATA, T., KANO, M. & YAMAMOTO, N. 2010. Role of pre- and postsynaptic activity in thalamocortical axon branching. *Proc Natl Acad Sci U S A,* 107, 7562-7.
YAMAWAKI, N., BORGES, K., SUTER, B. A., HARRIS, K. D. & SHEPHERD, G. M. 2014. A genuine layer 4 in motor cortex with prototypical synaptic circuit connectivity. *Elife,* 3, e05422.
YANG, G., PAN, F. & GAN, W. B. 2009. Stably maintained dendritic spines are associated with lifelong memories. *Nature,* 462, 920-4.
YIN, H. H. 2009. The role of the murine motor cortex in action duration and order. *Front Integr Neurosci,* 3, 23.
YTTRI, E. A. & DUDMAN, J. T. 2016. Opponent and bidirectional control of movement velocity in the basal ganglia. *Nature,* 533, 402-6.
ZARIWALA, H. A., BORGHUIS, B. G., HOOGLAND, T. M., MADISEN, L., TIAN, L., DE ZEEUW, C. I., ZENG, H., LOOGER, L. L., SVOBODA, K. & CHEN, T. W. 2012. A Cre-dependent GCaMP3 reporter mouse for neuronal imaging in vivo. *J Neurosci,* 32, 3131-41.
ZHANG, S., XU, M., CHANG, W. C., MA, C., HOANG DO, J. P., JEONG, D., LEI, T., FAN, J. L. & DAN, Y. 2016. Organization of long-range inputs and outputs of frontal cortex for top-down control. *Nat Neurosci,* 19, 1733-1742.
ZINGG, B., CHOU, X. L., ZHANG, Z. G., MESIK, L., LIANG, F., TAO, H. W. & ZHANG, L. I. 2017. AAV-Mediated Anterograde Transsynaptic Tagging: Mapping Corticocollicular Input-Defined Neural Pathways for Defense Behaviors. *Neuron,* 93, 33-47.
ZIS, V. P., SPYRAKI, C. & PAPADOPOULOS, G. 1984. Acquisition and extinction of L-maze and conditioned avoidance behaviours following kainic acid-induced lesions of the ventromedial thalamic nuclei in rats. *Brain Res Bull,* 12, 617-23.